# The suitability of ovine as a cell source for cultured meat applications

V.M.B. Andriessen

*Supervisors*

Dr. L. J. Domigan, University of Auckland

Dr. A. D. van der Meer, University of Twente

Master's thesis Biomedical Engineering

University of Twente

April 2021

# The suitability of ovine as a cell source for cultured meat applications

by

V. (Vicky) M. B. Andriessen

to obtain the degree of Master of Science in Biomedical Engineering

at the University of Twente,

to be defended publicly on Monday 3 May 2021, at 12.00.

| | | |
|---|---|---|
| Student number: | 1248693 | |
| Thesis committee: | Prof. dr. P.C.J.J. Passier | University of Twente, chairman |
| | Dr. A. D. van der Meer | University of Twente, supervisor |
| | Prof. dr. ir. L. I. Segerink | University of Twente, external member |
| External supervisor: | Dr. L. J. Domigan | University of Auckland |

UNIVERSITY OF TWENTE.

THE UNIVERSITY OF AUCKLAND
Te Whare Wānanga o Tāmaki Makaurau
NEW ZEALAND

# Preface

When I found out about the concept of cultured meat 4 years ago, I was immediately intrigued. Producing meat without the need to slaughter an animal - could this be real? I investigated how this could become reality, and for a short moment I was satisfied reading that a small group of people was developing the product. Then suddenly, it hit me. I could contribute to the development as well! At that moment, I was following a pre-master to transfer to Mechanical Engineering at the TU Delft. I finished the pre-master, went back to the University of Twente, and started a master in Biomedical Engineering. I followed the Bioengineering track and included all the courses that would increase my knowledge about tissue engineering. I am extremely grateful to Andries van der Meer, Robert Passier, and the exam committee for approving my personalised master curriculum and thereby allowing me to follow extracurricular courses in Food Technology, intern at a cultured meat company, and perform my thesis research at the University of Auckland within the field of cultured meat. I want to stipulate my gratitude for Andries van der Meer, as he assisted me in getting this research approved. I moreover want to thank Loes Segerink for being my external committee member.

Finding a project for my thesis took a long time, until I contacted Laura Domigan. She shared my excitement and passion for cultured meat, and invited me to join her research group at the University of Auckland, New Zealand. The impact of COVID-19 could not have been foreseen and has made my time abroad different than expected. Despite this, I am glad that I went and extremely thankful to Laura and colleagues for having me. I especially want to thank Manmeet Kaur for her insights, her positive energy, and overall being lovely. Moreover, I want to thank James Dickson for the insightful discussions about tissue engineering, native New Zealand birds, and basically anything that can be discussed about life. I want to thank Kai Steinmetz for being my cultured meat buddy, and Morgan Dolfing for his limitless excitement about every little step I made in my research. I want to thank Vaughan Feisst and Thaize Chometon for guiding me through the process of cell identification. Moreover, I want to thank Mosa Meat, especially Joshua Flack, for providing me with purified ovine and bovine satellite cells for this research.

Last year consisted mostly of strict lockdowns alternated with long days in the lab to compensate for missed time. I want to thank Jade Houenoussi for being my friend and every so often pulling me out of the lab to explore the country. Moreover, I am especially grateful to my boyfriend Rutger for always being there for me and keeping me sane on a distance. And of course, I want to thank my family and friends for their unconditional support.

I am extremely grateful to New Harvest for rewarding my research proposal with the New Harvest Seed Grant. It is an honour to be supported by such an innovative research institute. A special thanks goes out to Jeremiah Johnston who always made time for meeting me. Moreover, I want to thank the Jo Kolk Scholarship for financially supporting me to perform my thesis research in New Zealand.

### Declaration of competing interest

The author of this thesis performed an internship at cultured meat company Mosa Meat prior to this thesis research and has signed for a job after graduation. Purified bovine and ovine cells were supplied by Mosa Meat and the isolation protocol used during the research presented here was based on their protocol. Mosa Meat has not been involved in the contents of this thesis work in any form, nor has it been involved in discussions about this thesis research. Moreover, the New Harvest Seed Grant was awarded to this research. Although employees of New Harvest have been involved in discussions about the research, they have not been involved in the writing of this thesis.

## English abstract

The meat industry imposes an immense pressure on the Earth and its inhabitants. The global meat consumption is expected to increase by up to 70% in the coming decennia. A proposed solution is cultured meat: a product that aims to replicate the appearance, texture, and flavour of conventionally produced meat through tissue engineering techniques. Cultured meat is made by isolating stem cells from an animal, expanding the cells by proliferation, and differentiating the cells in a 3D environment into muscle and fat tissue. Cells sourced from bovine, porcine, and avian are of greatest interest at presence. Interest in ovine as a cell source is also expressed, but no extensive research to this species has been previously reported. The research presented in this thesis investigates the properties of cells isolated from ovine and lays the groundwork for tissue engineering research with interest in ovine as a cell source. Cells were isolated from the two hindlimb muscles *m. semitendinosus* and *m. semimembranosus*. The cell types present in the samples were identified as myogenic cells and fibroblasts. Myogenic properties were confirmed as the cells expressed the myogenic protein myosin after differentiation was initiated by serum starvation. It was observed that a higher percentage of ITGA7+ cells resulted in a higher population doubling rate. A system was designed for formation of myofibres. A control model was established with a C2C12-laden hydrogel containing collagen and Matrigel. The C2C12 constructs expressed spontaneous contraction after 4 days of culture. Ovine constructs were created with an enzymatic isolated cell sample, containing 76% myogenic cells and 24% fibroblasts. The ovine sample was observed to form a construct in the system, however detaching from the anchor points was observed within five days. According to the results presented in this thesis, ovine isolated myogenic cells are expected to meet the requirements of cultured meat research and it is therefore concluded that ovine is an eligible cell source for cultured meat production.



## Dutch abstract/Nederlandse samenvatting

De vleesindustrie vergt veel van de Aarde en haar inwoners. De verwachting is dat de globale vleesconsumptie zal toenemen tot 70% in de komende decennia. Een voorgestelde oplossing is kweekvlees: een product that streeft om het uiterlijk, de textuur en de smaak van conventioneel geproduceerd vlees te repliceren door middel van weefselkweek technologie. Kweekvlees wordt geproduceerd door stamcellen te isoleren van een dier, de cellen te prolifereren en vervolgens in een 3D omgeving te differentiëren in spier- en vetweefsel. Momenteel krijgen cellen van koe, varken, en pluimvee de meeste interesse. Interesse in schaapcellen for kweekvlees productie is ook geuit, maar uitgebreid onderzoek naar deze soort is hedendaags nog niet gepubliceerd. Het onderzoek gepresenteerd in deze thesis onderzocht de eigenschappen van geïsoleerde schaapcellen en legt de basis voor weefselkweek onderzoek met schaap als bron van cellen. Cellen werden geïsoleerd van twee spieren op het achterbeen, de *m. semitendinosus* en *m. semimembranosus*. De celtypes in de samples werden geïdentificeerd als myogene cellen en fibroblasten. Myogene eigenschappen werden bevestigd door expressie van het motoreiwit myosine, nadat differentiatie was geïnitieerd door een gelimiteerde toevoeging van serum. Een hoger percentage ITGA7+ cellen resulteerde in een hogere verdubbelingssnelheid van de populatie. Een systeem was ontworpen voor de formatie van spiervezels. Een controle model was opgezet met een C2C12 cellen bevattende hydrogel, gebasseerd op collageen en Matrigel. De C2C12-constructen vertoonden spontane contractie na 4 dagen kweken. De constructen waren ook gemaakt met een enzymatisch geïsoleerde schaapcellen mix van 76% myogene cellen en 24% fibroblasten. De schapencellen vormden een construct in het systeem, maar bleven niet langer dan vijf dagen intact. Gebasseerd op de resultaten gepresenteerd in deze thesis wordt verwacht dat myogene schapencellen voldoen aan de eisen van kweekvlees onderzoek en dat schapen derhalve een geschikte celbron zijn voor de productie van kweekvlees.

# Contents

# List of Figures

# List of Tables

# List of abbreviations

**A-A** antibiotic-antimycotic solution

**B1** biopsy 1

**B2** biopsy 2

**BEC** bovine endothelial cell

**bFGF** basis fibroblast growth factor

**BSMC** bovine smooth muscle cell

**DMEM** Dulbecco's modified Eagle's medium

**DMSO** dimethyl sulfoxide

**FACS** fluorescent activated cell sorting

**FBS** fetal bovine serum

**FSB** flow staining buffer

**GHG** greenhouse gas

**HS** horse serum

**LCA** life cycle assessment

**MFI** mean fluorescence intensity

**PBS** phosphate buffered saline

**PDL** population doubling

**PDMS** polydimethylsiloxaan

**PFA** paraformaldehyde

**PLA** polylactic acid

**SC** satellite cell

**SI** stain index

**SM** m. semimembranosus

**ST** m. semitendinosus

**TNS** tryplE neutraliser solution

**TSP** textured soy protein

**WB** wash buffer

# 1 Introduction

The meat industry is imposing an immense pressure on the Earth and its inhabitants. The complications are known and documented, but demand for meat is still growing. This chapter provides an overview of the impact of the meat industry, categorised in sustainability, animal welfare, and public health and safety, and it provides one proposed solution.

## 1.1. Sustainability

The effects of climate change become increasingly apparent every year. Natural disasters have cost the lives of an innumerable amount of people, with certainly more to come [1]. The main cause of climate change is the increase in greenhouse gas (GHG) emissions [2]. These emissions are heating up the planet, and the amount of emissions is expected to rapidly increase in the near future. The meat industry contributes a significant amount to the GHG emissions. In 2018, 13.2% of the global GHG emissions were produced by livestock, compared to 8% emitted by non-animal food [3, 4, 5]. GHGs are produced at farms by methane emissions from bovine (cows) and by farm machinery, followed by emissions caused by deforestation for land-use change and emissions produced during processing of animal feed. It is noteworthy that deforestation decreases the ability of greenhouse gas sequestration even more, since there is less vegetation. Figure 1.1 depicts a comparison of greenhouse gas emissions produced by meat of several species and the plant-based product tofu. Tofu is chosen as comparison as it contains all essential amino acids and has a protein digestibility of 93% (compared to 91% of meat protein digestibility) [6]. It stands out from figure 1.1 that meat from bovine and ovine (sheep) have the highest emissions in terms of conversion to both kilocalories as well as proteins.


Figure 1.1.: Greenhouse gas emissions are measured in kilograms of carbon dioxide equivalents per 1000 kilocalories and per 100 grams of protein. Data retrieved from [3].

Moreover, one of the main causes of water shortage throughout the world is the industrialisation

of the meat industry [7, 8]. In 2017, it was reported that globally 1.2 billion people suffered water shortage [7]. As water is essential for health, food, and energy, the inherent consequences of water depletion are massive on human survival. It is expected that in the coming decades 3.9 billion people will be suffering from water shortage [7]. 27% of the globally used fresh water in 2013 was directly or indirectly used for animal production [9]. Figure 1.2 visualises a comparison of meat of different species and tofu, based on their water use. It stands out that the production of meat has a high water footprint, especially porcine and ovine, when compared to the plant-based product.

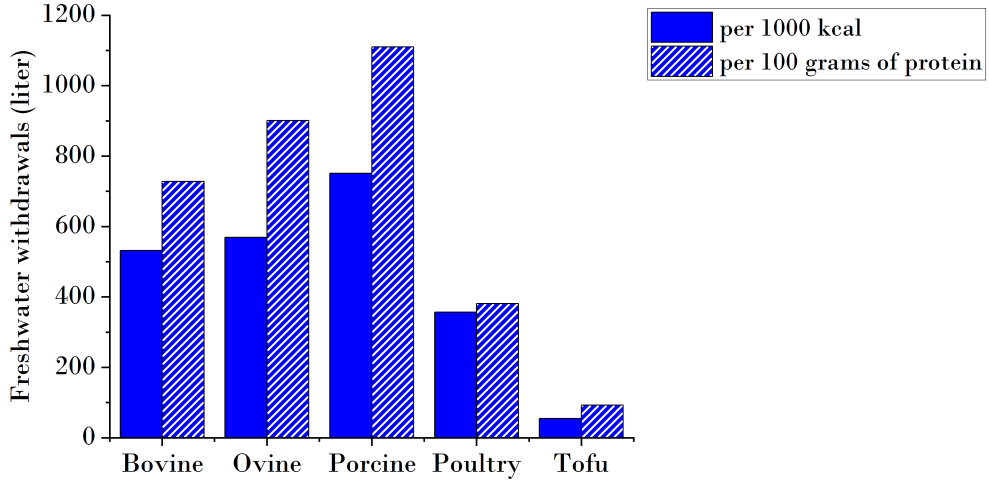


Figure 1.2.: Freshwater withdrawals measured in liters per 1000 kilocalories and per 100 grams of protein of meat and tofu. Data retrieved from [3].

Another effect of the meat industry is that some species demand a large amount of land. Land is an important resource, as it is essential for housing, infrastructure, setting up industries, forestry, flora, and fauna [10].These categories all contribute to survival and prosperity of humanity. However, the amount of available land is limited, while human demand for it seems unlimited. Globally, 40 million $km^2$ is used for animal agriculture, which is more than the surface area of Europe and Africa combined [11]. This means that 39% of globally habitable land and 77% of agricultural land is designated to animal agriculture, which covers the land used for farmhouses, grazing, and growing animal feed (e.g. soy and cereals). An approach to create more usable land is deforestration. Deforestation has a negative impact on climate change as it decreases the amount of forest available for greenhouse gasses sequestration. Meanwhile, deforestation itself and the purposes of deforestation increase the amount of greenhouse gas emissions. Although the negative impact of deforestation is known, the urge to increase meat production to meet global demand is prioritised and large areas are deforested [12]. Figure 1.3 visualizes the amount of land that is needed to produce 100 grams of proteins across various food products. Ovine and bovine are excessive in land use, compared to porcine, poultry, and tofu.

Additionally, the meat industry imposes a pressure on the food production system, causing food shortage. Protein conversion of meat production is rather inefficient, as the ratio of protein feed input converted to final protein product for consumption are 3.8%, 6.3%, 8.5%, and 19.6%, for bovine, ovine, porcine, and poultry, repectively [13, 14]. In 2018, 821 million people (roughly 11% of the global population) were undernourished [15]. Meanwhile, the annual feed grown for livestock consumption would be sufficient to feed 3.5 billion people [16].

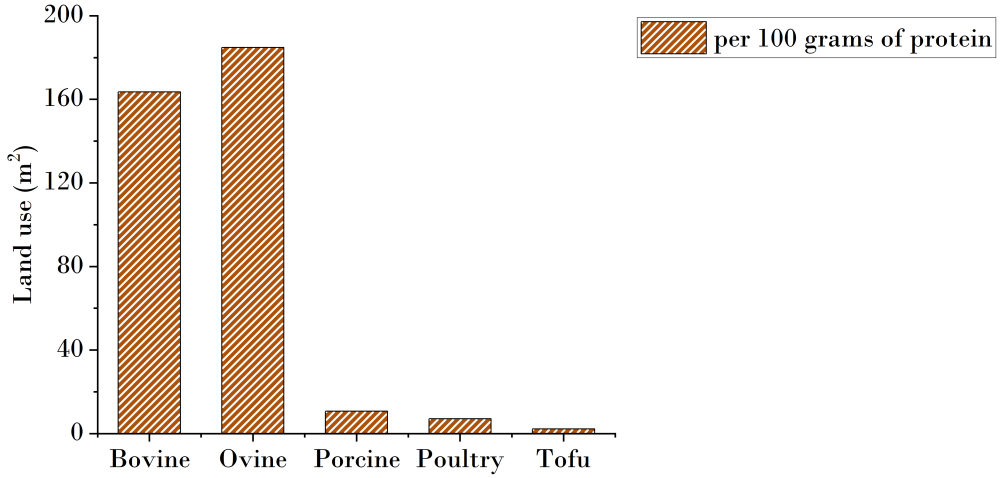


Figure 1.3.: Land use measured in meters squared per 100 grams of proteins for meat and tofu. Data retrieved from [11].

## 1.2. Animal welfare

Figure 1.3 presents that the land use of porcine and poultry per 100 grams of protein is rather low. From this graph, it can be concluded that porcine and poultry meat is very efficient to produce. To produce the meat at this level of efficiency, the animals are farmed in cramped spaces. For example, the maximum allowed amount of chickens per square meter was 21 in The Netherlands in 2020 [17]. This comes down to 0.05 square meter per chicken on average. A higher level of efficiency is inherent to a lower level of animal welfare: efficiency improves when animals move less, are bred to grow faster, and are slaughtered younger [9]. Regulations are applied to the treatment of farmed animals during farming and slaughtering, but the attempt of legislated regulation is constantly violated by the urge of maximising profit, condoned by the under-regulation of the animal industry [18], as confirmed by an investigation of slaughterhouses in The Netherlands in 2019 [19]. Annually, 70 billion animals are slaughtered for global meat consumption [13]. That means that 2500 animals are slaughtered every second. As only a miniscule fraction of these animals are fortunate enough to graze outside, most animals are born and raised in cramped spaces indoors without access to sunlight or fresh air [18]. In 2017, only 2.9% of livestock in The Netherlands was raised on organic farms [20] and it is estimated that 99% of livestock in the US lived on factory farms and was not allowed to go outside [21]. It is shown that farmed animals experience stress due to confinement, because of e.g. lack of space, artificial lighting, loud sounds, arousing odors, and uncomfortable temperatures [22]. The animals are bred to grow as fast as possible, inducing skeletal, respiratory, and cardiovascular diseases [23, 24, 25, 26]. Additionally, most animals suffer injuries during their journey to the slaughterhouse [27]. Once in the slaughterhouse, the animals do not experience a painless death [18]. Some slaughterhouses use electrical stunning, as it is intended to be less painful than the traditional throat cutting [28]. However, improper handling makes the stunning ineffective and thereby increases animal suffering, and studies indicate that improper stunning occurs frequently [29]. Although legally not allowed, it is common practise that animals are still conscious and breathing as they face their killing [30]. It is confirmed that the sector is under-regulated and that rules are breached [19]. Hence, in addition to the environmental factors that the meat industry imposes on the Earth, the animal cruelty is surprisingly higher than the public is made aware of.

## 1.3. Public health and safety

The meat industry also causes medical problems. Subject of discussion is the use of antimicrobials; a comprehensive term for antibacterials, antifungals, antivirals, and antiparasitics. 80% of the globally available antimicrobials is used for animal agriculture, to suppress health issues of the animals and maintain efficiency of the production line [31]. However, human consumption of food carrying antimicrobial-resistant bacteria contributes to the development of antibiotic resistance [31, 32, 33, 34, 35]. Therefore, utilising these antimicrobials causes a threat to public human health, and the use of these in animal agriculture is a subject for debate [23, 31].

Medical problems that are less publicly discussed and understood are the mental health problems suffered by slaughterhouse workers. For instance, 4.4% of US slaughterhouse workers suffer from serious psychological distress, describing symptoms of post-traumatic stress disorder (PTSD) [18, 36, 37]. The employment situation of slaughterhouse work is comparable to conventional environments where development of PTSD is common; large scale violence and deaths of hundreds of beings every day, during which brutal handling, skinning and boiling of conscious individuals are common, in a cold, bloody, and smelly environment [18, 36]. The symptoms of PTSD are e.g. expressed as recurring dreams regarding the violent acts, heightened emotive responses, personality changes, and engaging in destructive coping tactics. A study conducted to a poultry plant in North Carolina, United States, by Lipscomb *et al.* in 2007 concluded that the prevalence of depressive symptoms was 80% higher among poultry workers than among people working other occupations in the same geographic area [38].

An elaborate study of Fitzgerald *et al.* in 2009 concluded that crime rates increased significantly in communities where large slaughterhouses were located [39]. A comparative study was performed with the industries of iron and steel forging, truck trailer manufacturing, motor vehicle metal stamping, sign manufacturing, and industrial laundering. It was also confirmed that the increase could not be explained by unemployment, social disorganisation, or demographic variables. The study presented correlations between an increase in slaughterhouse employment and increases in rape arrests and other sex offences. Victims of such offences were mostly of vulnerable groups. For example, child abuse in towns with slaughterhouses was 50% higher than the state average. Fitzgerald *et al.* interpreted this to be evidence that the slaughterhouse work might spillover to violence against vulnerable groups, such as women and children, due to the lowered ability to emphathise. No increase in sexual assaults was observed in analyses of comparative industries. However, more studies should be performed to determine the exact relationship between slaughterhouse work and psychological trauma.

## 1.4. Cultured meat

As previously elaborated on, the meat industry affects the planet and its inhabitants in multiple ways. Although the nutritional needs of humans can be satisfied with a meat-free or plant-based diet [40, 41, 42, 43, 44], only 8% of the world population followed a vegetarian or vegan diet in 2018 [45]. In 2019, the United Nations published a report in which they urged the world population to consume less meat [46]. Unfortunately, the small growth in the vegetarian and vegan population is not sufficient to compensate for the current meat-consuming population. It is expected that the total world population will increase from the currently 7.7 billion people to 9.7 billion people in 2050 [47]. A correlation is seen between an increase in wealth and an increase in meat consumption, and as developing countries are becoming more wealthy it is expected that the global meat consumption will increase by up to 70% in the coming decennia [13, 48]. Therefore, alternatives have to be explored, and scientists in the tissue engineering field are developing a suitable alternative: cultured meat.

Cultured meat aims to replicate the appearance, texture, and flavour of conventionally produced meat through tissue engineering techniques [49, 50]. The technology is derived from regenerative medicine, where the goal is to restore disfunctional organs by functional *in vitro*-grown tissue [51]. Cultured meat is made by isolating stem cells from an animal, expanding the cells by proliferation, and differentiating them into muscle and fat tissue. See figure 1.4 for a visualization of the current process. The first step is to harvest the cells, for example by taking a muscle or fat biopsy. The cells can be isolated from the tissue biopsy by enzymatic or explant isolation, followed by cell identification and separation to obtain a pure population. Subsequently, the number of cells is exponentially increased by proliferation. The cells are then introduced to a 3D environment, where they differentiate into muscle fibres or fat. The tissue constructs are assembled and the result is hamburger patty. Under the right conditions, primary cells isolated from a biopsy could expand in up to 50 population doublings in a timeframe of 7-8 weeks [51]. Around 10,000 cells can be isolated from a 0.5 gram biopsy, according to Post *et al.* [50], which could grow into $11 * 10^{18}$ cells in 8 weeks under the right conditions. In 2013, cultured meat company Mosa Meat presented a cultured meat hamburger as a proof-of-concept [51]. This hamburger was 85 grams in weight and $1.5 * 10^{10}$ cells were used to produce it. Using this information as a reference, it should be theoretically possible to grow 10,000 cells of one biopsy into 63.8 million kilograms of meat. It should be noted that this is under perfect theoretical circumstances. The global meat production in 2018 was 340 billion kilograms [13]. Assuming the theoretical amount of 63.8 million kilograms of meat resulting from one biopsy, the demand of 2018 could have been met with 5329 biopsies of 0.5 gram developed under perfect conditions.

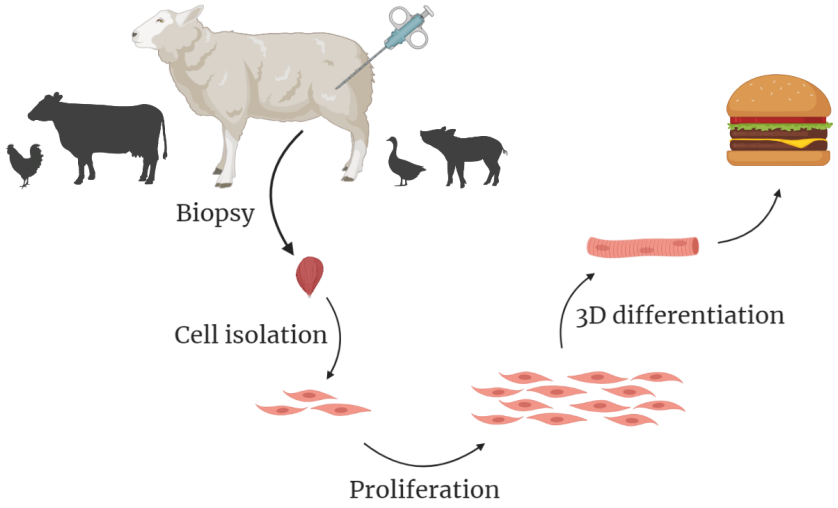


Figure 1.4.: Visualization of the current production process of cultured meat. First, a tissue biopsy is obtained from an animal. Cells are isolated from the tissue and expanded by proliferation. The cells are introduced to a 3D environment where they differentiate into muscle fibres or fat tissue. When mature differentiation is achieved, the cells are assembled into a meat-like structure, like a hamburger patty.

As cultured meat is still under development, it is not yet possible to guarantee that all problems imposed by the meat industry will be solved by this alternative product. The benefits for climate change need more elaboration and will be discussed in the next section. Animal welfare, however, will be undoubtedly higher than in the conventional meat industry, which solves the problem of high animal cruelty. The goal is to produce cultured meat with less to none antibiotics and hormones than conventional meat. As antibiotics are commonly used for cell culture and tissue engineering, it will be a challenge to exclude antibiotics fully from the

cultured meat process. The production process has to be very well controlled and extraordinarily sterile. Cultured meat companies are aiming for excluding or drastically reducing the amount of antibiotics used, which is currently under research [48]. Medical health problems are not expected to be comparable to those in conventional meat production, as the working environment is not expected to be PTSD inducing, and by virtue of that the public safety is expected to increase. It can be argued that the previously mentioned problems are, partly, resolved.

Multiple life cycle assessment (LCA) studies of cultured meat are performed over the years to determine the impact on climate change [52, 53, 54, 55]. Recently, an LCA was published based on primary data from multiple cultured meat companies and from associated companies in the cultured meat supply chain [55]. This is the most recent and therefore expected to be the most probable LCA of future cultured meat production, and will therefore be discussed. The LCA reported on the expected environmental impact of a ground-meat product, cultured at 37 °C, produced in a future commercial-scale facility in 2030. This scenario was compared to an ambitious benchmark for conventional meat products in 2030, to produce conclusions as robust as possible. The LCA concluded that cultured meat will be able to compete with all conventional meat regarding greenhouse gas emmisions and all round environmental impact, and that it scores much better than conventional bovine meat. If more than 30% of energy use for production of cultured meat is sourced sustainably, it is the most environmental friendly option for meat production of any species. Components of the cultured meat production process that have a large impact on the sustainability are medium quantity, medium composition, and processing energy. All these aspect are energy related, as the production of medium components requires a lot of energy, and can be improved by switching to sustainable energy. In terms of land use, cultured meat will have a significantly lower footprint than conventional meat products and a comparable footprint to tofu. Regarding water use, cultured meat will be comparable to poultry [3, 55]. The previously mentioned LCAs presented comparable conclusions [52, 53, 54]. Note that cultured meat is presented as a sustainable alternative for meat, however it does not approach vegetable derived protein in level of sustainability [13, 55, 56].

### 1.4.1. Consumer acceptance

The first cultured meat hamburger was presented as a proof-of-concept at a public tasting in 2013 [48, 51, 57, 58]. The event introduced the concept of cultured meat to the public and gained a lot of media attention. Since then, newspapers have been covering the concept in both a positive and negative manner [57]. If cultured meat becomes commercially available, it is of uttermost importance to make sure that the product is accepted by the public. Studies show that nomenclature influences the consumer acceptance, as well as the level of information provided about the product [59, 60]. A public survey among 15,000 participants of the Dutch population conducted in 2013, asked if the participants would buy '*in vitro*' meat if it would be available in the local supermarket [61]. 29% of the participants answered 'yes, probably', and 23% answered 'certainly'. Additionally, a study conducted in 2020 indicated that perceived benefits of cultured meat could result in a willingness to pay a higher price for the product in 36% of the participants - when information on the benefits of cultured meat was provided [59]. When the content of information is framed positively, the tasting experiences are favourable, and the benefits are clearly marketed, consumer acceptance of cultured meat is potentially high. Naturally, the general consensus is that positive marketing and low price will provide the highest chance of consumer acceptance.

### 1.4.2. Scaling up and costs

In order to get cultured meat available at a competitive price, it is essential to scale up cultured meat production. Scaling up can be achieved by culturing the cells in large bioreactors, as they provide scalability and controllability [50]. The goal of the bioreactor would be to increase the medium conversion ratio, in other words the ratio between the percentage of medium nutrients converted to edible animal tissue - the equivalent of feed conversion in conventional meat production. Most mammalian cells are adherent cells, and it is therefore essential to maximise the surface area in the bioreactors [62]. Stirred tank bioreactors are the standard for mammalian cells, in which surface area can be increased by microcarriers in suspension [50]. These microcarriers should be approved for food regulations, while also offering suitable structure and surface chemistry to the cells. Ongoing research is exploring several options: non-edible, non-degradable microcarriers; non-edible, degradable microcarriers; or edible microcarriers embedded in the final product [62]. Non-edible and non-degradable microcarriers seem unfeasible, as a dissociation and separation step would be required to remove the microcarriers of the final product, which would be challenging. Degradable or edible microcarriers seem more feasible, as they can be degraded prior to or included in assembly of the final product. Another interesting point of research is to use microcarriers as controllable-releasers of nutrients.

A recent techno-economic assessment (TEA) presented an estimation of cultured meat production costs in a full-scale, industrial installation in 2030 [63]. The TEA is based on primary data from multiple cultured meat companies and from associated companies in the cultured meat supply chain, and it was modelled for a ground-meat product, cultured at 37 °C, produced in a future commercial-scale facility in 2030 (this research is connected to the LCA described previously [55]). The TEA concluded that the current cultured meat production costs are at least 100 times higher than benchmark values for comparable conventional meat products. In the current situation, with average amount and price of culture medium, the production costs are $1707 per kilogram. Culture medium is concluded to be the main driver of costs. However, the TEA also presented different future scenarios that can substantially reduce costs and are expected to be feasible. See table 1.1 for an overview of the scenarios. The scenarios are organized by expected feasibility, starting with the highest feasibility at the top. Each scenario reduces the product price per kilogram, and the resulting product price per kilogram is given in the right column.

Ultimately, a price of $5.66 per kilogram could be achieved. The market costs for comparable conventional meat products are around $2 per kilogram, so the difference is still significant. In order to get the price further down, cultured meat companies could apply for subsidy. To provide a specific example: the Europian Union provides funding opportunities solely for promotion of agricultural products, like for example €17.5 million for meat promotion in multiple countries in 2017 [64] and €1.85 million for Dutch beef promotion in South-Korea and China in 2020 [65]. If cellular agriculture products are considered for certain subsidies, cultured meat companies could propose to get subsidy for promotion of their products by lowering of the selling price.

### 1.4.3. Cell sources for cultured meat

Cells sourced from bovine [63, 66, 67], porcine [68], and avian [63] are of greatest interest at presence. Cultured meat companies are also expressing an interest in ovine. Studies have reported on the promising skeletal muscle regenerative potential of satellite cells isolated from ovine, making this an interesting cell source [69, 70]. Rodriguez *et al.* compared the two posterior limb muscles *m. soleus* and *m. semimembranosus* to the two facial muscles *m. zygomaticus major* and *m. masseter*, as primary ovine cell sources for 3D tissue engineered skeletal muscle structures [69]. The study concluded that the *m. semimembranosus* is the

| Additional scenario | Explanation | $/kg |
|---|---|---|
| Low-medium usage with low current medium prices | This can be the current scenario if focus is on efficient use of medium and low prices for individual ingredients. | 149 |
| Lower prices for growth factors | It is assessed that lower production prices of growth factors will be feasible in 2030. | 116 |
| Lower costs for recombinant proteins | Recombinant proteins account for 80% of medium costs. Reduction of recombinant protein usage and lower production prices are expected to be feasible and would significantly lower the costs. | 17 |
| Social investment criteria | Commercial payback time of investments is around 4 years. If payback time is stretched to 30 years, this would reduce capital expenditures. This could be feasible due to social motives of investors. | 8 |
| Higher cell density | More cells in a bioreactor of the same volume would reduce equipment and energy use. The baseline cell density is modelled at $50*10^6$ cells/ml, which could be increased to $200*10^6$ cells/ml. | 6.52 |
| Shorter production time | It is estimated that production run time could be reduced by 25%. | 5.74 |
| Larger cell volume | At constant cell density and larger cell volume, a decrease in energy, medium, and equipment demand is expected. | 5.66 |

Table 1.1.: Overview of future cost reduction scenarios and the resulting price in dollars for one kilogram of cultured meat [63]. The scenarios are organized by expected feasibility, starting with the highest feasibility at the top, and each scenario is an addition to the scenario mentioned prior.

muscle that is best suited as a cell source for muscle-derived cells, based on its proliferative capacity, differentiative capacity, and depth of invasion when taking a biopsy. However, not much research to the cellular properties of ovine is published yet. As presented in figure 1.1, 1.2, and 1.3, conventional ovine meat is high in GHG emissions, freshwater withdrawal, and land use, showing the importance of finding a suitable alternative for conventional ovine meat. The research presented in this thesis is carried out in New Zealand, known for its high-quality lamb. The global export of lamb in January 2020 alone was worth US$291 million, testament to the global popularity of this source [71]. Cultured ovine meat is therefore likely to be of large commercial interest.

## 1.5. Research question

The goal of this research project is to determine the potential of ovine to function as a cell source for cultured meat applications. The results of this research will lay the groundwork for future cultured meat development with a focus on ovine. The research is performed in New Zealand, and therefore the cells will be isolated from a New Zealand ovine. Differences between cells from ovines in New Zealand and from other countries will not be investigated. However, it is assumed that the cells will be similar enough for the results of this research to be applicable to ovines elsewhere in the world. To be suitable for cultured meat applications, the cells should proliferate at an appropriate rate, be able to form myotubes during differentiation, and form a muscle fibre when introduced to a 3D environment. As there is no research published on requirements for

cells to be used for cultured meat, performance of the ovine cells will be compared to bovine and ovine satellite cells provided by Mosa Meat, and C2C12 cells. The bovine satellite cells are currently used by Mosa Meat for cultured meat research and development, which makes these cells perfect for control experiments. The ovine satellite cells of Mosa Meat are purified by fluorescent activated cell sorting, which makes them interesting as a pure satellite cell control population of the same species. C2C12s are robust cells that are commonly used for skeletal muscle tissue engineering, which makes them useful as a control group and for setting up a working 3D model. The scope of this research will be on skeletal muscle tissue engineering and the ability of the ovine cells to be integrated in a working 3D model. The isolated cells will be assessed in terms of their proliferation rate in 2D and the differentiation capability in 3D, as these are most crucial in commercialisation of cultured meat. Although fat is an important aspect in flavour design, as will be described in section 2.1, fat tissue will not be studied. Consumer acceptance will not be studied either.

# 2 Theory

When imitating conventional meat, it is important to achieve a high level of similarity in flavour, appearance, and texture - if not a perfect replicate. Flavour is influenced by smell, taste, mouthfeel, and vision [72, 73, 74]. This chapter outlines the aspects of conventional meat that are important to mimic with cultured meat for consumer acceptance. Furthermore, this chapter lays the theoretical groundwork for the practical research described in chapter 3 and 4.

## 2.1. Flavour

The characteristic flavour of meat is mainly formed by vitamin degradation, the Maillard reaction, and lipid degradation, which are thermally induced reactions and are dependent on cooking temperature, cooking time, and animal species [75, 76]. Vitamin degradation forms certain flavour precursors, that contribute to the characteristic meat flavour [75]. For example, thermal degradation of vitamine B1 produces sulfur compounds, of which the smell contributes to cooked meat aroma [75, 76]. The Maillard reaction creates the brown-coloured surface layer on cooked food, and is responsible for most of the aroma compounds [75]. It is initiated by condensation of amino groups on reducing sugars, and eventually forms malenoidins, which cause browning [77]. Lipid degradation results in volatile compounds responsible for the fatty aromas [76]. Although the volatile compounds derived from the Maillard reaction play an important role in the flavour of meat, research showed that volatile compounds resulting from lipid degradation are most important for meat palatability (i.e. hedonic reward, pleasure) [75]. It was concluded that an increase of intramuscular fat content was correlated with an increase in preference of US consumers. The minimum level of US consumer acceptance was at 3% of intramuscular fat content, to describe a slightly intense fat flavour and mouthfeel. Moreover, it was stated that a clear distinct in taste was perceptable between fatty and lean pieces of meat: fatty meat provides a taste specific for species, while lean meat only provides a basic meat flavour [76]. It is noteworthy that bovine and ovine have lower intramuscular fat content than porcine and poultry, and that lipid degradation products distinguish characteristic flavours of the different species [76]. This shows that the amount of fat in a meat product plays a large role in the all round flavour experience, making it of high importance to closely mimic this in cultured meat products. In conventional meat, aspects like animal breed, sex, age, feed, and cooking and aging conditions play a role in flavour development as well [75]. It is not yet published how certain aspects can be included in the production process of cultured meat.

## 2.2. Appearance

As customers are not able to judge the odor or texture of meat without opening a package, the colour of meat is the most important factor influencing purchase decisions [78]. A fresh cut of meat has a bright, cherry-red colour, but meat discolouration is inevitable during storage and retail. Myoglobin is the heme protein primarily responsible for the colour of meat. In packaged meat, myoglobin exists in four redox states. Three of these are in ferrous state and are red in colour, but when these oxidize they form metmyoglobin, which is brown in colour and responsible for discolouration [78]. Discolouration is prevented by the use of certain packaging

conditions or antioxidants. Pre-packed meat products are enclosed in gas-barrier materials of which the gaseous composition is altered. One of the used conditions is high oxygen (80% $O_2$ and 20% $CO_2$). The $O_2$ binds with the myoglobin to prevent oxidation and retain the desirable colour. It is suggested that hypoxia influences the regulation of myoglobin transcription in skeletal muscle [79]. This could be applied during the cultured meat production process, during incubation. Although myoglobin is not naturally present in artificial muscle tissue, it can be derived from plant tissue and added to the cultured meat tissue [80]. Myoglobin can be used in cultured meat products to enhance the colour, and the packaging strategy can be used for cultured meat packaging likewise.

Antioxidants can improve meat colour even before slaughtering the animal [78]. Vitamin E and plant extracts rich in antioxidant compounds has been shown to increase colour stability in conventional bovine and ovine meat, when integrated in their feed. It would be interesting to investigate if this would also have an effect on the colour of cultured meat, during the production process. Furthermore, it is observed that chitosan improves surface redness of ground beef burgers [78]. This is interesting, as chitosan is commonly used in biomaterials for skeletal muscle [81, 82, 83] and fat [84] tissue engineering techniques. It would be interesting to study the effect of chitosan on cultured meat surface colour and the effect of integrating chitosan in the 3D environment: if chitosan proves to have a positive impact on both, it could for example be integrated as a scaffold in the 3D environment and therefore enhance meat colour and 3D cell behaviour simultaneously.

Another aspect contributing to the appearance of meat products, is the red aqueous solution that leaks out of meat. Consumers often expect this to be blood. However, except for small amounts of residual blood within large skeletal muscles, the majority of blood is removed during slaughter [78]. The red solution consists of water, myoglobin, and proteins leaking out of the cells [85, 86]. As this does not largely influence the taste of cultured meat, mimicking this aspect is not an urgent matter if it does not naturally occur. However, if the visual leaking of red fluid turns out to be important for the consumer experience, it can be mimicked with a plant-based dye.

## 2.3. Texture

As described in section 2.1, it is essential to incorporate fat in meat products, as it adds flavour, juiciness, and tenderness [84]. The intramuscular fat content needs to be at least 3% to provide pleasure to the consumer. Therefore, a mixture with muscle cells wherein 3% of the mixture is occupied by fat cells could be used as a guideline to mimic the palatability of conventional meat. Ideally, the fat and muscle cells would be proliferated and differentiated in the same environment. However, co-culture of these cell types poses a difficult challenge and separate culture of the cell types followed by mixed assembly in the final product seems more feasible on short-term [51]. Fat tissue can be found in the body as white and brown adipose tissue. Adipogenic stem cells can be derived from both of these tissues and they can additionally be derived from muscle tissue [51]. Transdifferentiation of satellite cells into adipogenic cells has been achieved by inhibition of Wnt signaling, high glucose exposure, and culture in adipogenic medium [84]. Transdifferentiation is interesting, as this would eliminate requiring multiple tissues biopsies for cell isolation.

While fat tissue is important for meat flavour, muscle tissue is important for meat texture. The development of meat texture is influenced by the architecture of the muscle, and the characteristic texture of meat is a result of the parallel organisation of muscle fibres in a fascicle [87]. In order to approach the texture of conventional meat, it is important to mimic the cellular

organisation of *in vivo* muscle as close as possible. Achieving a texture that mimics conventional meat is currently one of the biggest hurdles of cultured meat development. Therefore, the scope of this research is on tissue engineered muscle. In the following section fat tissue engineering will briefly be described, after which skeletal muscle tissue engineering will be elaborated on.

## 2.4. Skeletal muscle engineering

### 2.4.1. Intramuscular fat

Intramuscular fat forms when fibroblasts in the muscle differentiate into adipocytes (adipogenesis) and when triglycerides accumulate inside the adipocytes (lipogenesis), which is regulated by transcription factor Zfp423 [88]. Those triglycerides consist of glycerol and three fatty acids, and they accumulate in lipid droplets. Lipid droplets are encapsulated by a phospholipid monolayer and their size, composition, and number varies per cell [89]. In order to produce *in vitro* fat tissue in an efficient manner, it is important that the cells accumulate as many triglycerides as possible [90]. Large, unilocular adipocytes are preferred. Luckily, while cell culture in 2D mostly yields multilocular adipocytes, 3D culture has shown to produce large unilocular adipocytes [84]. Moreover, it is shown that the extent and efficiency of differentiation into adipocytes is higher when cultured in 3D than 2D. A commonly used 3D environment for culture of adipocytes is an alginate scaffold, and alginate scaffolds have shown to support 3D culture of both bovine and porcine adipocytes [84]. Alginate is used in both commercial food products as well as in molecular gastronomy for thickening, gelling, and film forming [91, 92, 93]. It is already approved for food applications by the Food and Drug Administration (FDA), and is therefore an interesting component for engineered fat tissue for cultured meat applications. However, to improve the functionality of an alginate hydrogel the alginate is often modified with RGD-peptides [94, 95], which are not yet approved by the FDA.

### 2.4.2. Skeletal muscle

Skeletal muscle is one of the three types of muscle in mammal bodies, alongside cardiac muscle and smooth muscle. Its main function is to generate force or produce movement, which is facilitated by contraction of the tissue [96]. Figure 2.1 provides a visualisation of the anatomy of a skeletal muscle. Every skeletal muscle in the body is made up of fascicles and blood vessels, bundled by the outermost connective tissue sheath known as the epimysium [97]. The epimysium covers the entire surface of the muscle, restraining it from blending with other muscles [96]. Each individual fascicle is encased by another kind of connective tissue, known as the perimysium. By dividing the muscle into fascicles, the perimysium enables the major blood vessels and nerves to run through the muscle belly without being constricted. The fascicles in turn are bundles of myofibres, surrounded by connective tissue called endomysium. Contraction is initiated within the myofibre by the proteins myosin and actin. Therefore, the myofibre is the smallest contractile unit of skeletal muscle tissue [98].

Satellite cells (SC) are progenitor cells that can grow, maintain, and repair postnatal skeletal tissue [100, 101, 102]. While SCs are naturally quiescent, they can be activated by a signal delivered from myofibres. Myofibres will send this signal in response to damage caused by exercise, injuries, or diseases [103, 102]. Figure 2.2 visualizes the formation of a myofibre. An activated SC proliferates and produces myoblasts. When myoblasts commit to differentation, they are called myocytes [104]. Myocytes can fuse with other myocytes to form myotubes, or they can fuse with existing myotubes [100, 105]. Myotubes are elongated, multinucleate cells, containing at least three nuclei and some peripherally located myofibrils [106]. Myofibrils are long, cylindrical organelles of the myotube, constituting the contractile apparatus. At some point during maturation, myotubes develop into myofibres. Myofibres have peripherally located nuclei and

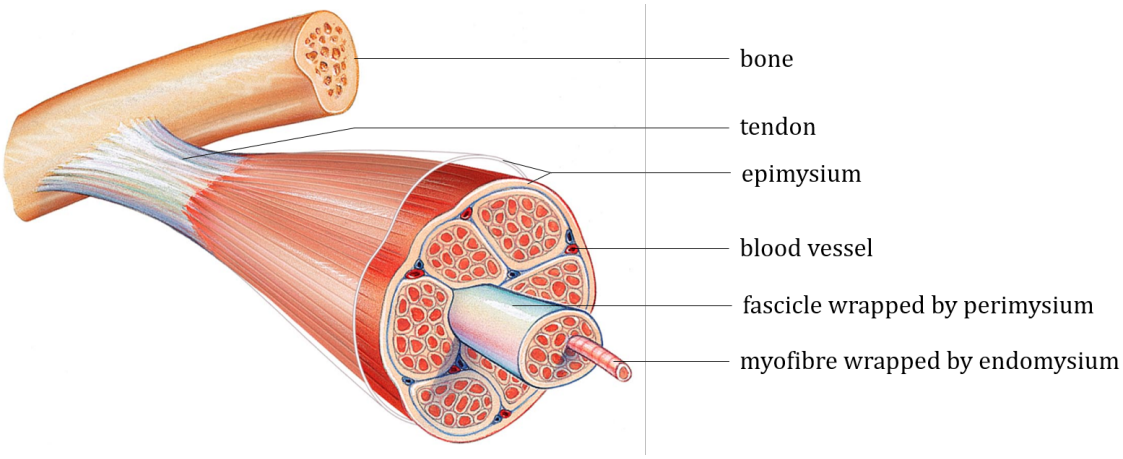


Figure 2.1.: Anatomy of a skeletal muscle. Figure retrieved from [99] and edited.

the cytoplasm is filled with myofibrils. There is no clear distinction of when a myotube develops into a myofibre [106].

### 2.4.3. Skeletal muscle markers

Figure 2.2 furthermore visualises the expression of essential muscle transcription factors during the formation of a myofibre. Essential skeletal muscle transcription factors are Pax7, Pax3, MyoD, myogenin, and myosin, among others. Pax7 is essential for the regulation of proliferation and differentiation of SCs [102]. Pax7 is expressed in all SCs, starting at the quiescent state. Most SCs, but not all, also express Pax3 [103]. Pax3 and Pax7 direct the activation signal that leads to activation of the quiescent SCs and are therefore suitable biomarkers to indicate activated SCs. When SCs are activated, MyoD is upregulated and coexpressed with Pax7 [107, 108]. In the case that cells return to the quiescent state, the expression of MyoD is downregulated. If the cells mature and initiate terminal differentiation, MyoD is retained and Pax7 is downregulated [107]. While MyoD is a master regulator of the skeletal myogenic program, some research suggests that MyoD could functionally be substituted by Myf5, and vice versa [109, 110]. Myf5 and MyoD both play an essential role in skeletal muscle development [111]. Research of Rudnicki *et al.* in 1993 presented that mice lacking both MyoD and Myf5 did not develop any skeletal muscle tissue and no skeletal muscle-specific mRNA was detected [111]. Other studies showed that skeletal muscle tissue did develop when lacking only one of Myf5 or MyoD [111, 112, 113]. However, follow-up studies reported that the skeletal muscle development was impaired when lacking one of Myf5 or MyoD [114, 115]. It is suggested that Myf5 is activated prior to MyoD, which could indicate that the transcription factors have complementary functions during myofibre development, instead of being able to substitute one another [116, 117]. Additionally, it is suggested that Myf5 directs myoblast proliferation, and MyoD prepares myoblasts for differentiation [118]. Another suggestion is that either Myf5 alone or MyoD alone is expressed after activation of the satellite cell, before coexpressing with the other to proceed myogenic development [114]. It can be concluded that there is no clear consensus on the exact difference between Myf5 and MyoD [108]. Moreover, it is noteworthy that all studies presented here focusing on Myf5 and MyoD, are performed by the same research group. Despite the uncertainty between the exact functions of Myf5 and MyoD, MyoD has proven to be a reliable biomarker for myoblasts with the intention of differentiation [119].

Another essential transcription factor is myogenin. Myogenin is required for early differentiation of committed muscle progenitor cells into myofibres [108, 120, 121]. Expression of myogenin

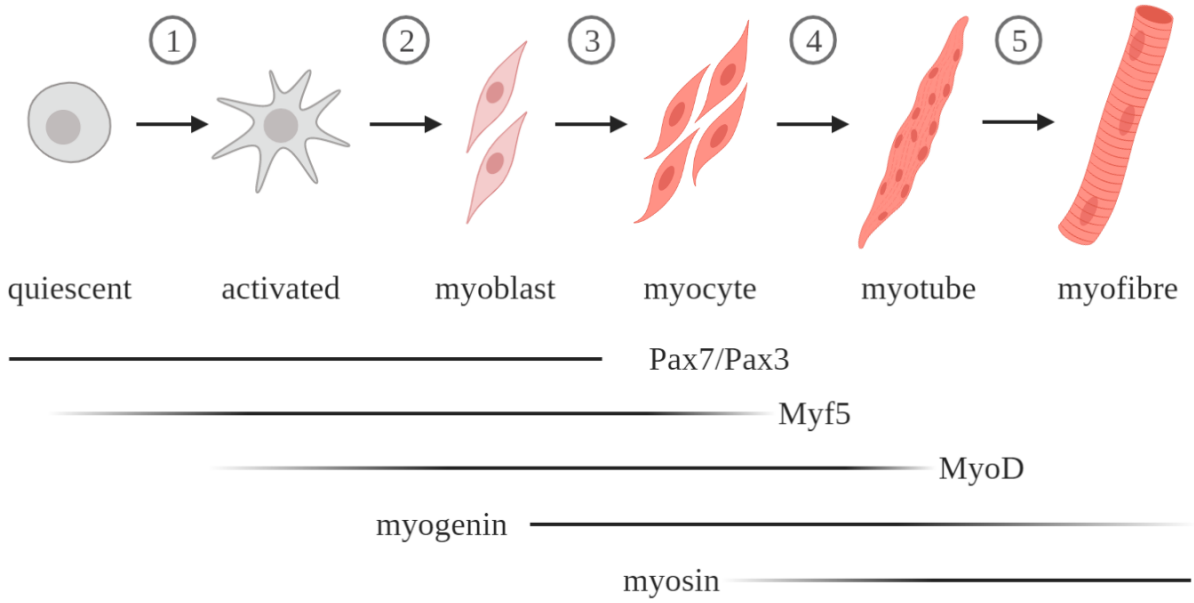


Figure 2.2.: Formation of a myofibre, including visualisation of when essential transcription factors are expressed in the process. The transcription factors with a solid line will be analysed during this research. Transition steps are numbered: (1) activation, (2) proliferation, (3) differentiation, (4) fusion, (5) maturation. Figure based on [100] and edited.

directly induces terminal myoblast differentiation and fusion into myofibres [103, 122]. It also regulates myofibre size, making it essential for muscle regeneration. A study of Ganassi *et al.* in 2018 presented the crucial importance of myogenin for the formation of multi-nucleated myofibers, when the study showed that almost no multi-nucleated myofibers were formed in mice in which myogenin was mutated [122]. Myogenin is therefore an excellent marker to stain for terminal myoblast differentiation. Another marker that is expressed in terminally differentiated muscle cells is myosin heavy chain MYH1 [123]. Myosin heavy chain MYH1 is part of the myosin family, which comprises around half of the total protein in skeletal muscles and is important for muscular contraction [124, 125]. Myosin heavy chain MYH1 (hereafter referred to as just 'myosin') is expressed in myotubes and is therefore an appropriate marker to indicate full maturation of the cells [126, 127].

In conclusion, Pax3, Pax7, MyoD, myogenin, and myosin are suitable markers to monitor myogenesis. These markers indicate at what point of differentiation the cells are. Wu *et al.* specifically confirmed that Pax7, MyoD, and myogenin are suitable markers for ovine SCs. Cancellara *et al.* confirmed the expression of myosin in ovine skeletal muscle tissue [128]. The markers will be used during the research presented here to gain knowledge about the cells properties. Pax3, Pax7, MyoD, and myogenin are expressed in the nuclei, myosin is expressed in the cytoplasm of myotubes.

## 2.5. State of the art

The concept of cultured meat is to create *in vitro* skeletal muscle tissue for consumption. Although the current process is based on assembling many muscle fibres into a hamburger patty, the ultimate goal is to create large, steak-like structures. The biggest challenge is not cultured meat specific but known by the whole tissue engineering industry: to create a large construct without formation of a necrotic core. Necrotic cores occur when oxygen and nutrients can not

diffuse to the center of the construct, while metabolites can not diffuse out of the center and accumulate to toxic levels. The current limitations require a cell to be within 200 $\mu$m of a nutrient source to remain viable, resulting in a maximum tissue thickness of 400 $\mu$m [129]. However, before tackling this major challenge, smaller hurdles need to be overcome. A main hurdle in the cultured meat field is to create a 3D construct with the isolated animal cells and to achieve full differentiation into a myofibre. Luckily, a large amount of research has been published in the field of regenerative tissue engineering for skeletal muscle, which can be applied to cultured meat research. This section provides an overview of interesting techniques for creating skeletal muscle tissue with mammalian cells.

*In vivo* skeletal muscle consists of highly aligned multinucleated myofibres and it experiences tension. When designing an *in vitro* tissue engineering model for skeletal muscle, it must support alignment and differentiation of the cells, while also supporting tension or contractile force generation in the tissue. To achieve this, the *in vivo* extracellular matrix (ECM) of the cells needs to be mimicked. One approach to achieve this is by seeding the cells in a hydrogel to provide the cells with a 3D environment. To create the tension that is experienced by skeletal muscles *in vivo*, cell-laden hydrogels are often seeded around at least one pillar to provide the cells with an anchor point [61, 130, 131]. See figure 2.3a for a visualisation. A study of Li *et al.* presented formation of rings consisting of C2C12 cells around a PDMS pillar, resulting in spontaneous muscle twitching [131]. The hydrogel was based on collagen type 1 and Matrigel, both at a final concentration of 2 mg/ml, and the cells were seeded at a seeding density of $2.5 * 10^6$ cells/ml. The one-pillar system creates circular tension and was also used by Post *et al.* for the production of the proof-of-concept hamburger of Mosa Meat in 2013 [61]. No recent papers are published on how Mosa Meat is currently producing muscle fibres, but a patent published in 2019 suggests that their current protocol is likewise based on hydrogel casting around one pillar [132]. PDMS is often used as material for the pillars, as it is bio-compatible, transparent, gas permeable, suited for autoclaving, and reusable[133].

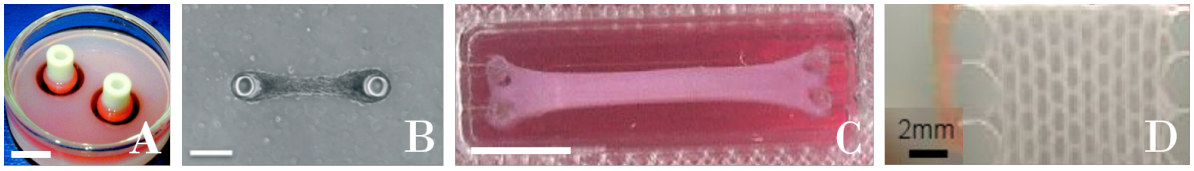


Figure 2.3.: Pillar systems described in literature. Cell-laden hydrogels seeded in a (A) one-pillar system [130]; (B) two-pillar system [134]; (C) four-pillar system [133]. (D) Tissue grown in a pillar array system [135]. The white network is the tissue containing wholes for where the pillars were located. Scalebars: (A) 10 mm; (B) 150 $\mu$m; (C) 5 mm; (D) 2 mm.

Another approach is seeding the cells in a hydrogel around two pillars [134, 136, 137, 138, 139]. The use of two pillars supports the formation of uniaxially aligned cylindrical tissue constructs, mimicking the *in vivo* structure of skeletal muscle. Agrawal *et al.* seeded C2C12s in a hydrogel of gelatin methacrylate (which is collagen derived) and reported that intact, aligned muscle strips formed around the two PDMS pillars, which is visualised in figure 2.3b [134]. A study of Capel *et al.* integrated two more pillars, resulting in a system in which the cell-laden hydrogel was seeded around four pillars, see figure 2.3c [133]. In this study, the pillars were made by 3D printing of polylactic acid (PLA) and C2C12 cells were seeded at a seeding density of $4 * 10^6$ cells/ml in both a collagen-based hydrogel as well as a collagen/Matrigel-based hydrogel. The collagen-Matrigel constructs showed three times as many myotubes per 100 $\mu$m when compared to the collagen constructs. Constructs were formed in volume sizes ranging from 25-500 $\mu$l

construct volumes and cross-striations were clearly visualised by expression of actin after 14 days in culture.

As pillars have proven to provide suitable anchor points to the cells, Bian *et al.* designed a PDMS system containing an array of pillars [135]. C2C12s were seeded in a hydrogel consisting of different ratios of fibrinogen and collagen, and 10% of Matrigel. The cells were seeded at a seeding density of $5 * 10^6$ cells/ml. The gels compacted properly and expressed myogenin, showed abundant cross-striations, and generated spontaneous tissue contractions. It is noteworthy that the gels consisting of collagen and Matrigel ruptured on day 3-4 of differentiation, while gels including fibrinogen ruptured on day 10-11 of differentiation. See figure 2.3d for a picture of the tissue grown in the system. The previously described examples of pillar systems published in literature present benefits: the systems are variable in size, distance, and material, they are easy to manufacture and clean, and they are often reusable. These systems are suitable for research and development. However, upscaling of these systems seems less practical.

Another approach of providing the cells with anchor points is by seeding them in an existing scaffold. Research of Ben-Arye *et al.* used textured soy protein (TSP) scaffolds seeded with bovine cells [66]. TSP is a by-product of soybean oil production and used as a plant-based meat replacer. It is dry, porous, and high in protein, and it expands and turns soft when soaked in liquid. Micro-CT scans showed that the pores of the scaffold are highly interconnected and that they show pore directionality, proving it is suitable for cell adhesion, growth, spread, and differentiation. See figure 2.4 for a confocal image of the pore structure. The cells were seeded in a hydrogel consisting of a 1:1 ratio of fibrinogen and thrombin, at several seeding densities, ranging from $5.4 * 10^7$ to $10.7 * 10^7$ cells/ml. Cell were seeded in monoculture with bovine SCs, co-culture with bovine smooth muscle cells (BSMC), and a tri-culture with addition of bovine endothelial cells (BEC). All cell cultures adhered to the TSP scaffold and differentiated into myotubes. The co-culture and tri-culture improved ECM deposition and myogenic differentiation. This was concluded after the TSP scaffold partially degraded during culture, and the scaffolds seeded with co-culture and tri-culture maintained their mechanical properties. See figure 2.4 for a picture of TSP scaffold seeded with the co-culture (at unknown days of culture). It is noteworthy that before cell seeding, the bovine SCs were grown in proliferation medium supplemented with various growth factors. This supports cell functioning and might make comparison with studies that did not supplement with growth factors less reliable. The isolated SC sample was pre-plated to purify the SC population, but it is not reported if the cells in the sample were identified and separated. Therefore, the population referred to as SCs could be a heteregenous population including other cell types like fibroblasts. The BSMCs and BECs were commercially obtained and are expected to be homogenous.

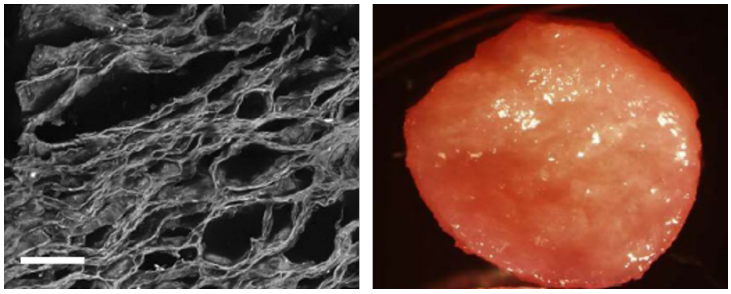

Figure 2.4.: Confocal image of the TSP scaffold pores of Ben-Arye *et al.*, scalebar 500 $\mu$m (left) and picture of a 6-mm cylinder TSP scaffold seeded with a co-culture of bovine satellite cells and smooth muscle cells (right) [66].

To enhance oxygen, nutrients, and metabolites transport, the possibilities of decellularising

plant tissue are being explored [129]. Research of Gershlak *et al.* showed that mammalian tissue and plant tissue are highly similar in their vascular network regarding their branching pattern, as depicted in figure 2.5a and 2.5b [140, 141]. Due to this similarity, decellularisation of plant tissue provides us with a prevascularised scaffold. Gershlak *et al.* and Jansen *et al.* presented successful decellularisation of leafs of several plant species, providing different scaffolding geometries [140, 142]. Dikici *et al.* decellularised a spinach leaf in 7 days until the leaf was colourless and translucent [143]. The DNA content of the decellularised leaf was measured and it was showed that 98% of the DNA content was removed when compared to the DNA content of a fresh spinach leaf. The vascular network was perfused with a blue dye, which visualised a mostly intact network with a minor leakage and ability of the food dye to reach the small branch points, see figure 2.5c. This indicates that the vascular network was mostly maintained after decellularisation. The surface of the decellularised leaf was subsequently seeded with human dermal fibroblasts that became fully confluent on culture day 11. Human dermal microvascular endothelial cells were seeded on the inside of the vascular channels, but did not penetrate into the smaller branches and were mostly found along the main channel of the leaf.

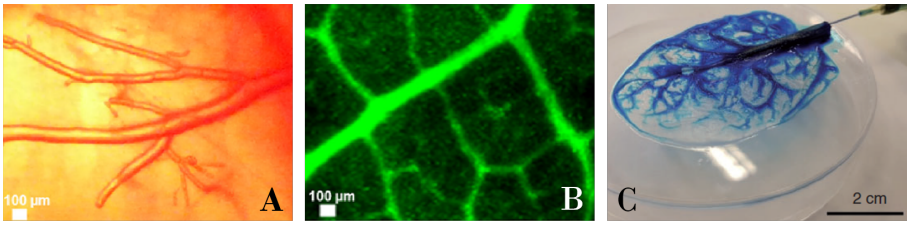


Figure 2.5.: Branched vascular networks in decellularised tissue. (A) Branched vascular network of decellularised tissue of a rat heart, showing similarities with (B) the branched vascular network of decellularised tissue of a *Buddleja davidii* leaf [140]. (C) A decellularised spinach leaf of Dikici *et al.* perfused with blue food dye to demonstrate the maintained vascular network [143].

Motivated by the results of Gershlak *et al.*, Jones *et al.* studied the potential of decellularized spinach as an edible scaffold for cultured meat applications [129]. The spinach leaves were decellularized by submergence in deionized water supplemented with 1% sodium dodecyl sulfate (SDS) for 5 days, refreshing the solution daily, followed by 48 hours in deionized water supplemented with 0.1% Triton X-100 and 10% concentrated bleach. Biopsy punches of 12 mm in diameter were used to create the scaffolds. According to the article, primary bovine cells were seeded on the scaffolds and it was confirmed that these cells can survive on spinach scaffolds for at least 14 days, with a viability of more than 98% compared to the control group cultured on gelatin. The article does not mention characterisation of the cells, but it does mention cell sorting to purify the satellite cell population as a future refinement for commercial use. This indicates that it is unknown which cell types are exactly present and in which ratio. However, after 14 days of culture on the spinach scaffolds, the cells expressed myosin, indicating that myogenic cells are present in the samples. The cells formed multinucleated myotubes and no significant difference in myosin expression was seen between the control group cultured on gelatin and the cells cultured on the spinach scaffold. The research presented by Jones *et al.* could be improved by characterisation of the cell population and by increasing the sample size (3 scaffolds were used per 3 bovines), to draw a more reliable conclusion about the significance of the results. However, these preliminary results are promising for future experiments. The vascular network of decellularised plant tissue provides a perfusable scaffold at low cost. Moreover, it is free of animal derived materials while common hydrogel components as collagen and Matrigel are not.

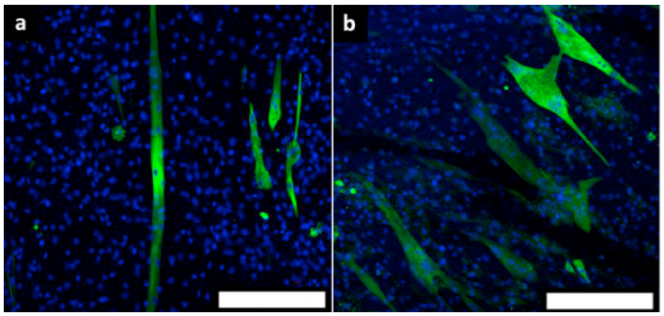


Figure 2.6.: Primary bovine cells cultured on a (a) gelatin coated substrate and (b) decellularised spinach scaffold. Multinucleated myotubes are visible in both samples. Cells are stained for myosin (green) and DAPI (blue). Scalebar: 250 $\mu$m.

Aiming to resemble a piece of steak, Furuhashi *et al.* investigated the feasibility of stacking multiple layers of cell-laden hydrogels to engineer a tissue thickness in the millimetre range [144]. Hydrogel layers seeded with bovine myoblasts and SCs were individually cultured until they contained aligned myotubes that were able to contract under influence of electrical stimulation. Subsequently, 40 layers of the cell-laden hydrogels were stacked and immobilised with 3D printed pillars as anchor points. After 7 days of culture, the layers were fused and the construct dimensions were 8 mm $*$ 10 mm $*$ 7 mm (width $*$ length $*$ height). Due to poor light transmission, analysis was difficult on the 40-layer thick structure and was instead performed on a 5-layer thick structure. The myotubes were oriented in the longitudinal direction of the tissue and no enucleated cells were observed in the center of the 5-layer construct. It is therefore suggested that this technique maintains cellular viability without a necrotic core and that this technique is interesting for future cultured meat research. It is unclear why the 40 layer construct was not divided into smaller pieces for analysis.

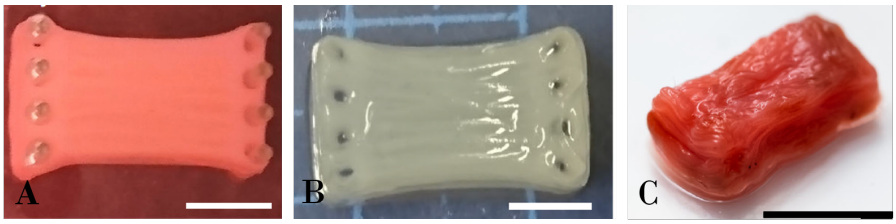


Figure 2.7.: Bovine muscle tissue created by stacking 40 layers of cell-laden hydrogels by Furuhashi *et al.*. (A) Picture of day 7 of stacked culture, scalebar: 5 mm. (B) Top view of the tissue after release of the pillars, scalebar: 5 mm. (C) The 40-layer thick bovine muscle tissue coloured using red food colouring, scalebar: 1 cm [144].

## 2.6. Developmental process

The production process of cultured meat typically includes the following steps: obtaining a tissue sample, isolating cells from the sample, identifying the cells present, expanding the cells, and introducing the cells to a 3D environment promoting differentiation, motivating the cells to fuse and grow into a muscle fibre. A similar process will be performed during the research presented here, as the goal is to determine if ovine cells are suitable for creating muscle fibres. This section provides theoretical information of the main steps that will be undertaken during this research. Figure 2.8 depicts a visualisation. In addition to cell identification, the different cell types would normally also be separated to obtain pure cell populations. However, due to COVID19-restrictions at the time of research, this was not possible.

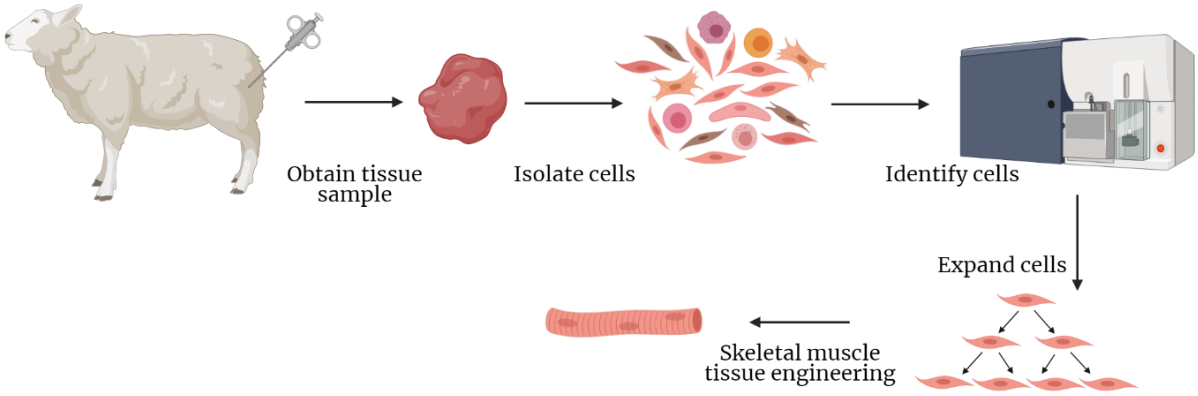


Figure 2.8.: The process of creating a muscle fibre, highlighting the main steps that are taken during the research presented here. First, a muscle biopsy is obtained from an animal, in this case an ovine. Cells are isolated from the muscle tissue and identified. The cells are then expanded and introduced to a 3D environment, where they fuse and differentiate into a muscle fibre.

### 2.6.1. Muscle tissue biopsy

The aim is to isolate SCs from ovine muscle. A study of Rodriquez *et al.* compared the hindlimb muscles *m. soleus* and *m. semimembranosus* (SM) and the facial muscles *m. zygomaticus major* and *masseter* of ovine, based on their protein expression and formation of myotubes [69]. Pax7 and MyoD were used to identify myogenic cells, and isolations of all muscles had an average myogenic cell population of 5-10%. SM derived cell populations showed the highest amount of myotubes/mm$^2$ of all muscles, with a difference of 24-32%. The study did not draw a hard conclusion, but suggested that the SM was the muscle best suited for isolation of muscle-derived cells. It should be noted that their sample size is unclear, which is important as obtaining a cell sample from a muscle is a variable process which can result in variable ratios of several cell types, like fibroblasts or other non-myogenic cell types. Another muscle that is interesting is the *m. semitendinosus* (ST), as it is commonly used as an ovine satellite cell source. Raja *et al.*, Hathaway *et al.*, and Rihan *et al.* presented successful isolation of SCs from the *m. semitendinosus* of ovine [145, 146, 147]. Therefore, the SM and ST will be used for cell isolation.

### 2.6.2. Cell identification

Cells will be isolated by enzymatic isolation and explant isolation. The isolations will result in heteregenous mixtures of several cell types. Cell types that are most likely to be present are SCs, fibroblasts, endothelial cells, and immune cells. Heterogenous samples are best identified and separated, to obtain purified populations. Fluorescent activated cell sorting (FACS) is commonly used for this purpose [148]. Antibodies used for FACS are conjugated with fluorophores at specific wavelengths and target specific surface proteins, enabling detection of multiple markers simultaneously, at the level of individual cells [149]. SCs and fibroblasts will be targeted by CD29 [67, 150], while CD56 and ITGA7 will be used to target SCs. Ding *et al.* showed that CD56 is suitable for FACS as positive selection for SCs in an enzymatic cell isolation sample of bovine [67]. Additionally, CD56 is mentioned in multiple papers as a marker for SCs [151, 152, 153, 154]. However, Castiglioni *et al.* indicate that Pax7-expressing cells coexpress CD56 and ITGA7 in fetal and adult human musle, while stipulating that these markers on their own are not sufficient to distinguish the cells [155]. Pax7 is active during both proliferation and differentiation of SCs, which raises the idea that ITGA7 and CD56 could express at different points of maturation of the SCs [102]. Other researchers also used ITGA7 as a positive marker for SCs [152, 156]. None of these studies had tested the antibodies on ovine

SCs. The uncertainty around these two antibodies, and the lack of time to properly test them on control samples during the research presented here, led to the decision to use both CD56 and ITGA7 for FACS analysis. Endothelial cells will be targeted with antibodies against CD31 [157, 158]. CD45 is a hematopoietic cell marker, and will therefore be used to identify immune cells [67, 159].

### 2.6.3. Skeletal muscle engineering

The state of the art described in section 2.5 presents several possibilities for skeletal muscle tissue engineering. The goal of the research presented here is to determine if ovine cells are suitable for cultured meat applications and to reach this goal it is essential to study the 3D properties of the cells by mimicking the *in vivo* skeletal muscle environment. As the myofibre is the smallest contractile unit of skeletal muscle tissue, as described in section 2.4.2, that is the structure to be mimicked. The four-pillar system of Capel *et al.*, described in section 2.5, is selected as model for the 3D system, considering the convenient manufacturing by 3D printing and simple adjustability of the design, making it suitable for design iterations. Moreover, monitoring the compaction of a hydrogel is easier whenseeded around multiple pillars instead of one. The four pillars will provide the anchor points for a cell-laden hydrogel based on a combination of collagen and Matrigel.

## 2.7. Hypothesis

Ovine as a satellite cell source is not extensively described in literature. However, the available literature has presented promising results for ovine cell isolation and proliferation. Meanwhile, the use of primary bovine cells has been elaborately covered, and as ovine and bovine are closely related mammalian species it is expected to see similarities in cell behaviour. When isolation of ovine cells is achieved, it is important to determine the ratio of different cell types present in the isolation samples. As cell isolation is a highly variable process, the expectations of this research are linked to the ratios of cell types present. Assuming a pure population of SCs as isolation samples, the cells are expected to proliferate at a comparable rate to bovine SCs. If fibroblasts are present in the sample, the proliferation rate might be higher due to a higher growth rate in fibroblasts than in myogenic cells, according to literature [160]. Myogenic differentiation and formation of myotubes is expected to occur in pure SC populations but also in heteregenous populations. Fibroblasts do not survive in myogenic differentiation medium, and will therefore not intervene with the myogenic development. The formation of 3D muscle fibres will be dependent on the cell type ratio of the isolated sample likewise. A 3D control model will be established with C2C12 cells. It is expected that the C2C12-laden hydrogels will compact into myosin expressing muscle fibres.

# 3 Methods and Materials

The goal of this research is to determine the potential of ovine cells for cultured meat applications. Cells will be isolated from ovine and assessed in terms of their proliferation capacity in 2D and their differentiation capacity in 3D. This chapter provides an overview of the experimental approach.

## 3.1. Cell isolation

Cell isolations were performed following the protocol of Ding *et al.* with a few alterations [67]. Ding *et al.* used collagenase type 2 for SC isolation of bovine. The study confirmed that the cells were myogenic, as they expressed Pax7 and could be induced to differentiate into myosin expressing cells by culture in myogenic differentiation medium consisting of DMEM supplemented with 2% FBS (fetal bovine serum). This protocol was followed by Mosa Meat to isolate the ovine and bovine SCs that were provided for the research presented in this thesis. A study solely focusing on ovine for SC isolation used collagenase type 1 [70]. The study confirmed that the isolated cells were myogenic cells, as they could be induced to differentiate into cells expressing myogenin and myosin, by culture in myogenic differentiation medium consisting of DMEM supplemented with 2% horse serum. The research presented here has isolated cells of two biopsies, by enzymatic and explant isolation. Enzymatic isolation of biopsy 1 was performed with collagenase type 1, while isolation of biopsy 2 was performed with collagenase type 2. The ovine cells were isolated twice from *post mortem* biopsies. Biopsies were performed at the Large Animal Unit of the University of Auckland, New Zealand.

### 3.1.1. Collagenase type 1 satellite cell isolation - biopsy 1

A biopsy was taken from a female ovine. The ovine was between 3 and 5 years old and was used as a control animal in an animal study. It had not received drug treatments, but it did undergo a thoracotomy surgery to implant probes around the heart. The ovine was euthanised with pentobarbital overdose through an intravenous line in the jugular vein. This is not expected to affect the cell population at the place of biopsy. Five minutes after euthanisation, the leg was shaved and the locations of the *m. semimembranosus* (SM) and *m. semitendinosus* (ST) were identified. The skin was cleared with 70% ethanol, and a 5 centimetre long vertical incision was made. After cutting through the skin, subcutaneous tissue, and fascia, the fascia was lifted and separated from the muscle. Fascia was pulled back by tweezers, exposing the muscle and allowing space for the biopsy. Biopsy punches of 10 mm diameter were used to obtain the muscle samples, and transferred to PBS (Gibco, 10010-023) supplemented with 1% antibiotic-antimycotic solution (A-A) (Sigma-Aldrich, A5955) on ice for one hour. The weight of the biopsies was not logged. After rinsing the muscle samples with PBS supplemented with 1% antibiotic antimycotic solution once, any traces of fat and connective tissue were removed. The muscle samples were dissected into pieces of around 3 mm $*$ 3 mm $*$ 3 mm. This procedure was performed for both the SM as the ST. See figure 3.1 for a visual overview of the cell isolation process.

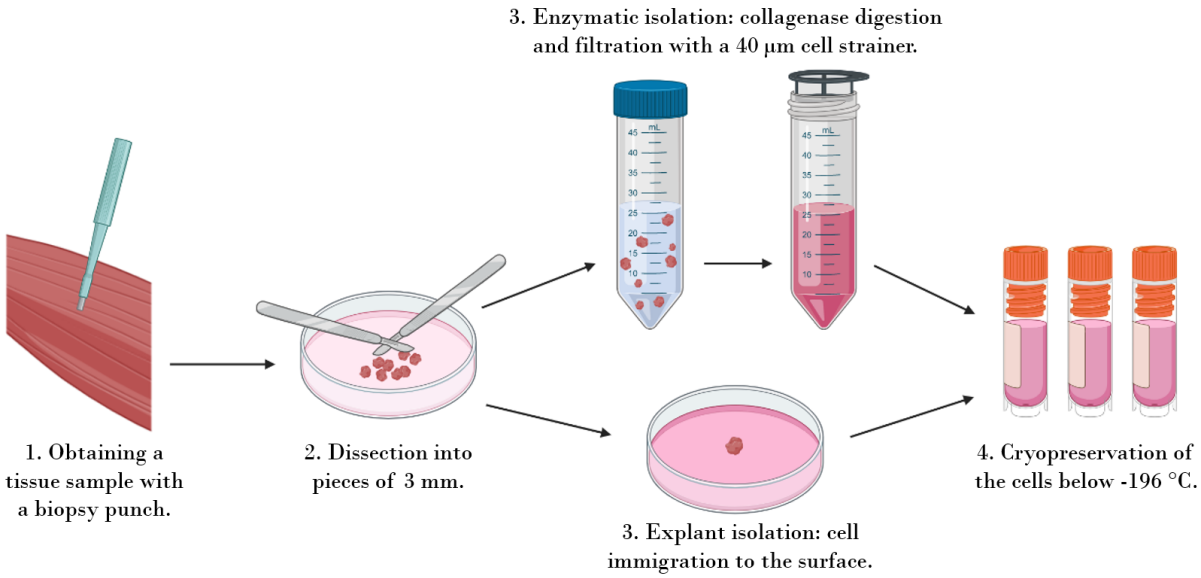


Figure 3.1.: Visualization of the main steps of the cell isolation process. The tissue samples were obtained by punch biopsies of the *m. semimembranosus* and *m. semitendinosus*. The tissues were dissected into smaller fragments of ± 3 mm, followed by enzymatic or explant isolation. For long term storage cells were preserved at below -196 °C.

**Explant isolation** was conducted by placing the dissected pieces of tissue on 35 mm tissue culture Petri dishes, one piece per dish. Three different types of Petri dishes were used: uncoated, coated with collagen coating solution (type I rat tail collagen (3447-020-01, Cultrex, Biotechne) diluted to 0.5 mg/ml in 0.02 M acetic acid), and coated with Matrigel coating solution (Matrigel (356234, Corning, Life Sciences) diluted 1:200 in phosphate buffered saline (PBS) (10010-023, Gibco). Around 1 ml of growth medium was added to the tissue, less if needed to avoid floating of the tissue. Explants were stored at 37 °C and 5% $CO_2$ for 1-3 hours, allowing attachment of the tissues to the dishes. After attachment, tissue was flooded with growth medium (Ham's F-10 (11550043, Gibco), supplemented with 20% fetal bovine serum (FBS) (10091-148, Gibco), 1% A-A, and 5 ng/ml recombinant human bFGF (13256029, Gibco) until just covered, or 5 ml maximum. Explants were checked daily for migration of cells out of the tissue. After cells were migrating out and reaching 50% confluency around the explants, cells were passaged into flasks. As no difference in migration rate, confluency, or morphology was seen between the different coatings, all cells of each muscle type were passaged into one flask. The cells were expanded to reach 70% confluency and were subsequently frozen in freezing medium (80.1% DMEM (4.5 g/L D-Glucose, GlutaMax$^{TM}$ supplement, 10569-010, Gibco), 9% FBS, 0.9% A-A, 10% DMSO (AJA2225, Univar)) at -80 °C for 1-3 days and in liquid nitrogen below -196 °C for long term storage.

**Enzymatic isolation** was conducted by enzymatic digestion with 400 units/ml collagenase type 1 (17018029, Gibco) in DMEM, supplemented with 2% A-A, in a shaking water bath at 37 °C for one hour, after mincing the dissected pieces in smaller pieces of approximately 1 $mm^3$. After digestion, the tissues were broken down by titration with a serological pipette and digestion was stopped by addition of growth medium (Ham's F-10 (11550043, Gibco), supplemented with 20% FBS, 1% A-A, and 5 ng/ml recombinant human bFGF) and PBS. The mixture was filtered through a 100 $\mu$m strainer, and spinned down for 5 minutes at 800 $g$. Erythrocyte lysis buffer was added for 1 minute at room temperature, and stopped by adding PBS. The mixture was centrifuged for 5 minutes at 800 $g$, the pellet resuspended in growth medium, and the suspension was filtered through a 40 $\mu$m strainer. The cells were plated in culture flasks or frozen in freezing

medium (80.1% DMEM, 9% FBS, 0.9% A-A, and 10% DMSO) at -80 °C for 1-3 days and in liquid nitrogen below -196 °C for long term storage.

### 3.1.2. Collagenase type 2 satellite cell isolation - biopsy 2

The difference of biopsy 1 and biopsy 2 was the type of collagenase used. Collagenase type 2 was used during cell isolation of the second biopsy. The biopsy for this cell isolation was taken from a pregnant ovine, between 3 and 5 years old, and used for an animal study. Surgery was performed on the fetus, the mother only had a maternal vein catheter. The experiment was hypoxia-ischemia in the fetus, followed by hypothermia. The animals were not treated with drugs. The ovines were euthanised with a pentobarbital overdose through an intravenous line in the jugular vein. This is not expected to affect the cell population at the place of biopsy. The rest of the procedure was performed as described in section3.1.1. The biopsy of the ST and SM weighed 4 and 1 gram, respectively.

**Explant isolation** was conducted following the protocol described in section 3.1.1.

**Enzymatic isolation** was conducted following the protocol described in section 3.1.1, with the only difference that collagenase type 2 was used instead of collagenase type 1.

## 3.2. Cell identification

As described in section 2.6.2, a common approach to identify what cell types are present in the isolated samples is by using FACS. However, the process of designing a FACS panel and titrating the antibodies can be quite time consuming. It was therefore attempted to distinguish the different cell types by cell analysis without the use of antibodies. This is not used to separate the cells, only to distinguish different cell populations. The technique is based on forward and side scatter, where forward scatter provides information about the size of the cells and side scatter provides information about the granularity of the cells. If the different cell types in a sample have an evident variation in cell size and granularity, this technique can be sufficient to determine a ratio between cell populations within the sample. However, the cell types showed such similarity in size and granularity that different cell populations could not be distinguished. Therefore, antibodies were included in the analysis and a FACS panel was designed nevertheless. This section describes the how cell analysis without antibodies and with antibodies was performed, including the titration of the antibodies.

### 3.2.1. Cell analysis without antibodies

Cells were washed with PBS and detached from culture flasks by covering the surface with tryplE (TryplE$^{TM}$ Express, 12605-028, Gibco) for 5 minutes at 37 °C. After cells were detached, an equal amount of tryplE neutraliser solution (TNS) (PBS supplemented with 2% FBS) was added to neutralize the cell suspension. The cell suspension was centrifuged for 5 minutes at 350 $g$ at 24 °C, after which the supernatant was discarded and the cells were resuspended in growth medium (DMEM (4.5 g/L D-Glucose, GlutaMax$^{TM}$ supplement, 10569-010, Gibco), supplemented with 10% FBS (10091-148, Gibco), and 1% A-A (Sigma-Aldrich, A5955)) at a temperature of 37 °C. Two million cells were collected per sample and resuspended in 2 ml of wash buffer (WB) (PBS (10010-023, Gibco) supplemented with 1% FBS and 1% 0.2 M EDTA (0.5 M EDTA (AM9260G, Thermo Fisher Scientific) diluted with D-PBS (14190-250, Gibco))). The cell suspension was centrifuged for 5 minutes at 350 $g$, supernatant was discarded and cells were resuspended in 400 $\mu$l FACS buffer. The samples were stored on ice until acquisition. Acquisition was performed by the BD FACS Aria II cell sorter (BD Biosciences).

### 3.2.2. Titration of antibodies

Making use of antibodies to identify the cell types in a mixed population gives a more accurate result. When incorporating antibodies in analysis techniques, the optimal working concentration needs to be determined by titration. Using suboptimal concentrations of antibodies can result in poor separation of the different cell populations and it increases the chance of non-specific staining [148, 149]. The outcomes of titration are the separation dose and saturation dose. When deciding on the optimal working concentration, these two need to be taken into account. The separation dose is the dose with the clearest separation between the positive and negative population, and the saturation dose is the dose with the highest staining index value. Staining index (SI) value is calculated by the using the mean fluorescence intensity (MFI) [161]:

$$SI = \frac{MFI_{pos} - MFI_{neg}}{2 * SD_{neg}} \tag{3.1}$$

with $MFI_{pos}$ as the mean fluorescence intensity of the positive population, $MFI_{neg}$ as the mean fluorescence intensity of the negative population and $SD_{neg}$ as the standard deviation of $MFI_{neg}$. The ideal combination of separation and saturation dose depends on the application. However, for this research it is of uttermost importance to have a clear separation between positive and negative colonies and therefore separation dose is prioritized over saturation dose.

Antibodies were titrated to determine the optimal working concentration. The highest concentration for the titration was the recommended working concentration, and serial dilution was performed five times to obtain six different concentrations. The dilutions were stored in round bottom polystyrene test tubes (Corning, 352058) on ice, protected from light. Cells were washed with PBS and detached from culture flasks by covering them with tryplE for 5 minutes at 37 °C. After cells were detached, an equal amount of TNS was added to neutralize the cell suspension. The cell suspension was centrifuged for 5 minutes at 350 $g$ at 24 °C, after which the supernatant was discarded and the cells were resuspended in flow staining buffer (FSB) (PBS supplemented with 4% FBS and 1% 0.2 M EDTA) at a concentration of 2 million cells per 50 $\mu$l. 50 $\mu$l of cell suspension was transferred to the dilution tubes prepared by serial dilution and the cells were vortexed and incubated on ice for 30 minutes, protected from light. After incubation, 1 ml of WB was added and the tubes were centrifuged for 5 minutes at 350 $g$ at 4 °C. Supernatant was discarded, and cells were resuspended in 0.5 ml of WB. Tubes were centrifuged for 5 minutes at 350 $g$ at 4 °C once more, followed by discarding the supernatant and resuspending the cells in 100 $\mu$l of WB. Cell suspensions were stored on ice and protected from light until acquisition. Right before acquisition, DAPI was added and the cell suspension was vortexed.

### 3.2.3. FACS

The antibodies of interest were added to one solution containing all antibodies. The optimal concentration per antibody was determined by titration, see section 4.2.2. The antibody cocktail consisted of: 10 $\mu$l ITGA7 conjugated with PE-Vio 770 (130-103-357, Miltenyi), 10 $\mu$l CD31 conjugated with FITC (MCA1097F, BioRad), 10 $\mu$l CD45 conjugated with R-PE (MCA2220PE, BioRad), 0.3125 $\mu$l CD56 conjugated with BV711 (563169, BD), and 0.15625 $\mu$l CD29 conjugated with APC (303008, Biolegend), topped up to 100 $\mu$l with FSB. Cells were washed with PBS and detached from culture flasks by covering them with tryplE for 5 minutes at 37 °C. After cells were detached, an equal amount of TNS was added to neutralize the cell suspension. The cell suspension was centrifuged for 5 minutes at 350 $g$ at 24 °C, after which the supernatant was discarded and the cells were resuspended in FSB at a concentration of 2 million cells per 50 $\mu$l. 50 $\mu$l of cell suspension was transferred to the dilution tubes prepared by serial dilution and the cells were vortexed and incubated on ice for 30 minutes, protected from light. After

incubation, 1 ml of WB was added and the tubes were centrifuged for 5 minutes at 350 $g$ at 4 °C. Supernatant was discarded, and cells were resuspended in 0.5 ml of WB. Tubes were centrifuged for 5 minutes at 350 $g$ at 4 °C once more, followed by discarding the supernatant and resuspending the cells in 100 $\mu$l of WB. Cell suspensions were stored on ice and protected from light until acquisition. Right before acquisition, DAPI was added and the cell suspension was vortexed. Acquisition was performed by the Cytek Aurora 3 laser (Cytek Biosciences).

## 3.3. Biomarker profile

As said in section 2.4.3, Pax3, Pax7, MyoD, myogenin, and myosin are important markers during development of a satellite cell into a myofibre. To set up a biomarker profile, these markers are used to indicate when the proteins come to expression. Ovine B1 ST enzymatic isolated cells of passage 4 were used for this experiment. 3T3 cells of passage 5 were used as negative control, and purified ovine satellite cells supplied by Mosa Meat were used as a positive control. Cells were seeded at seeding density of 10,000 cells/cm$^2$, in four different 96-wells plates. All three cell types were included on one plate and proliferated in the same growth media: DMEM (4.5 g/L D-Glucose, GlutaMax$^{TM}$ supplement) supplemented with 10% FBS and 1% A-A. On culture day 5, proliferation media was replaced by differentiation media: DMEM supplemented with 2% horse serum (HS) (26050088, Gibco) and 1% A-A. The plates were stained for all biomarkers at the following time points: early proliferation, late proliferation, early differentiation, and late differentiation, and each biomarker was stained in 4 wells per cell type. The cells were fixated at day 2 and day 5 of proliferation, and on day 2 and day 7 of differentiation. Cells were analyzed by immunofluorescence, as described in section 3.8.3. The expression of transcription factors Pax3, Pax7, MyoD, and myogenin was determined by counting the marker expressing nuclei. The expression of myosin was assessed by nuclei count in myosin expressing cells.

## 3.4. Proliferation in 2D

The isolated cells were proliferated in growth medium consisting of DMEM (4.5 g/L D-Glucose, GlutaMax$^{TM}$ supplement), supplemented with 10% FBS and 1% A-A. The cells were proliferated and stored in liquid nitrogen to set up a cell bank.

**Passaging** of the cells was performed by aspirating the culture media and rinsing the cells with PBS. Consequently tryplE was added and incubated at 37 °C for 5 minutes, or until cells were detached. TryplE neutraliser solution (TNS) (2% FBS in PBS) was added in the same amount as tryplE, and the cell suspension was transferred to a centrifuge compatible tube. The culture flask was rinsed with PBS, which was added to the tube likewise. Cells were spinned down in the centrifuge at 350 $g$ for 5 minutes. Supernatant was aspirated and discarded, and the cells were resuspended in growth medium to reach a concentration of approximately 1 million cells per ml. The cells were counted with the automated cell counter Countess II (A27977, Thermo Fisher Scientific). Cells were then seeded at preferred cell density and excess of cells was discarded or stored in liquid nitrogen.

**Liquid nitrogen** enables long term storage of the cells. After counting the cells, the required amount of cells was transferred to a separate tube and spinned down again at 350 $g$ for 5 minutes. The supernatant was aspirated and discarded, and the cells were resuspended in freezing medium (10% DMSO in growth medium) at a concentration of 1 million cells per ml. The cell suspension was divided over the preferred amount of cryovials, followed by cryovial storage in a freezing container (Mr. Frosty$^{TM}$, 5100-0001, Thermo Fisher Scientific) at -80 °C overnight. Cryovials were transferred to liquid nitrogen storage after 1-3 days.

### 3.4.1. Population doublings

The proliferative capacities of the isolated ovine cells were determined by proliferating all isolation samples for multiple passages and calculating their population doublings. At each passage, the cells were seeded at a seeding density of 2,000 cells/cm$^2$ (150,000 cells per T75 culture flask) and passaged and counted after 3 days of incubation at 37 °C and 5% $CO_2$. Cells were counted with the an automated cell counter (Countess$^{TM}$, A27977, Thermo Fisher). The time of passaging was logged, so proliferation time per passage could be exactly calculated. This was performed from passage 2 to 7 and the total passaging experiment was performed in duplicate. The population doublings of the samples were meant to be measured for a longer period, but in both instances an infection terminated the experiments.

### 3.4.2. Evaluating the effect of coating

Mammalian cells are often proliferated and differentiated on surface coatings, to improve cell adherence and performance. Common coatings are collagen and Matrigel. Collagen has been used to promote outgrowth during explant isolation [119], to promote myofibre formation [160], and as a scaffold in hydrogels [162]. Matrigel has been shown to stimulate outgrowth of myogenic progenitors [119], and maintain differentiation capacity [162]. However, the batch-to-batch variations in terms of adhesion receptors and growth factors make Matrigel unreliable, and is therefore not ideal for continuous production processes. Literature is contradictory on whether a collagen or Matrigel coating results in the biggest improvement on proliferation and differentiation of skeletal muscle cells, as studies get different results when comparing the two coating components [160, 162]. An experiment was performed to determine which coating works best for ovine cells. The results on this can be used as a suggestion for future research on ovine cells, for example to improve proliferation rate or as coating for microcarriers. Independently of the results, all other experiments of the research presented here are performed without coating to analyse the cells behaviour with minimal external influences.

Collagen and Matrigel coating solutions were prepared by diluting collagen (5 mg/ml, 3447-020-01, Cultrex, Biotechne) 1:10 in 0.02 M acetic acid, and diluting Matrigel (356234, Corning, Life Sciences) 1:200 in cold PBS, respectively. Subsequently, the coatings were adhered to 24-wells plates by adding 0.25 ml coating per well, incubating it overnight, and aspirating the remaining liquid afterwards. The coating was washed with room temperature PBS twice, after which the plates were ready for cell seeding. A 24-wells tissue culture plate without additional coating was used as control. All isolated cell samples were seeded in triple and all ovine cell samples were passage 6. The cells were compared to C2C12s of passage 9. The cells were seeded at seeding density 2,000 cells/cm$^2$ (day 0) and proliferated in 0.5 ml growth medium (DMEM 4.5 g/L D-Glucose, GlutaMax$^{TM}$ supplement, supplemented with 10% FBS and 1% A-A) per well. The high-content analysis system Operetta$^{TM}$ (OPRT1134, Perkin Elmer) was programmed to take 15 brightfield images at the exact same locations in each well on day 1, 2, and 3 of proliferation. Analysis of the images was carried out by the corresponding software Columbus (Image Data Storage and Analysis System, Perkin Elmer). This experiment was performed once. The experiment was aimed to perform twice more, and to also include analysis of the effect of coating on differentiation, but due to sudden closure of the lab (due to COVID-19 restrictions) and contamination, no additional results were obtained.

## 3.5. Differentiation in 2D

When cells reached complete confluency, the cells were starved from serum to initiate differentiation. Differentiation medium consisted of DMEM (4.5 g/L D-Glucose, GlutaMax$^{TM}$ supple-

ment), supplemented with 2% HS and 1% A-A. The cells were monitored daily, and medium was refreshed every 3 days. Cells were differentiated until multiple nuclei could be seen in the swollen regions of the cytoplasm. This varied in time dependent on isolation sample and confluency. Cells were analyzed by immunofluorescence as described in section 3.8.2.

## 3.6. 3D system and hydrogel

The 3D system to grow the myofibres in was based on the design of Capel *et al.*, as described in section 2.5. Their design and hydrogel composition were used during initial experiments. However, due to a lack of hydrogel compaction, both the system design and hydrogel composition were altered. This section provides a more detailed description of the experiments that were performed with the system of Capel *et al.* and explains the motivation for the alterations. C2C12 cells were used during experiments to set up a working model as a control for the ovine cells.

### 3.6.1. 3D printed PLA systems

The design of Capel *et al.* is depicted in figure 3.2a and 3.2b. The systems were designed in SolidWorks (Dassault Systèmes SolidWorks Corporation). They were 3D printed with PLA (resolution of 0.2 mm nozzle diameter, by the Original Prusa i3 MK3, available in-house), cleaned with 70% ethanol and attached to a 6-wells plate with a bioadhesive. The plate was cleaned with ethanol, washed with PBS, and sterilized by UV light for 30 minutes. Two different compositions of cell-laden hydrogels were seeded in separate systems, one based on collagen and one based on both collagen and Matrigel, as per the study of Capel *et al.* [133]: (1) 85% v/v type I rat tail collagen (at a protein concentration of 5 mg/ml) (3447-020-01, Cultrex, Biotechne), 10% growth medium, 1 M sodium hydroxide (NaOH) dropwise to neutralise the pH of the solution (indicated by a colour change to pink), and C2C12 cells at a seeding density of $4 * 10^6$ cells/ml in 5% v/v growth medium (DMEM 4.5 g/L D-Glucose, GlutaMax$^{TM}$, supplemented with 10% FBS and 1% A-A); (2) 65% collagen, 10% growth medium, 1 M NaOH dropwise to neutralise the pH of the solution, 20% Matrigel (356234, Corning, Life Sciences), and C2C12 cells at a seeding density of $4 * 10^6$ cells/ml in 5% v/v growth medium. The hydrogels were seeded around the pillars in the systems and allowed to set for 1 hour at 37 °C and 5 $CO_2$. Growth medium was added and the gels were incubated at 37 °C and 5% $CO_2$. Both hydrogels were tested in triple. The hydrogels did not show full compaction and they certainly did not compact around the pillars. This raised the question if the parts connecting the pillars to the rest of the system, referred to as 'pillar bridges' in figure 3.2b, interfered with the hydrogel compaction. The height of the pillar bridges was 0.4 mm in both systems. This could be too high and withhold the hydrogel from ascending the pillar bridges and compacting around the pillars. Therefore, the system was designed to be completely made of PDMS, with PDMS pillars attached to a bottom of PDMS, as depicted in figure 3.2d, eliminating the requirement of pillar bridges. Additionally, the initial process of 3D printing, adhering, and cleaning the systems was experienced as labour intensive, and this process is simplified when producing the systems with PDMS. The bioadhesive used to attach the systems of Capel *et al.* to the plates was silicone aquarium glue (9300697100382, Glass Silicone Sealant, Selleys). Preliminary tests culturing C2C12 cells directly on the adhesive had indicated that the cells attached to the silicon polymer and survived on it. Further experiments were planned to confirm cell viability when using the adhesive, however due to the alterations of the design no adhesive was required hereafter.

### 3.6.2. PDMS systems

PDMS systems can be sterilized by autoclaving, are reusable, and by making the whole system of PDMS no pillar bridges are required. See figure 3.2d for the PDMS design. Additionally,

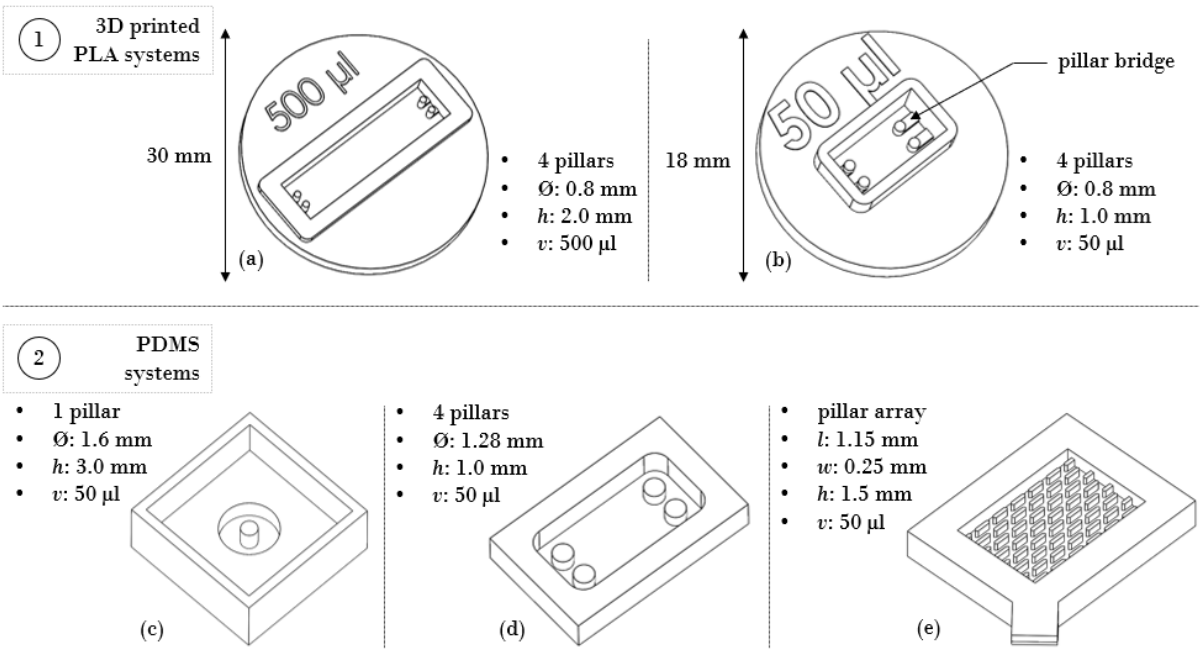


Figure 3.2.: Overview of the 3D printed PLA systems and the PDMS systems, designed in SolidWorks. ø indicates the pillar diameter, $h$ indicates the pillar height, and $v$ indicates the hydrogel volume. (a - b) Systems mimicking the designs of Capel *et al.* [133]; (c) one pillar system; (d) four pillar system; (e) pillar array system. $l$ indicates the length of the pillars and $w$ indicates the width of the pillars.

the function of four pillars was questioned and two additional systems were designed: a system containing one pillar, inspired by the study of Li *et al.* described in section 2.5, and a system containing an array of pillars, inspired by the study of Bian *et al.* described in section 2.5 likewise. It was decided to proceed with a hydrogel volume of 50 $\mu$l instead of 500 $\mu$l for all systems, to limit the amount of resources and cells needed. The system with one pillar is depicted in figure 3.2c and was chosen because the cells in the hydrogel do not need to cross a distance to connect pillars with one another. The system with a pillar array, as depicted in figure 3.2e, does require the cells to cover a distance to connect the pillars. However, the distance is a 20-fold smaller than in the design of Capel *et al.*. This short distance was expected to increase the compaction of the hydrogels around the pillars. The three systems were designed with SolidWorks and the negatives were created to function as molds for the PDMS. At first, the systems were created by 3D printing PLA, but protrusions of the PLA got stuck in the PDMS pillars, disrupted the smoothness of the pillars, and thereby disrupted the hydrogels. Alternatively, the systems were made by laser etching multiple layers into acrylic acetate (resolution of 0.08 mm laser diameter, with the Speedy 360, Trotec, available at Unleash Space (Centre for Innovation and Entrepreneurship at the University of Auckland)) which provided the pillars with the required smoothness. Moreover, the hydrogel composition was adjusted and the major alteration was a two-fold increase in seeding density: $8 * 10^6$ cells/ml. The hydrogel composition was adjusted to be as follows: 65% collagen (dissolved in growth medium to a protein concentration of 2.035 mg/ml), 10% growth medium, 1 M NaOH added dropwise until a colour change to pink was observed to neutralize the pH, 20% Matrigel, and cells seeded at a seeding density of $8 * 10^6$ cells/ml in 5% growth medium.

PDMS was made by thoroughly mixing silicon elastomer and corresponding curing agent in a ratio of 1:10 (Sylgard$^{TM}$ 184 Silicone Elastomer Kit, 04019862, Dow). The PDMS was poured in the moulds, and bubbles were removed by introducing the moulds to a vacuum environment.

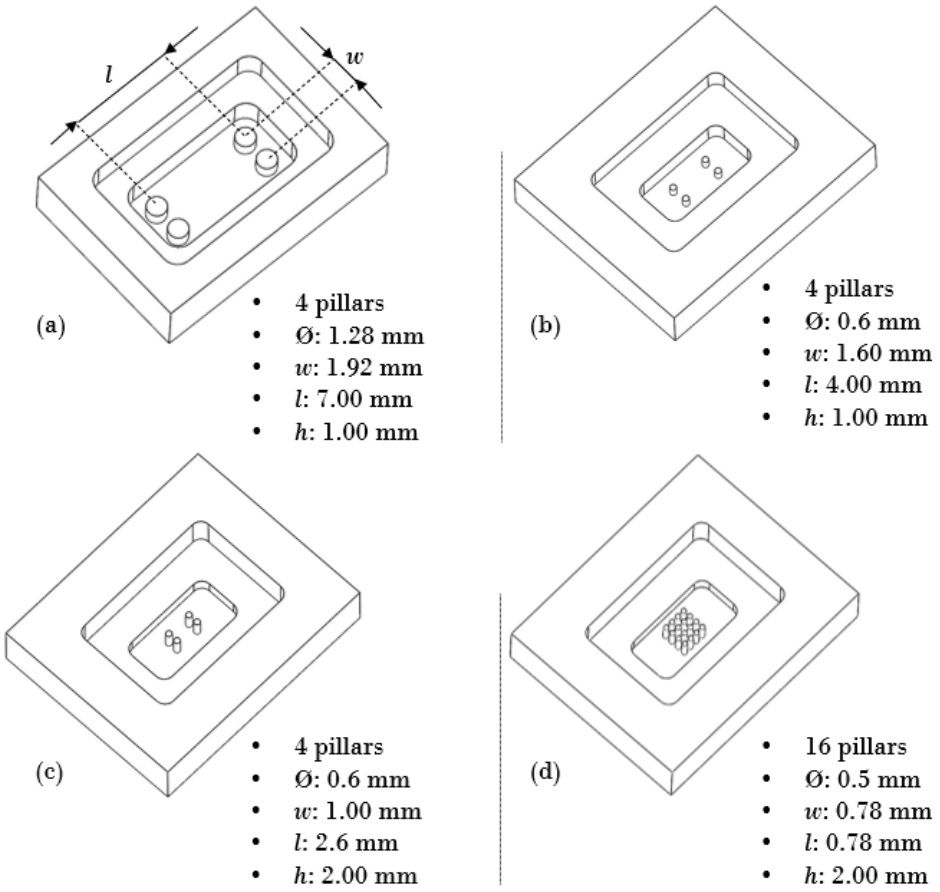


Figure 3.3.: Overview of the final 3D system designs. ø indicates the pillar diameter, $h$ indicates the pillar height. Hydrogel volume in all systems is 50 $\mu$l. (a-c) Four pillars, $l$ indicates the length distance between two pillars and $w$ indicates the width distance; (d) 16 pillars, $l$ and $w$ indicate the distance between two pillars (non-diagonal).

The PDMS was cured in an oven at 80 °C overnight. The systems were carefully removed from the moulds and sterilized by autoclaving. The hydrophobicity of the PDMS withheld the hydrogel of integrating in and around the small areas between the pillars of the pillar array of the design in figure 3.2e. This could have been solved by treating the PDMS surface with a solution containing a surfactant, such as Pluronic F-127 [163]. However, this product was not available in-house and the results obtained with the designs of figure 3.2c and 3.2d were promising enough to not proceed with this pillar array system.

The system containing one pillar was used as a stepping stone towards the final design. Compaction needed to be achieved and it was expected that compaction could be easiest achieved with one pillar. When the first compaction was seen around one pillar, compaction was also seen in the four pillar system. Monitoring the compaction of the hydrogel over time is easier to monitor in a system with multiple pillars than one pillar. Therefore, it was decided to proceed with the four pillar system. The system with four pillars was optimised: an extra deepening was added where the growth medium could be added in. Moreover, the distance of the pillars was shortened, to decrease the tension on the constructs, and the pillars were made taller, to avoid the constructs floating off of the pillars. When cells compacted around all four pillars, rupturing of the constructs around at least one pillar was common. This decreased the total tension on the constructs which could affect the differentiation of the cells. Therefore, a system was designed to intercept the rupturing of the constructs with extra 'back up' pillars. A system

of 16 pillars was designed with enough space in between to avoid impact of hydrophobicity of the PDMS. See figure 3.3 for the altered designs. As the pillar size became significantly smaller, a more accurate production method was required. The production of the systems was outsourced to University of Auckland's Technical Services Workshop, where the system was produced by milling in teflon (PTFE) with a CNC machine. Different compositions of hydrogels were experimented with, varying the cell seeding density, amount of hydrogel, amount of collagen, and amount of Matrigel. The hydrogel that worked best in the systems contained cells at a seeding density of $32 * 10^6$ cells/ml, which is eight times the seeding density used by Capel *et al.* The final hydrogel composition was: 65% collagen (dissolved in growth medium to a protein concentration of 2.035 mg/ml), 10% growth medium, 1 M NaOH added dropwise until a colour change to pink was observed to neutralize the pH, 20% Matrigel, and cells seeded at a seeding density of $32 * 10^6$ cells/ml in 5% growth medium.

## 3.7. Medium composition

One of the primary challenges of cultured meat is the price. One component that is driving up the costs is the culture medium. A standard solution of commonly used culture medium for basic proliferation cell culture consists of DMEM supplemented with FBS and the antibiotic mixture PenStrep. FBS is a standard component of culture medium as it maintains the cells and stimulates proliferation [164, 165]. It is a complex mixture of a wide variety of components like growth factors, proteins, vitamins, fatt acids, and hormones [164, 165, 166, 167]. However, it is indisputable that FBS should be eliminated from the culture medium of cultured meat, as it is animal derived and a by-product of the meat industry [165, 166, 167]. Additionally, the FBS composition has not been fully characterized and therefore shows batch-to-batch variations, resulting in inconsistent results [164, 165]. Many cultured meat companies have claimed to have developed culture medium without FBS, but their medium compositions are not published. The research that is presented in this thesis was performed with culture media supplemented with FBS, as finding a replacement for FBS was not the scope of this research.

Another point of discussion is the use of antibiotics and fungostatics in culture medium. Standard cell culture protocols include them to prevent contamination [168]. It would be ideal to completely eliminate antibiotics from the solution. The first reason being the health benefits of antibiotics-free food, as described in section 1.3. Another reason is the effect of antibiotics on cell behaviour. Ryu *et al.* investigated the effect of antibiotics on the 2D culture of HepG2 cells (human liver cancer cells) [168]. The culture medium was supplemented with 1% PenStrep and 10% FBS. Their findings show that PenStrep responsive genes are involved in pathways related to drug and insulin response, fatty acid activation, apoptosis, cell growth, and unfolded protein response. This suggests that PenStrep can significantly affect cell behaviour of HepG2 cells, and might have similar effects on other cell types. Additionally, Skubis *et al.* investigated the effect of various antibiotic mixtures on human adipose-derived stem cells [169]. They found that antibiotics alter the proliferation rate of the cells and that they can promote natural osteogenesis and adipogenesis. They also concluded that the influence of antibiotics depends on the duration of exposure and on the combination of the antibiotics compounds. This suggests that antibiotics could actually enhance certain cell behaviour in a positive manner, if used properly. However, setting up a suitable protocol for a single cell type would be very time consuming. Apart from these publications that suggest certain effects of antibiotics, little is known about the specific consequences of antibiotic supplementation in the culture process. This uncertainty, combined with the health benefits, make a compelling argument for eliminating antibiotics during the production process of cultured meat. Although cultured meat is aimed to be produced with a lower amount of hormones and antibiotics, or even no hormones and antibiotics at all, this is not implemented during the research presented in this thesis as it might cause complications

that distract from the scope of the research.

Dulbecco's modified Eagle's medium (DMEM) is a commonly used basal medium, consisting of amino acids, vitamins, salts, and other components [170, 171]. The DMEM used in this research contains 4.5 g/L D-Glucose, as studies showed that cells grow properly in this level of glucose [170]. Furthermore, the DMEM is supplemented with GlutaMax$^{TM}$, which is an alternative formulation of L-glutamine, designed to be stable in solution. This supplement leads to an efficient energy metabolism and high proliferation rate, without excess ammonia. Although DMEM is not the most expensive component of cell culture, it would be profitable to reduce its costs. One bottle of 500 ml DMEM GlutaMax$^{TM}$, 4.5 $g/L$ D-Glucose, costs around €20, and a bottle of 500 ml DMEM without supplements costs around €19 [172, 173]. As one T175 culture flask needs 35 ml of fresh culture medium every three days, the costs of a medium refreshment of only the DMEM part already costs €1.25 for one flask, which yields around 4 million proliferated cells. To reduce the costs of the medium, alternatives for DMEM were studied. An unconventional approach is investigated by the Shojinmeat Project: they propose to replace DMEM, partly, by energy drink. The Shojinmeat Project is an open source research collaboration, which is set up to enable individuals to contribute to cultured meat research. It focuses on DIY cellular agriculture and education. The Shojinmeat Project does not have official publications to refer to, but their experiments and protocols can be found on their website [174]. Their theory is that energy drinks are similar to DMEM, as both are composed of sugars, amino acids, vitamins, and minerals. The osmolarity and pH of the drink can be very different from DMEM, however this can be adjusted by adding baking powder to increase the osmolarity, and NaOH to increase the pH. Shojinmeat Project has presented comparable proliferation rates of mouse L6 cells cultured in a mixture of 60% DMEM and 40% energy drink, and a control group of 100% DMEM. An experiment to investigate the effect on the isolated ovine cells was set up. Table 3.1 provides an overview of the selected energy drinks.

Osmolarity and pH of the selected energy drinks were measured (with the VAPRO® Vapor Pressure Osmometer, EliTechGroup, and the SevenCompact pH meter S220, Mettler Toledo). Three drinks were selected for cell culture experiments: V-energy Original Guarana (V-energy) for investigation of the effect of guarana, Persist LIVE+ (LIVE+) for investigation of the effect of ginseng, and Gatorade Fierce Berry (Gatorade) because it is closest to DMEM in osmolarity. The three selected drinks were adjusted in osmolarity by adding baking powder (and MilliQ in case of an overshoot of baking powder), and adjusted in pH by adding NaOH (and MilliQ in case of an overshoot of NaOH). The final adjusted values can be found in table 4.4. After alteration of the energy drinks they were sterilised with a 0.2 $\mu$l filter. Both enzymatic isolated ovine cells ST B1 passage 5 and C2C12s passage 6 were used for this experiment. The cells were seeded in 96-wells plates at a seeding density of 1560 cells/cm$^2$, according to MTT assay recommendations of 500 cells per well. Per well, 100 $\mu$l of growth medium without energy drink (DMEM supplemented with 10% FBS and 1% A-A) was added. The cells were incubated in this medium overnight at 37 °C and 5% $CO_2$ to allow the cells to attach to the surface. After approximately 24 hours, the cells were washed with PBS and the mixtures of energy drink and DMEM were supplemented with 10% FBS and 1% A-A, and added to the cells. Cells were incubated at 37 °C and 5% $CO_2$ and cell viability was analysed by MTT assays on day 4 and day 10, as described in section 3.8.5. The medium was not refreshed.

Table 3.1.: The selected energy drinks for partial replacement of DMEM, the contents, and the reasons for selection.

| Energy drink | Contents | Reason for selection |
|---|---|---|
| V-energy Original Guarana | Carbonated water, sugar, acidity regulators (citric acid, sodium citrate), taurine, **guarana extract (0.12%)**, colour (caramel), glucuronolactone, caffeine, inositol, vitamins [niacin (B3), panthothenic acid, B6, riboflavin (B2), B12], flavours | It contains 0.12% guarana seed extract and caffeine. One gram of guarana is equivalent to 40 mg caffeine and guarana is released at a slower rate compared to pure caffeine [175]. Caffeine is suggested to have several effects on cell behaviour [176, 177]. |
| Persist LIVE+ | Carbonated water, sucrose, acidity regulators (citric acid, sodium citrate), flavour, potassium sorbate, caffeine, colour (caramel 4), **guarana seed extract (0.005%)**, ascorbic acid, **panax ginseng extract (0.003%)**, vitamins [thiamin (B1), niacin (B3)] | It contains 0.003% ginseng extract, 0.005% guarana seed extract, and caffeine. A primary active ingredient of Panax ginseng is ginsenoside Rg1. It is suggested that ginsenoside Rg1 can participate in the regulation of protein synthesis and degradation due to its structural similarity to human steroid hormones [178, 179]. |
| Mountain Dew | Carbonated water, high fructose corn syrup, concentrated orange juice, citric acid, natural flavour, sodium benzoate, caffeine, sodium citrate, gum arabic, erythorbic acid, calcium disodium EDTA, yellow 5 | It contains caffeine, without guarana seed or ginseng extracts. |
| Gatorade Fierce Berry | Water, sugar, dextrose, citric acid, salt, sodium citrate, natural flavour, monopotassium phosphate, gum arabic, red 40, glycerol ester of rosin | Gatorade is reported in literature to have an osmolarity of 348-362 mmol/kg [180], which is close to the osmolarity of DMEM at 310-350 mmol/kg [181, 182, 183]. Moreover, it does not contain caffeine in contrast to previously mentioned energy drinks. |
| Powerade ION4 Berry Ice | Water, sucrose, minerals (potassium citrate, magnesium sulphate, calcium chloride, sodium citrate, sodium chloride, potassium phosphate), food acid (330), flavour, colour (129), sweetener (955) | The ingredients are similar to Gatorade, but it is lower in cost. |
| Monster Energy Original | Carbonated water, sugar, glucose, citric acid, natural flavours, taurine, sodium citrate, color added, **panax ginseng extract**, L-carnitine L-tartrate, caffeine, sorbic acid, benzoic acid, niacinamide (B3), sucralose, salt, D-glucuronolactone, inositol, **guarana extract**, pyridoxine hydrochloride (B6), riboflavin (B2), maltodextrin, cyanocobalamin (B12) | It is an energy drink with a large market share [175], suggesting that many people experience an increase in energy after drinking this beverage. This raises the question how cells would perform on this drink. |

## 3.8. Cell analysis

This section describes the read-out methods used to analyse the cells.

### 3.8.1. Brightfield microscopy

To observe the cells in the cell culture lab, a brightfield miscroscope was available (Leica DM IL). This microscope was not equipped with a camera function. Microscopes with camera function were available in other labs in the building. The explant isolation tissues and the engineered tissue constructs were sensitive to movement and this could potentially disrupt the experiments. Therefore, these were not transported to other labs to obtain pictures, and pictures of the constructs were taken by phone (13mp, aperture: f/2.0, shutter speed: 1/172, ISO100) the the Leica microscope lense.

### 3.8.2. Immunofluorescence in 2D without serum

The cells were washed with PBS three times, for 5 minutes each time. Subsequently, the cells were fixated with 4% paraformaldehyde (PFA) for 30 minutes at room temperature. The cells were washed with PBS twice, for 5 minutes each time. The cells were incubated in permeabilisation solution (0.1% Triton X-100 in PBS) for 15 minutes, followed by three washing steps with PBS, for 5 minutes each. Blocking solution (2% BSA and 0.1% Triton X-100 in PBS) was added and aspirated after 30 minutes, followed by addition of primary antibody solution (MF20 (AB2147781, Developmental Studies Hybridoma Bank) at 2 $\mu$g/ml in blocking solution) for overnight incubation at 4 °C. The cells were washed with PBS three times, for 5 minutes each. Subsequently, secondary antibody solution (Alexa Fluor 488 (A-11030, Thermo Fisher Scientific) in blocking solution, 1:500) was added for 30 minutes. Cells were washed with PBS twice, for 5 minutes, after which DAPI (62247, Thermo Fisher Scientific) was added for 2 minutes. Cells were washed with PBS twice, for 5 minutes, and were visualised with fluorescent microscopy (inverted fluorescence microscope, Nikon Eclipse Ti). The plates were wrapped in parafilm and protected from light, while stored at 4 °C.

### 3.8.3. Immunofluorescence in 2D using serum

The cells were rinsed with PBS three times, for 5 minutes each, followed by fixation in 4% PFA for 40 minutes. Subsequently, the cells were washed with PBS twice, for 5 minutes each, and permeabilized in permeabilization solution (0.1% Triton X-100 in PBS) for 15 minutes. After removal of permeabilisation solution, blocking solution (50% BSA stock solution (2 wt% BSA in PBS), 40% PBS, and 10% goat serum) was added for 30 minutes. Primary antibody solution was prepared at a concentration of 5 $\mu$g/ml in blocking solution. The blocking solution was removed, primary antibody solution was added, and the cells were incubated overnight at 4 °C. The cells were washed with PBS three times, for 5 minutes each. Secondary antibody Alexa Fluor 488 (A-11030, Thermo Fisher Scientific) was diluted 1:500 in PBS and was added to the cells for 2 hours at room temperature. The cells were washed with PBS twice, DAPI was added for 2 minutes, the cells were washed with PBS twice more, and the cells were visualised with a fluorescent microscope. The plates were wrapped in parafilm and protected from light, while stored at 4 °C.

### 3.8.4. Immunofluorescence in 3D constructs

3D constructs were stained with primary antibody MF20 to target myosin and visualise myotubes. The 3D constructs were rinsed with PBS three times, for 5 minutes each time. Subsequently, the cells were fixated with 4% paraformaldehyde (PFA) for 50 minutes at room temperature. The cells were washed with PBS twice, for 5 minutes each time. The cells were

incubated in permeabilisation solution (0.1% Triton X-100 in PBS) for 15 minutes, followed by three washing steps with PBS, for 5 minutes each. Blocking solution (50% BSA stock solution (2 wt% BSA in PBS), 40% PBS, and 10% goat serum) was added for 40 minutes, followed by addition of primary antibody solution (MF20 (AB2147781, Developmental Studies Hybridoma Bank) at 3 $\mu$g/ml in blocking solution) for overnight incubation at 4 °C. The cells were washed with PBS three times, for 5 minutes each. Subsequently, secondary antibody solution (Alexa Fluor 488 (A-11030, Thermo Fisher Scientific) in PBS, 1:500) was added for 2 hours. Cells were rinsed with PBS after which DAPI (62247, Thermo Fisher Scientific) was added for 2 minutes. Cells were washed with PBS twice, for 5 minutes, and were visualised with fluorescent microscopy and confocal microscopy (live cell confocal microscope, Andor Revolution, Nikon Ti-E). The dishes were wrapped in parafilm and protected from light, while stored at 4 °C.

### 3.8.5. MTT assay

The colorimetric assay MTT is widely used to indicate cell viability, proliferation, and cytotoxicity [184]. It measures cellular metabolic activity, as the technique involves reduction of a water-soluble yellow tetrazolium salt thiazolyl blue (MTT) dye to insoluble purple formazan crystals, by metabolically active cells [185]. Subsequently, the formazan is solubilized and the concentration of formazan is measured by absorbance at 590 nm. Although it is suggested that that the amount of formazan is linearly correlated to the number of living cells, this has not been conclusively proven. Therefore, the results of MTT analyses will serve as an indication. In this research, the MTT assay is applied to measurements of proliferation rate and cell viability.

MTT assays were performed by seeding the cells at a seeding density of 15,000 cells/cm$^2$ in 96-wells plates. Cells were incubated for 3 days at 37 °C and 5% $CO_2$. Culture medium was aspirated, cells were washed with PBS, and a combination of 50 $\mu$l of serum free medium and 10 $\mu$l of MTT labeling reagent was added to each well. The plates were incubated for 3 hours at 37 °C, followed by aspiration of medium-reagent mixture. 150 $\mu$l of MTT solvent was added to each well. The plates were wrapped with aluminium foil, to protect it from light, and shaked until MTT crystals were dissolved. The absorbance was read by a plate reader (SpectraMax iD3, Molecular Devices, Bio-Strategy) at OD = 590 nm.

# 4 Results

The aim of the research presented in this thesis is to determine if ovine is a suitable cell source for cultured meat applications. This chapter presents the results of the experiments performed. An overview of the experiments is displayed in figure 4.1. The first step was to isolate cells from muscle biopsies of ovines, aiming for satellite cells. Two biopsies were obtained and cells were isolated by enzymatic and explant isolation. Enzymatic isolation was performed with collagenase type 1 during the first biopsy, and collagenase type 2 during the second biopsy. Six cell samples were obtained. As second step the cell types in the samples were identified. Through FACS three cell types were distinguished. The six cell samples presented significant variations in ratios of cell types. The proliferation rate was determined by population doublings, the differentiation capability was initiated by serum starvation, and the cells metabolic activity was measured by MTT assays for multiple passages. A 3D system was designed for formation of myofibres. Additional experiments were performed to determine coating preferences and to test cell metabolism with a cost effective DMEM alternative.

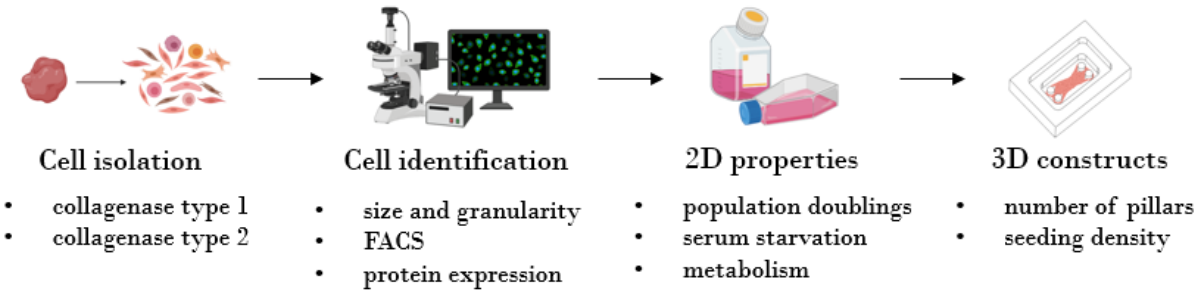


Figure 4.1.: Overview of the experimental approach.

## 4.1. Cell isolation

Cells were isolated from two *post mortem* biopsies by both explant isolation and enzymatic isolation. Explant isolation during biopsy 1 and 2 was performed following the identical protocol. The risk of contamination is high in environmental samples, and explant isolation of biopsy 1 was terminated due to contamination. Explant isolation of biopsy 2 was successful. The goal of explant isolation is to obtain activated cells that are migrating out of the tissue. See figure 4.2 for pictures of the explant and the cells migrating out. Explant isolation was performed on tissue culture dishes without coating, with collagen coating, and with Matrigel coating. No visual difference was observed in morphology or amount of cells by brightfield miscroscopy. It was decided to combine the cells from the identical muscle isolated on different coatings to minimise the number of samples. The cells obtained by explant isolation of the ST and SM during biopsy 2 will hereafter be referred to as 'B2 ST explant' and 'B2 SM explant', respectively.

Enzymatic isolation was performed with collagenase type 1 during biopsy 1, and collagenase type 2 during biopsy 2. Both collagenase type 1 and collagenase type 2 resulted in successful

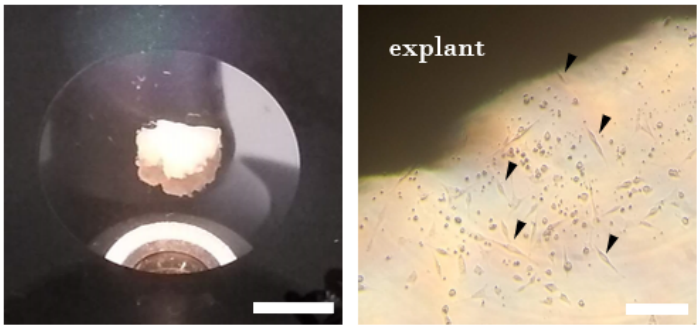


Figure 4.2.: Picture of a B2 SM explant cultured in a Matrigel coated Petri dish, scalebar 5 mm (left). Microscopic image of cells migrating out of the explant, indicated by black arrows, scalebar 500 $\mu$m (right).

cell isolation. Cell counts after enzymatic isolation from the ST and SM during the first biopsy were $9.9 * 10^6$ and $8.7 * 10^6$ cells, respectively. Cell counts after enzymatic isolation during the second biopsy were $14.5 * 10^6$ and $7.9 * 10^6$ cells for the ST and SM, respectively. Cells attached to the plates after approximately five days on average. The observed amount of attaching cells was lower than expected when compared to the cell count after isolation. Cells attachment did not occur simultaneously and it was therefore not possible to determine the amount of viable and attaching cells before cells initiated proliferation. It is noteworthy that cluster growth were observed during proliferation. See figure 4.3 for pictures of cell clusters that formed after enzymatic isolated cells of passage 0 were seeded. The cluster growth suggests that all cells in a cluster are derived from one cell, which suggest that a small amount of isolated cells attached. If isolation results in a higher cell yield, more cells will attach and more cells can contribute to expansion of the cell sample, enabling the sample to retain its stemness for longer. Although the amount of cells from these isolations was sufficient to set up a cell bank, it would therefore have been preferred to obtain a higher cell yield. Four cell samples were obtained: enzymatic isolated cells of the ST and SM by collagenase type 1, and by collagenase type 2. Samples will hereafter be referred to as 'B1 ST enzyme', 'B1 SM enzyme', 'B2 ST enzyme', and 'B2 SM enzyme', respectively.

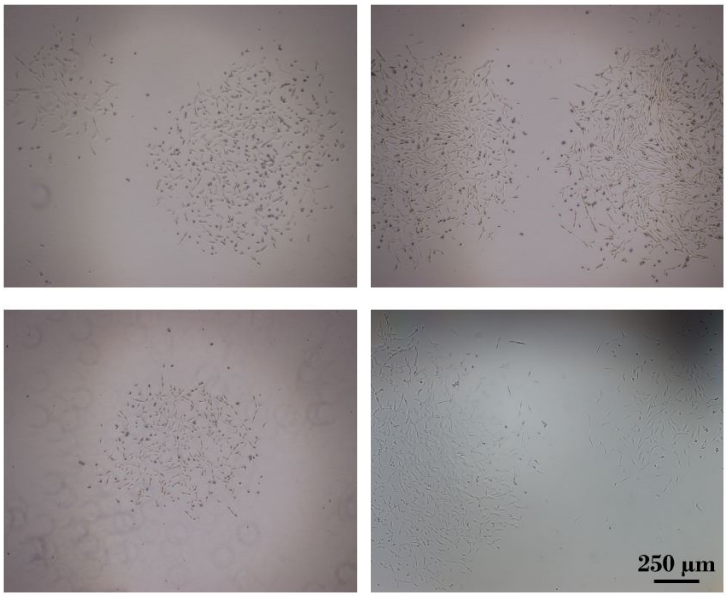


Figure 4.3.: Ovine B1 ST enzymatic isolated cells growing in clusters during proliferation at passage 1. Scalebar: 250 $\mu$m.

## 4.2. Cell identification

As described in section 2.6.2, it is essential to identify the cell types present in heterogeneous samples when investigating the properties of the isolated samples. Cell types that are expected in the samples are SCs and fibroblasts, and cell types that might be present are endothelial cells and immune cells. Identification of the cell types based on morphology is not accurate, as satellite cells and fibroblasts look eminently similar. Figure 4.4 depicts brightfield images of 3T3 cells (which are mouse fibroblasts), enzymatic isolated ovine B1 ST cells, and Mosa Meats purified bovine SCs for comparison. The cells in figure 4.4a and 4.4c are hard to distinguish from one another, and when presented with a mixed population as in figure 4.4b it is extra complicated. Therefore, other identification methods were explored.

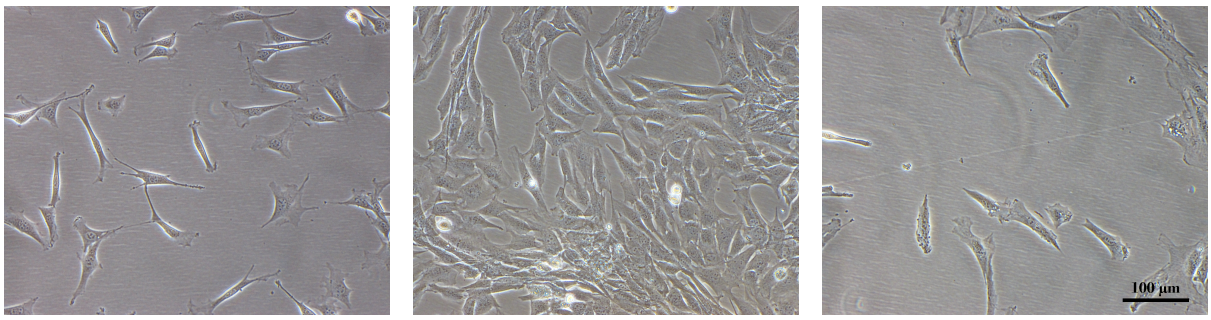


(a) 3T3 (b) Ovine B1 ST enzyme (c) Bovine satellite

Figure 4.4.: Brightfield pictures for comparison of morphology. Scalebar: 100 $\mu$m.

### 4.2.1. Cell analysis without antibodies

Cell analysis without antibodies was performed, to investigate if the cell types in the isolated samples could be distinguished based on size and granularity. This would have been possible if two clearly separated colonies would have been visible in the analysis plots. However, as depicted in figure 4.5, the cells are highly similar in cell size and granularity, and there is no clear separation between cell types visible. The 3T3 cells of figure 4.5a and the bovine satellite cells of figure 4.5c slightly differ, however not sufficient enough to identify cells in the plot of figure 4.5b. It was therefore decided to include antibodies in the analysis.

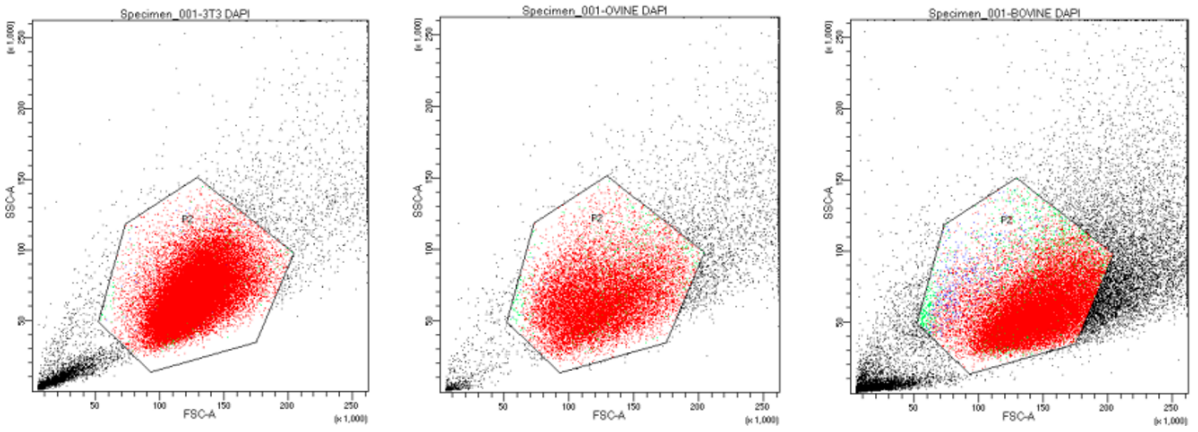


(a) 3T3 (b) Ovine B1 ST enzyme (c) Bovine satellite

Figure 4.5.: Results of cell analysis without antibodies.

### 4.2.2. FACS

As mentioned in section 2.6.2, it is expected that CD29 targets SCs and fibroblasts, CD56 and ITGA7 target SCs, CD31 targets endothelial cells, and CD45 targets immune cells. When designing a FACS panel, the antibodies need to be titrated to optimise the working concentration. The results of the titrations can be found in Appendix A. All ovine isolated samples were analysed with FACS, however only the enzymatic isolated B1 ST sample at passage 4 (P4) is presented in this chapter. Remaining FACS results can be found in Appendix B. Figure 4.6 presents the FACS results of the enzymatic isolated ST sample of biopsy 1. The graphs will be explained in this section. Graph 4.6a depicts a plot of the cell size to granularity. The area of interest is selected, to eliminate debris from the analysis, and analysed in graph 4.6b to select the single cells and remove double cells of the analysis. In graph 4.6c the living cells are selected and the cells positive for DAPI are removed. Graph 4.6e displays the living cells and their expression of CD31 and CD45. The whole population is negative for both CD31 as well as CD45. This indicates that endothelial cells and immune cells are not present in the sample. Graph 4.6d displays the living cells and their expression of ITGA7. It presents a negative ITGA7 population of 24% (green) and a positive ITGA7 population of 76% (red and blue). In graph 4.6g the ITGA7+ population is plotted presenting the CD56 to CD29 expression. The ITGA7+ population is clearly separated into a population that is negative for both CD56 and CD29 (red), and a population that is positive for both CD56 and CD29 (blue). The ITGA7- population (green) is positive for CD29 and is both positive and negative for CD56. Based on the theory that ITGA7 targets satellite cells, it is indicated that the ITGA7- population of graph 4.6d is not satellite cells. As the whole ITGA7- population is positive for CD29 in graph 4.6f, these cells are identified as fibroblasts.

Table 4.1.: FACS results expressed as expression percentages of all samples. *P* indicates the passage number. Three passages of the identical sample are in bold.

| Cell type | ITGA7- CD29+ CD56-/+ | ITGA7+ CD29+ CD56high | ITGA7+ CD29- CD56- | IGTA7+ |
|---|---|---|---|---|
| Biopsy 1 | *fibroblasts (green)* | *satellite cells (blue)* | *maturing myogenic cells (red)* | *total myogenic* |
| B1 SM P4 enzyme | 84.3 | 15.1 | 0.0 | 15.4 |
| **B1 ST P3 enzyme** | **48.4** | **11.3** | **39.1** | **51.4** |
| **B1 ST P4 enzyme** | **24.0** | **8.4** | **66.0** | **75.9** |
| **B1 ST P5 enzyme** | **11.2** | **2.1** | **85.2** | **88.8** |
| Biopsy 2 | | | | |
| B2 SM P4 enzyme | 92.6 | 6.6 | 0.0 | 6.9 |
| B2 SM P4 explant | 92.5 | 7.0 | 0.0 | 7.2 |
| B2 ST P4 enzyme | 99.3 | 0.7 | 0.0 | 0.7 |
| B2 ST P4 explant | 99.6 | 0.4 | 0.0 | 0.4 |

According to literature, ITGA7 can be expressed during both proliferation and differentiation of satellite cells [155]. Therefore, the ITGA7+ population might be satellite cells in quiescent state, active state, or a later stage. The ITGA7+ population clearly separates in two colonies in graph 4.6g, which could indicate a separation of myogenic cells at different points of maturation. Similar to ITGA7, CD56 should express in SCs, but the specific time point of expression is questioned [155]. It is suggested that the ITGA7+/CD29+/CD56high population is satellite cells and that the ITGA7+/CD29-/CD56- population is myogenic cells in a later stage of maturation. Additional experiments are required to identify the cell types with more certainty. Interestingly, the population expected to be fibroblasts also partly expresses CD56, which is unexpected.

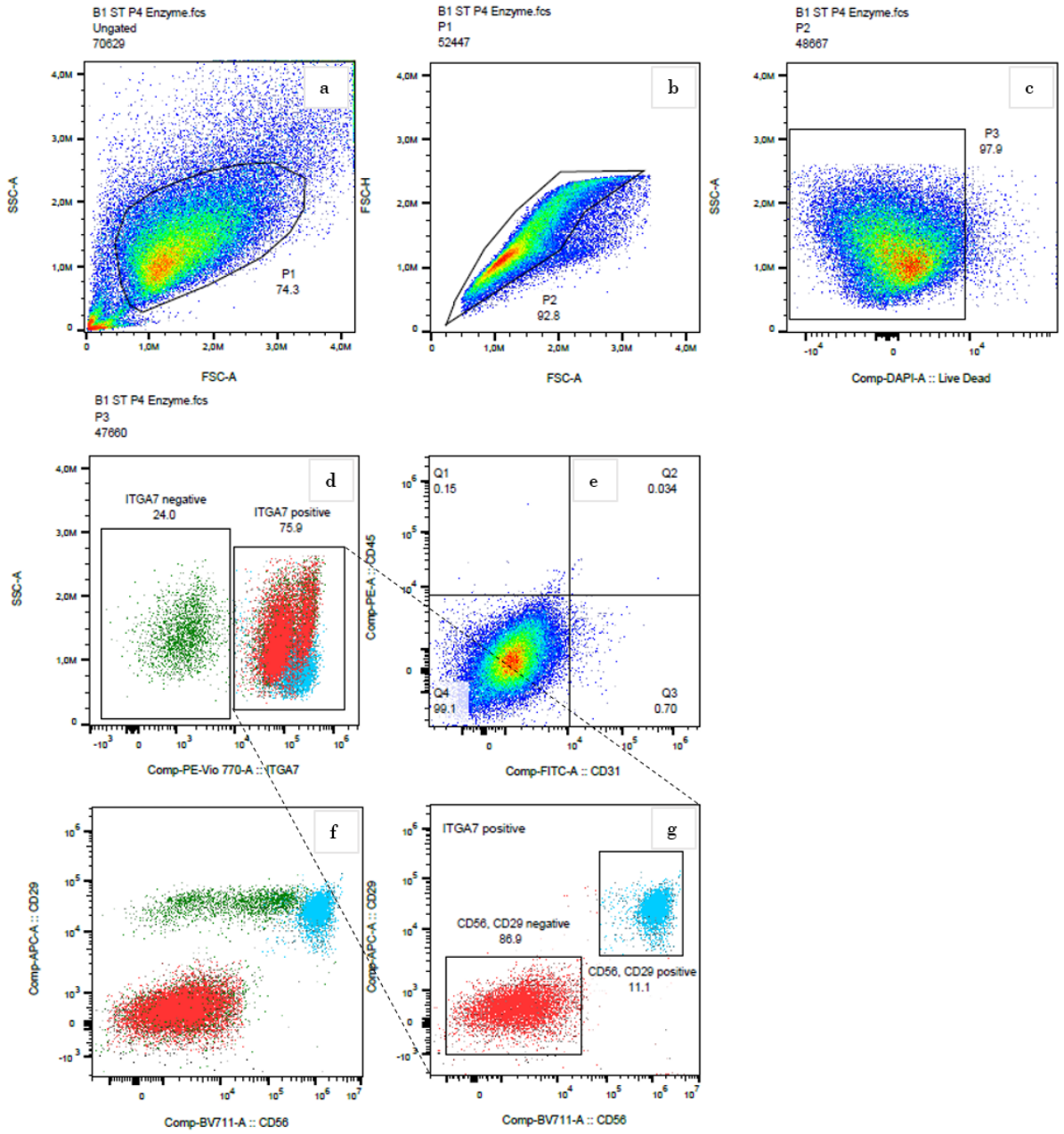


Figure 4.6.: FACS plots of enzymatic isolated ovine B1 ST P4 cells. Graphs are explained in the text.

The antibodies were not tested on pure satellite cell populations or pure fibroblast populations, due to a lack of time. Results of these experiments would have been useful as controls. To improve identification of the cells, the populations could be separated and assessed by Pax7 immunofluorescence and a differentiation assay. Pax7 indicates if the cells are myogenic. Pax7 is expressed during a certain time frame, so optimisation of the staining timing is advised. The aim of the differentiation assay is to starve the cells of serum and assess if the cells initiate differentiation by cell alignment and fusion into myotubes. Immunofluorescence with myosin will provide a clear indication of which populations are myogenic and which are not. Nevertheless, both assessments will not distinguish expression in quiescent satellite cells and expression in satellite cells at a certain stage of maturation.

Summarising the results: it is suggested that the ITGA7-/CD29+/CD56-+ population is fibroblasts, the ITGA7+/CD29+/CD56high population is satellite cells, and the ITGA7+/CD29-/CD56- population is myogenic cells in a later stage of maturation than satellite cells. Building on these assumptions, the FACS results of the other samples are analysed similarly and an overview of the expression percentages is presented in table 4.1. Enzymatic isolated B1 ST cells of passage 3 to 5 are in bold, because something interesting is observed. It can be seen that the fibroblast and SC populations are decreasing, while the maturing myogenic cell population is increasing. This is interesting, as the cell type ratio was not expected to change. The change might be caused by culturing the cells above 70% confluency and thereby activating the SCs to start the maturation process. The reason of decrease in fibroblast population might be caused by overgrowing of the satellite cells or in general not doing well on the ECM excreted by the myogenic cells, but this is only speculation. The decrease in fibroblasts contradicts literature, as fibroblasts are regularly seen to grow faster than myogenic cells, resulting in potential overgrowth by fibroblasts [186]. It is moreover observed that none of the SM samples or samples of biopsy 2 contain maturing myogenic cells and that both B2 ST samples contain mostly fibroblasts. The B2 SM samples contain a small amount of SCs, but the general SC yield of biopsy 2 is significantly lower than observed in biopsy 1. The enzymatic isolated samples were tested on differentiation capability by serum starvation and, although the samples of biopsy 2 are low in myogenic marker expression, all enzymatic isolated samples were capable of differentiation. See figure 4.7. The difference in amount of satellite cells could be due to the enzyme type, however it could be also be due to differences in the biopsies. Collagenase type 1 was used for biopsy 1, collagenase type 2 was used for biopsy 2. The biopsies were taken from different ovines, and therefore individual physiology can have caused variety in tissue samples. There is not enough data to conclude the influence of the collagenase type on the isolated cell populations.

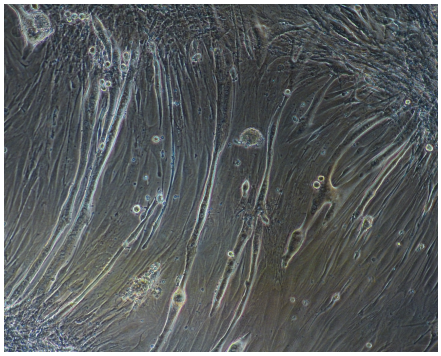

(a) B1 ST enzymatic isolated cells, passage 4.

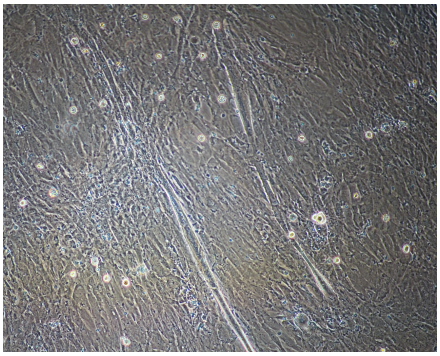

(b) B1 SM enzymatic isolated cells, passage 4.

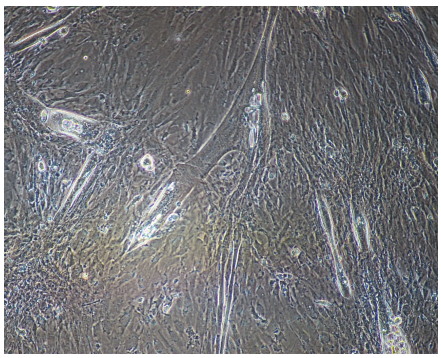

(c) B2 ST enzymatic isolated cells, passage 4.

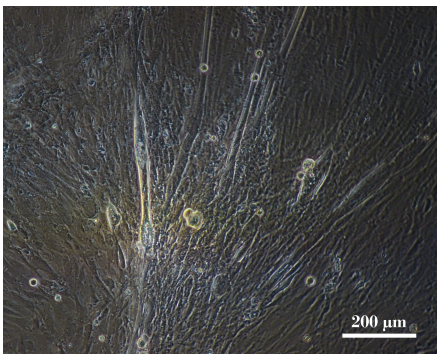


(d) B2 SM enzymatic isolated cells, passage 4.

Figure 4.7.: Differentiation of the enzymatic isolated cell samples. Scalebar: 200 $\mu$m.

To increase the chances of enriching the satellite cell population, the isolated samples could be pre-plated on collagen coated dishes [129]. Fibroblasts are known to adhere faster than myogenic cells. Therefore, seeding the hetereogenous cell samples on a collagen coated dish for 24 hours, followed by transferring the supernatant containing myogenic cells to a fresh dish has shown to reduce the percentage of fast adhering fibroblasts in the population [160]. Additionally, the growth of satellite cells could be enhanced by growth factors like IGF and FGF, which might support the satellite cells to overgrow the fibroblasts [187].

## 4.3. Biomarker profile

Expression of the proteins Pax3, Pax7, MyoD, myogenin, and myosin was analysed in the enzymatic isolated B1 ST ovine cells at passage 5 and the purified ovine SCs at passage 4. The time line of expression of these proteins can be found in figure 2.2. Pax3, Pax7, and MyoD are expected to express from early proliferation to early differentiation. Myogenin is expected to express from late proliferation to late differentiation, and myosin is expected to express during late differentiation. The protein expression of the enzymatic isolated B1 ST cells at passage 5 is presented in table 4.2 and figure 4.8, and the protein expression of purified ovine SCs for control is presented in table 4.3 and figure 4.9. Pax3 is not expressed during proliferation or differentiation of both the isolated sample and the purified SCs. As mentioned in section 2.4.3, not al SCs express Pax3, so this is not unexpected. Contrarily, Pax7 is clearly expressed during all stages. The highest expression of Pax7 is seen during late proliferation, and a significant decrease is seen during early differentiation. Expression during late differentiation is higher than early differentiation, which is unexpected, but the error at this stage is relatively large. However, a similar expression pattern is presented by the purified SCs. Moreover, Pax7 is expressed in 81.9% of the isolated cells during late proliferation, which approaches the 88.8% of ITGA7+ cells presented by the FACS results of B1 ST P5 enzyme in table 4.1. This suggests that the ITGA7+ cells are myogenic. It is noteworthy that the purified SCs have an expression of Pax7 during late proliferation of more than 100%, which is not possible. This indicates that the results of this experiment can not be treated as conclusive.

Table 4.2.: Percentages of protein expressing cells of the total amount of cells, for enzymatic isolated ovine B1 ST cells at passage 5. Percentages higher than 0.00 are in bold.

| Ovine B1 ST P5 | Pax3 | Pax7 | MyoD | myogenin | myosin |
|---|---|---|---|---|---|
| Early P | 0.0 | **21.3** | **4.0** | 0.0 | 0.0 |
| Late P | **0.2** | **81.9** | 0.0 | **5.4** | 0.0 |
| Early D | 0.0 | **3.7** | 0.0 | **1.6** | **1.1** |
| Late D | 0.0 | **12.7** | 0.0 | **10.0** | **10.3** |

Table 4.3.: Percentages of protein expressing cells of the total amount of cells, for purified ovine satellite cells at passage 4. Percentages higher than 0.00 are in bold.

| Ovine SCs P4 | Pax3 | Pax7 | MyoD | myogenin | myosin |
|---|---|---|---|---|---|
| Early P | 0.0 | **65.4** | **0.6** | 0.0 | 0.0 |
| Late P | 0.0 | **109.7** | 0.0 | **3.5** | 0.0 |
| Early D | 0.0 | **20.1** | 0.0 | **9.9** | **2.7** |
| Late D | 0.0 | **46.1** | 0.0 | **12.0** | **8.3** |

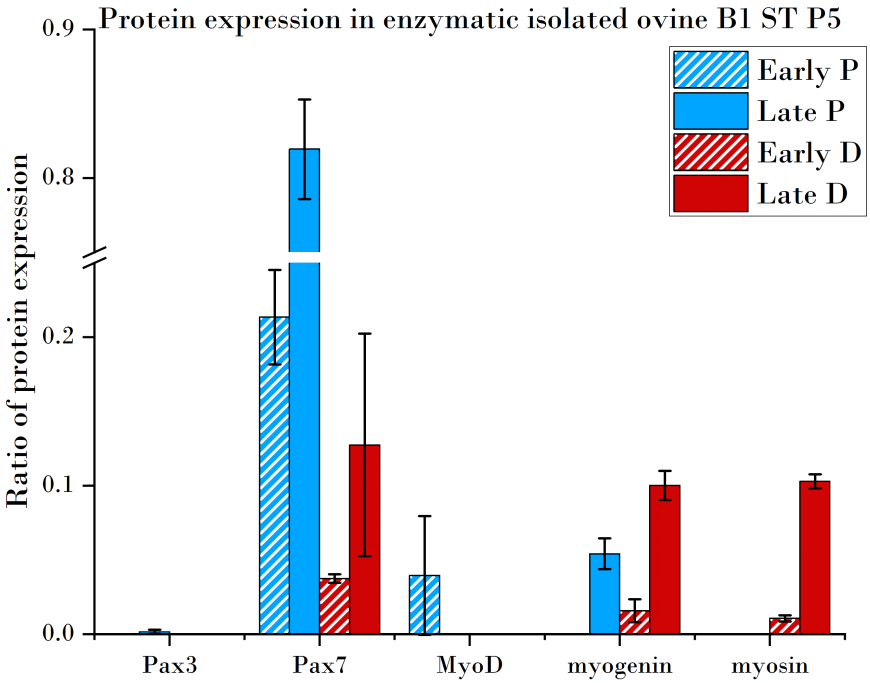


Figure 4.8.: Expression of proteins in enzymatic isolated ovine B1 ST cells at passage 5, during early proliferation (Early P), late proliferation (Late P), early differentiation (Early D), and late differentiation (Late D).

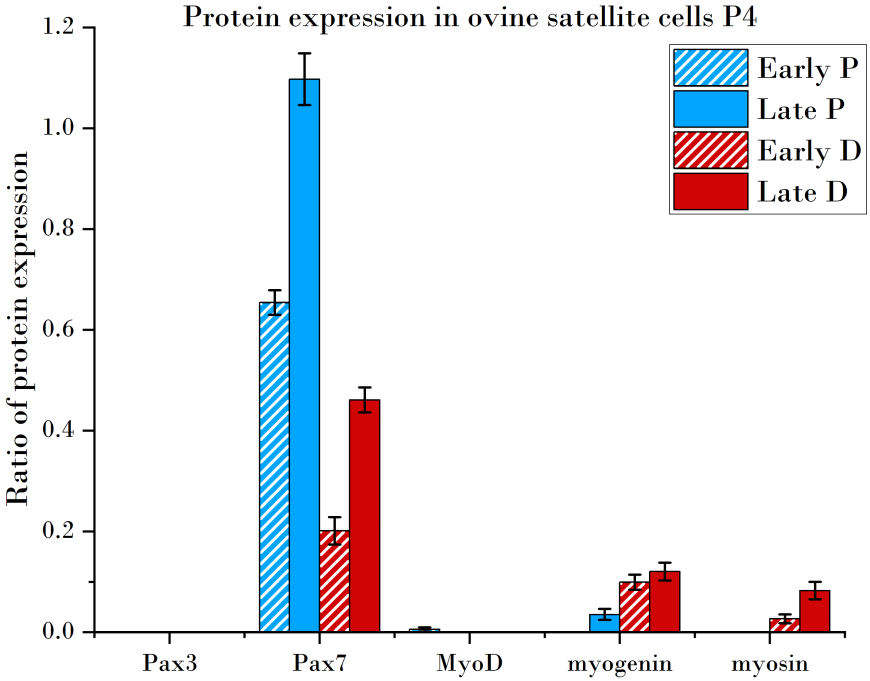


Figure 4.9.: Expression of proteins in purified ovine satellite cells at passage 4, during early proliferation (Early P), late proliferation (Late P), early differentiation (Early D), and late differentiation (Late D).

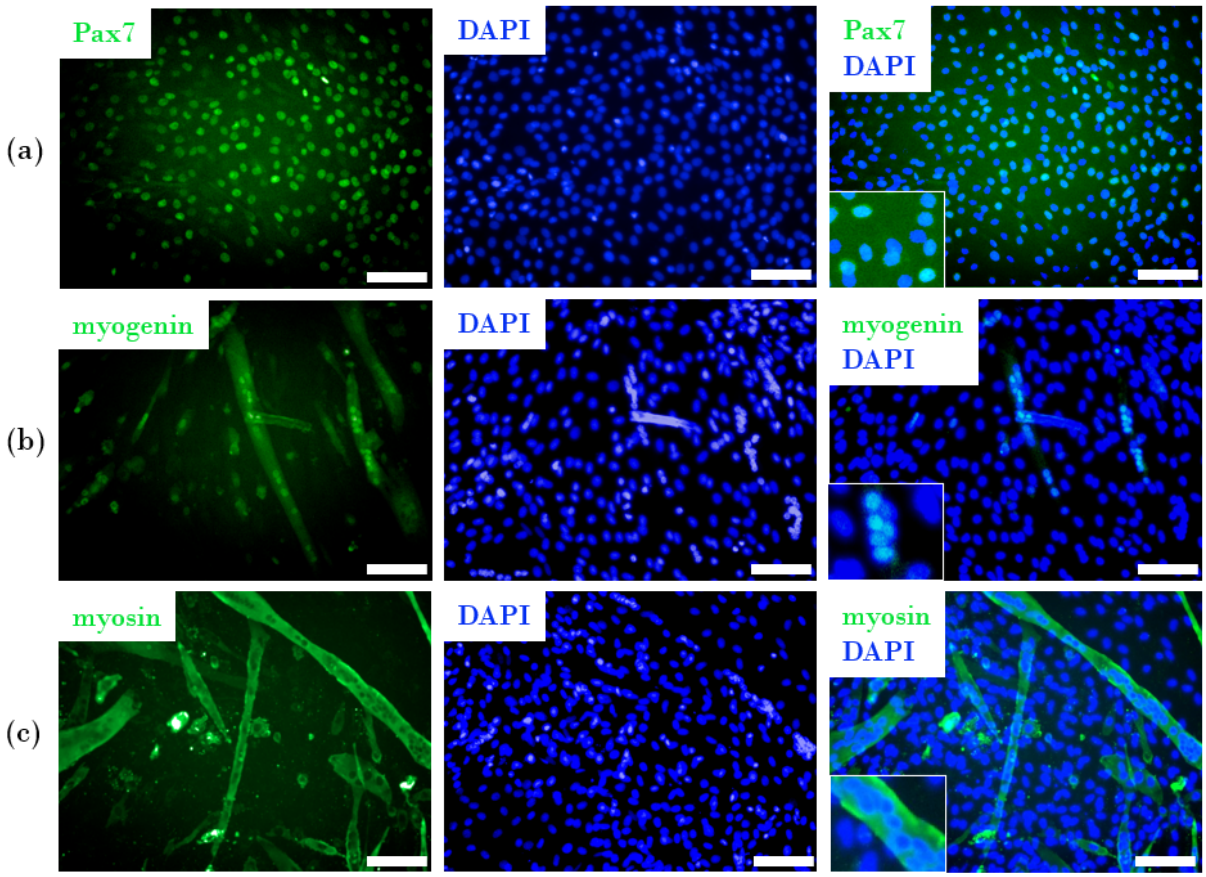


Figure 4.10.: Immunofluorescent images of marker expressions in the enzymatic isolated ovine B1 ST cells at passage 5. Scalebar: 200 $\mu$m. (a) Pax7 expression (green) and DAPI (blue) during late proliferation; (b) myogenin expression (green) and DAPI (blue) during late differentiation; (c) myosin expression (green) and DAPI (blue) during late differentiaton.

A small amount of MyoD is expressed only during early proliferation in the isolated sample, which is similar to the expression of the purified SCs. As described in section 2.4.3, early expression of MyoD indicates activated SCs. Furthermore, upregulation of MyoD is generated by Pax7, followed by coexpression of Pax7 and MyoD, which could explain the expression of MyoD during early proliferation. However, the low percentage of MyoD expressing cells during early proliferation (4%) and the corresponding error make this result insignificant. Unexpectedly, MyoD is not expressed at a later time point of analysis. The lack of expression could be caused bynon-optimal time points of analysis, with MyoD being expressed in between time points. However, even if this would be the case it would be expected to see a small amount of expression in the measurements of late proliferation and early differentiation.

Myogenin is expressed from late proliferation to late differentiation, as expected. The sudden decrease in expression during early differentiation is unexpected, and this phenomenon is not seen in the expression of purified SCs. Myosin is slightly expressed during early differentiation and late differentiation. Similarity is seen between the expression percentage of myogenin and myosin during late proliferation. It is expected that the difference between myogenin and myosin would be larger if the analysis of late differentiation was performed after longer differentiaiton of the cells. 3T3 cells were used in this experiment as a negative control and expression of the markers was 0% at all time points. This confirms that the used markers do not express in fibroblasts and that all cells expressing the markers are myogenic.

## 4.4. Proliferation

During proliferation, cells were cultured in growth medium (DMEM 4.5 g/L D-Glucose, GlutaMax™ supplement, supplemented with 10% FBS and 1% A-A) and analysed by brightfield microscopy on a daily basis. See figure 4.11 for two brightfield microscopy images that were taken two days apart, at the same location, of ovine B1 ST enzymatic isolated cells of passage 1. The cells were capable of proliferation and grew into a confluent culture.

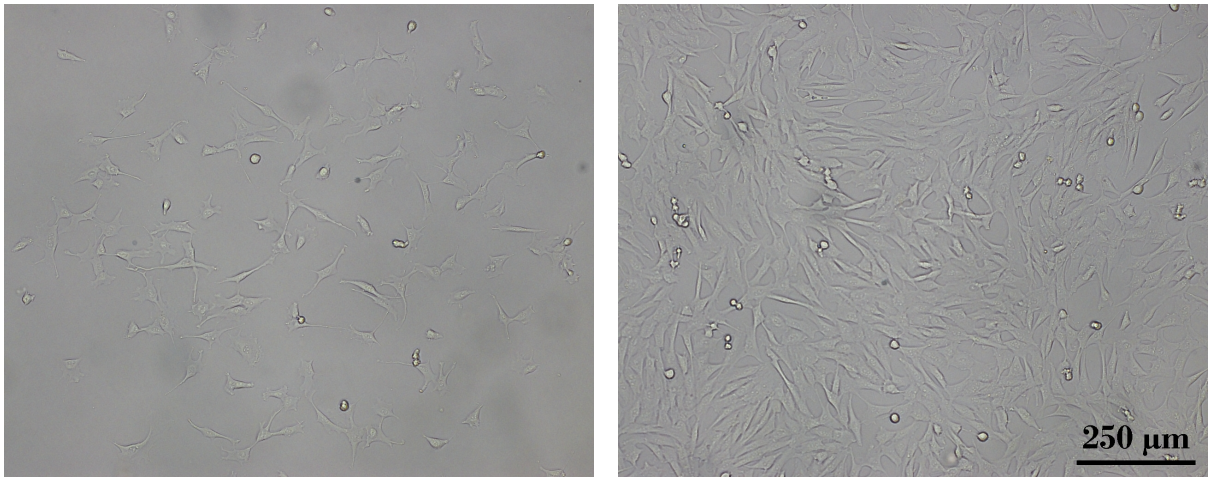


(a) Picture taken on day 4 of proliferation. (b) Picture taken on day 6 of proliferation.

Figure 4.11.: Ovine B1 ST enzymatic isolated cells passage 1, pictured 2 days apart at the same location. Scalebar: 250 $\mu$m.

Visual analysis gives an indication of the performance of the cells, however these results are not quantifiable. To obtain quantifiable data, the population doubling rate of all isolated samples was determined. All six isolated samples were included in this experiment. Purified bovine SCs were used as control. These cells are currently used for research and development of cultured meat at cultured meat company Mosa Meat, and can therefore indicate the expected cell performance of cells for cultured meat applications. C2C12 cells were also used as control, as these are elaborately studied for cell culture and tissue engineering applications. The population doubling rates are presented in figure 4.12, where the cumulative population doublings are set out to the proliferation time in days. The population doublings were logged from passage 2 to passage 7, including exact times of seeding and harvesting. The process was performed in duplicate, but the duplicate had to be terminated early due to contamination. Data points including error bars are averages of the duplicates. Bovine was terminated prior to the other samples, as it showed contamination likewise. The results present that sample 'B1 ST enzyme' demonstrates the most cumulative population doublings of all isolated ovine samples after 18 days of proliferation, approaching the number of doublings of the C2C12 cells. Surprisingly, the bovine SCs demonstrate a relatively low amount of cumulative doublings. It can be argued that the bovine SCs were affected by the contamination vested in the sample before termination, however this seemingly low proliferation rate could be a property of the cells as well. The bovine cells are purified SCs, while the isolated ovine cells are heterogenous samples of myogenic cells and presumably fibroblasts. The heterogeneity might influence the population doubling rate, as co-culture of myoblasts and fibroblasts can increase myoblast proliferation, according to literature [188, 189]. Long term passaging and replicates are advised for more complete representation of the cumulative population doublings.

As mentioned in the previous alinea, heterogeneity might influence the population doublings rate. According to literature, fibroblasts can increase myoblast proliferation. However, the

population doubling rates presented here suggest that an excess of fibroblasts will inhibit proliferation. When relating the cumulative population doublings to the identified cell types in the samples, presented in table 4.1, it stands out that the enzymatic isolated B1 ST sample produced the highest amount of population doublings and also contains the highest number of myogenic cells. The enzymatic isolated B1 SM sample produced the second highest amount of population doublings and contains the second highest number of myogenic cells. The samples isolated from biopsy 2 have produced the lowest amount of population doublings and also demonstrate the lowest percentage of myogenic cells. This indicates that the myogenic cells are responsible for the speed of the population doublings. More data needs to be obtained to confirm this. Additionally, if the cells were cultured to a confluency above 70%, it might be possible that the SCs were activated to start maturation, leading to loss of stemness and decreasing the population doubling rate in the samples demonstrating relatively low population doubling rates.

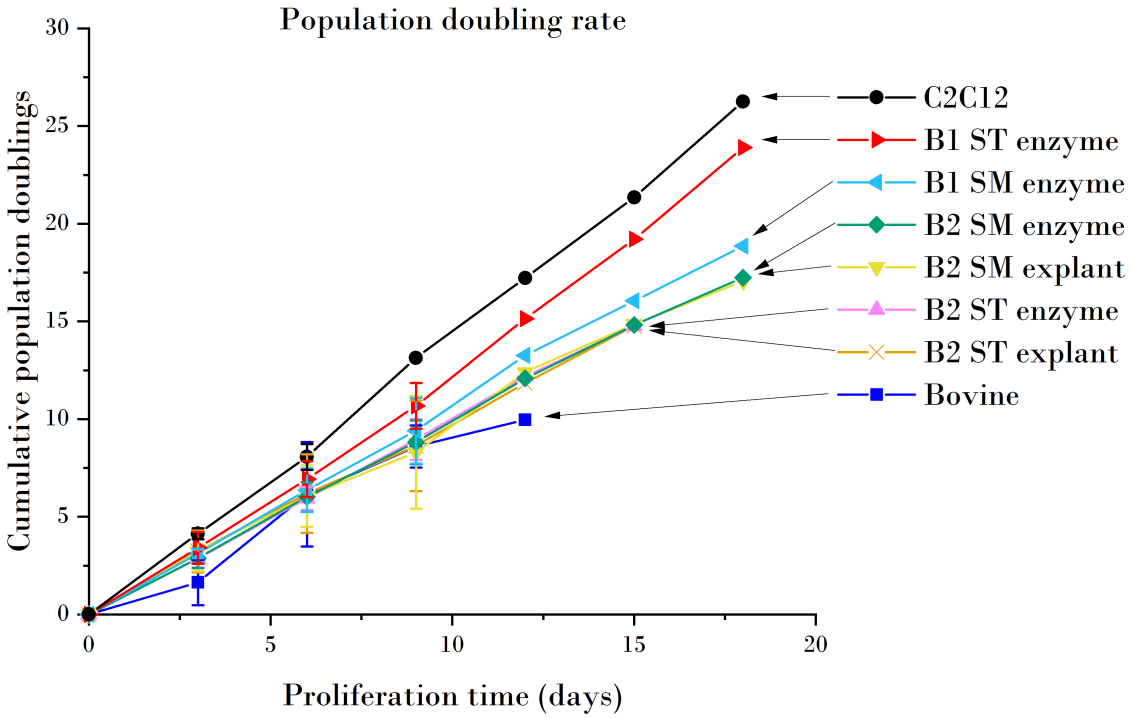


Figure 4.12.: Population doubling rate of the enzymatic isolated B1 ST cells, started at passage 2 for ovine cells and bovine SCs and passage 5 for C2C12 cells. Cumulative population doublings are set out to the proliferation time in days.

### 4.4.1. Metabolism

During one of the population doubling experiments, depicted in figure 4.12, the metabolism rate of all isolated samples was measured by an MTT assay at every passage. As described in section 3.8.5, the metabolism rate of a cell population is not inherently correlated with proliferation rate of the population. However, it does provide an indication of population growth, as it is assumed that the cells present in the isolated samples are comparable in speed of metabolism, and an increase in speed of metabolism therefore suggests an increase in cells. At every passage, all samples were seeded at a seeding density of 2,000 cells/cm$^2$ and proliferated for 3 days before the MTT assay was performed. As the cells had 3 days to proliferate before the metabolism rate

was measured, a higher absorbance during the MTT assay is assumed to be related to a higher proliferation rate. The MTT assay was included to support the measurements of the population doublings experiment. Figure 4.13 presents the results of the MTT assay, where the passage numbers are set out to the measured absorbance. The experiment was performed once, with each plotted point being the average of 6 wells. Some points include a large margin of error. Taking this into account, the results will not be treated as conclusive but as an indication. It stands out that the enzymatic isolated B1 ST sample presents a higher absorbance than the other isolated samples. This supports the population doubling results, presented in figure 4.12, where the enzymatic isolated B1 ST sample presented a higher proliferation rate than the other samples. C2C12 cells were included as a control group but were measured at different passages, which is indicated by the labels in the graph. The enzymatic isolated B1 ST sample approaches C2C12 cells in metabolism rate, which supports the results of the population doublings experiment. Bovine SCs demonstrate the lowest metabolism rate of all samples, supporting the results of the population doubling experiment likewise. The bovine SCs were terminated one passage prior to the other samples, due to an infection.

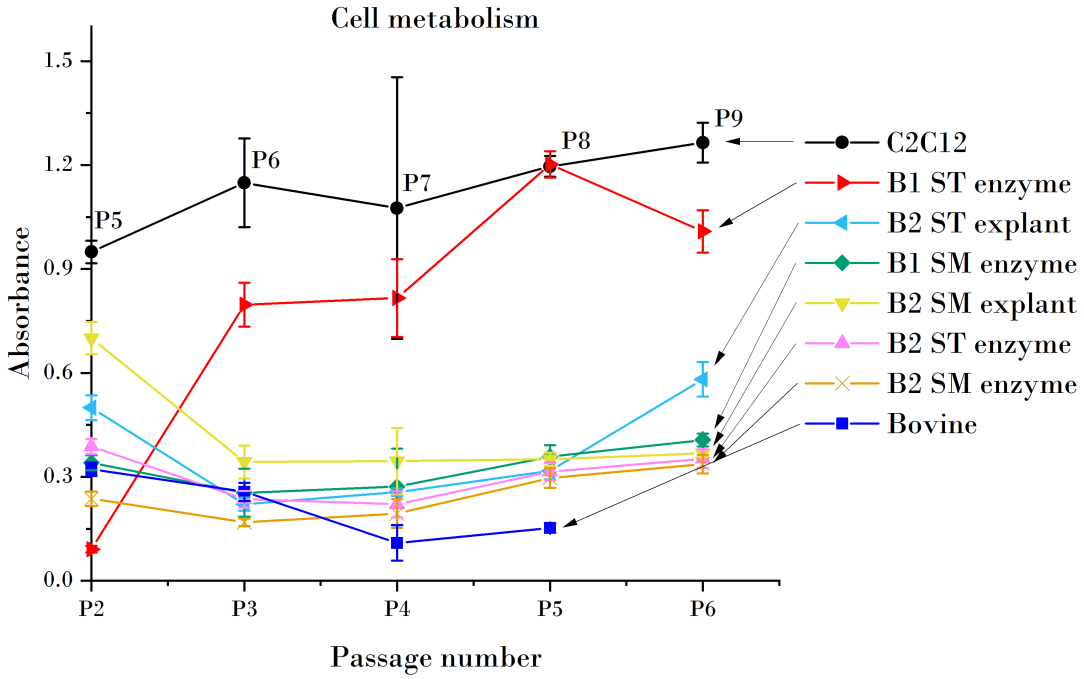


Figure 4.13.: Cell metabolism measured by an MTT assay. The C2C12 cells were started at a different passage, which is indicated by the additonal labels in the graph.

### 4.4.2. The effect of coating

Cells were cultured on collagen and Matrigel coating, to determine the effect on the proliferation rate. All isolated samples were cultured on non-coated tissue culture plates, collagen coated plates, and Matrigel coated plates. Figure 4.14 presents the average of all ovine isolated samples combined. Results of the individual samples can be found in Appendix C. Figure 4.14 demonstrates a strong cell preference for the collagen coating, as it results in the highest cell count after 3 days during proliferation. The Matrigel coating results in a slightly lower cell count when compared to uncoated tissue culture plates. This experiment was performed once with three wells per sample. Although more data should be included to be able to treat the results

as conclusive, these results indicate that proliferation of ovine cells is supported by a collagen coating. It should be noted that a different coating might be preferred during differentiaton.

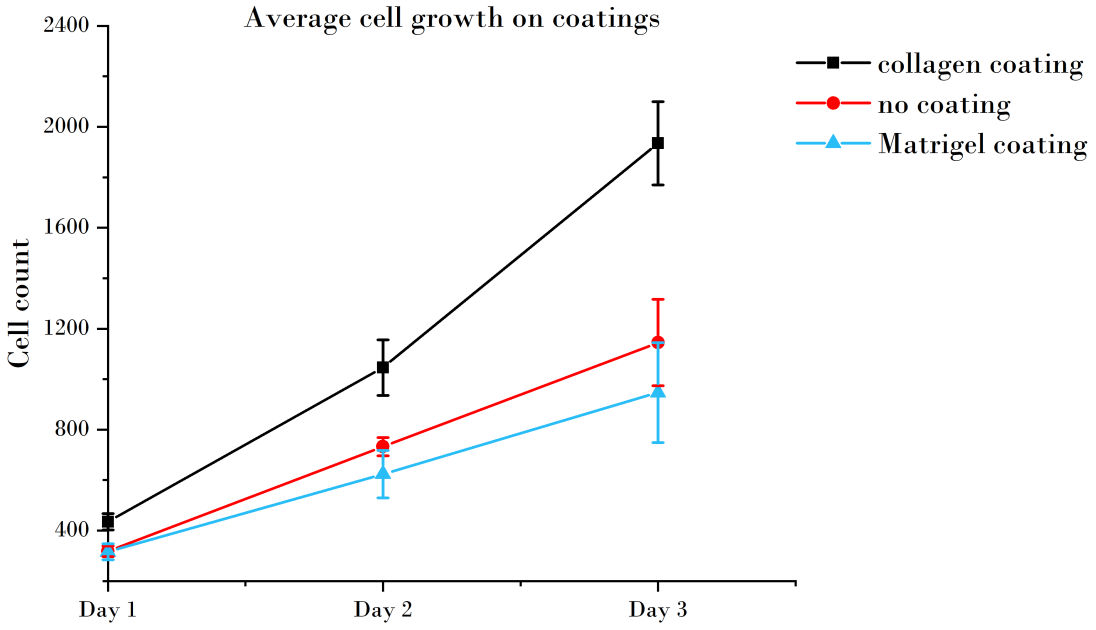


Figure 4.14.: Proliferation of the ovine cells on tissue culture plates without coating, with collagen coating, and with Matrigel coating. This graph represents the average of all isolated ovine samples. Cells were counted on day 1, 2, and 3 of proliferation.

## 4.5. Differentiation

To determine if the cells were capable of differentiation, the cells were proliferated into complete confluency and subsequently starved from serum in medium containing 2% horse serum. Cell alignment and fusion was observed by brightfield microscopy, as presented in figure 4.15. To confirm myogenic differentiation, enzymatic isolated B1 ST cells were stained for myosin. Figure 4.16 presents pictures of the immunofluorescent staining with myosin and DAPI. Myosin has clearly come to expression proving that the cells are capable of differentiation. This inherently provides an additional confirmation that myogenic cells are present in the sample. The other enzymatic isolated samples were likewise starved from serum and cell alignment and fusion was observed, as presented in figure 4.7, however these samples were not analysed on myosin expression.

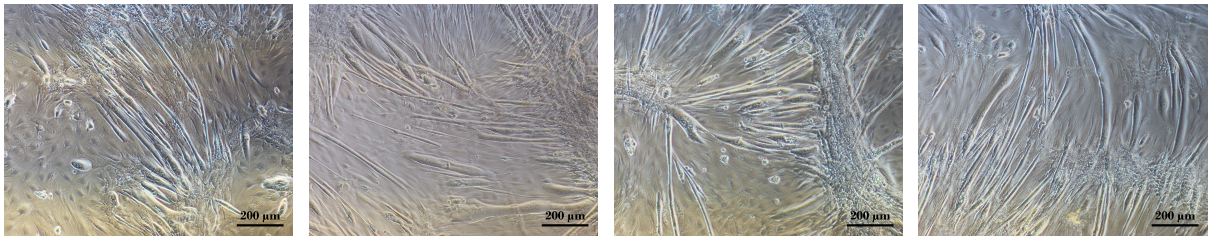


Figure 4.15.: Ovine B1 ST enzymatic isolated cells at passage 3. Pictures taken at different wells, on day 8 of differentiation. Scalebar: 200 $\mu$m.

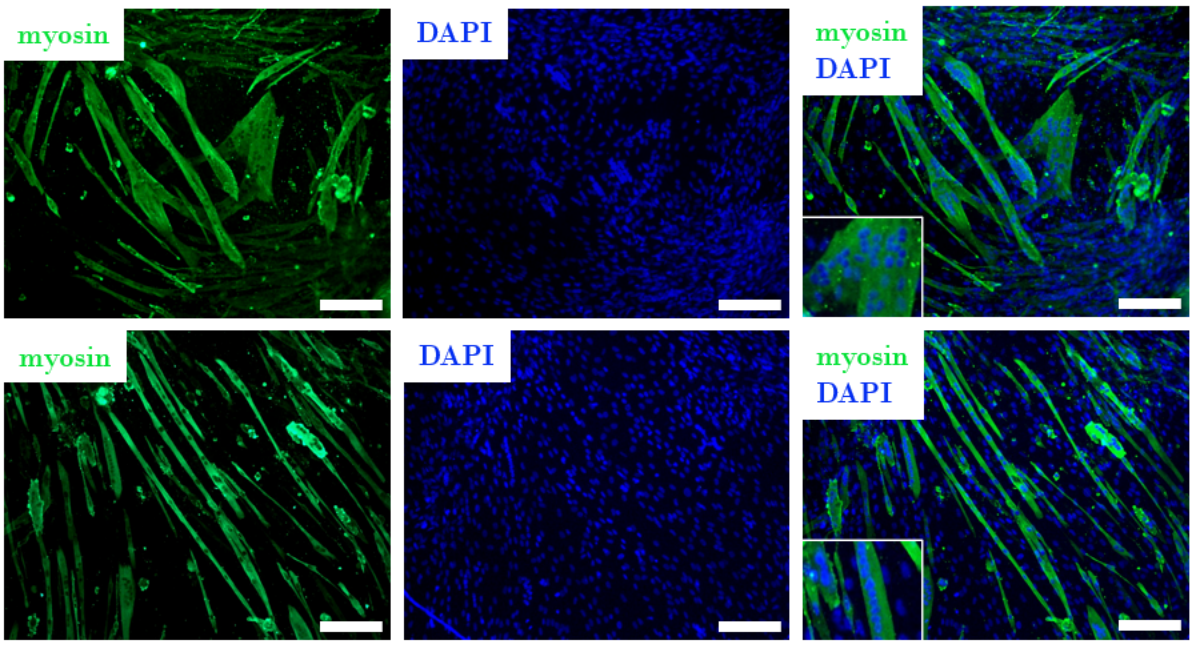


Figure 4.16.: Ovine ST B1 enzymatic isolated cells at passage 5, differentiated and stained for myosin (green) and DAPI (blue). Pictures taken at different wells. Scalebar: 200 $\mu$m.

## 4.6. Tissue constructs

A crucial aspect of cultured meat production is the capability of cells to form 3D muscle constructs. Therefore, the cells were introduced to a 3D environment that supports formation of myofibres. As described in section 3.6, the cells were seeded in a hydrogel containing collagen and Matrigel. Gradually increasing cell densities were experimented with before proper cell compaction was seen at a cell seeding density of $16 * 10^6$ cells/ml. The cell-laden hydrogels were seeded in the four pillar system presented in figure 3.3b. Figure 4.17 provides an overview of the development of one of the 3D constructs over time, containing enzymatic isolated B1 ST cells at passage 5. On day 1 and 2 a compacted 3D construct is observed. However, the construct is visibly experiencing tension and some parts of the construct appear to be translucent, indicating uneven distribution of the cells. Growth medium (DMEM supplemented with 10% FBS and 1% A-A) was replaced by differentiation medium (DMEM supplemented with 2% horse serum (HS) and 1% A-A) on day 3. On day 4, the tension caused the construct to detached from the upper right pillar. A high level of tension can be seen in the tissue around the lower right pillar. On day 5, the construct is detached from three of the four pillars. At this point, no more tension is excerted on the tissue and myofibre formation is unlikely.

The translucent patches and the detaching of the tissue presented in figure 4.17 suggest that the constructs might benefit from a higher cell density. This motivated the decision to double the cell seeding density to $32 * 10^6$ cells/ml. Figure 4.18 provides an overview of the development of one of the constructs containing this seeding density over time. The cells have compacted and the construct is less translucent. On day 2 and 3 it was observed that the construct decreased slightly in width, due to further compaction of the cells. Growth medium was replaced by differentiation medium on day 3. Although the tension on the construct is less clearly visible than in figure 4.17, the construct detached from three of the pillars on day 4, resulting in a non-structured cluster of cells similar to the previous results with $16 * 10^6$ cells/ml.

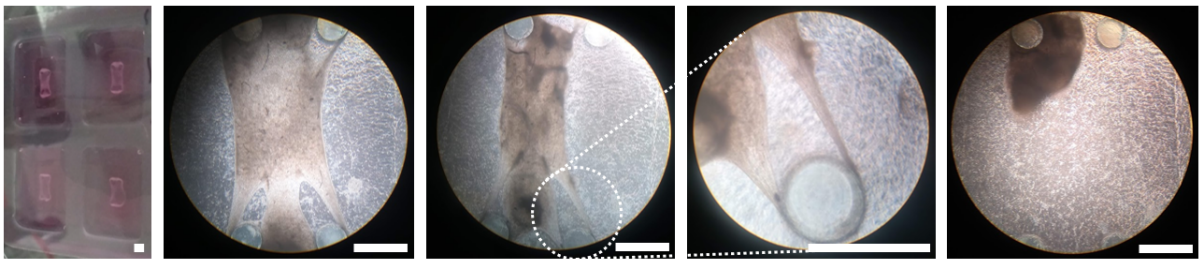


Figure 4.17.: 3D constructs made with enzymatic isolated ovine B1 ST cells at passage 5. Cell seeding density: $16*10^6$ cells/ml. Scalebars: 1 mm. Camera settings are described in section 3.8.1.

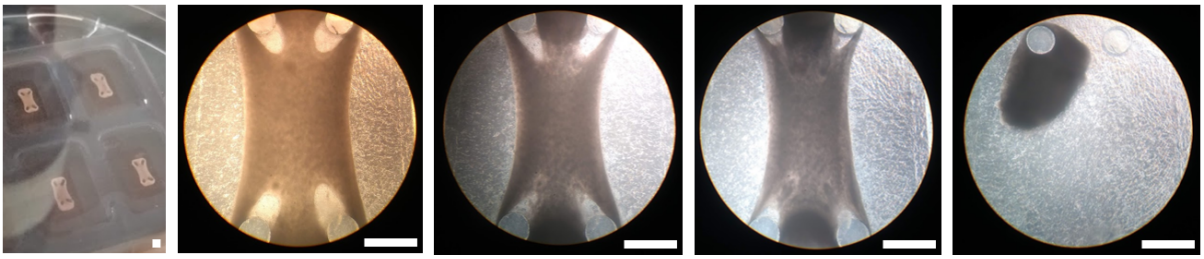


Figure 4.18.: 3D constructs made with enzymatic isolated ovine B1 ST cells at passage 5. Cell seeding density: $32 * 10^6$ cells/ml. Scalebars: 1 mm.

As the cell density was relatively high compared to literature, it was decided not to increase the cell density further. Instead, the system was tested with C2C12 cells to investigate if the constructs stay intact when using this cell line, as described in literature. An overview of the development of one of the C2C12 constructs over time is presented in figure 4.19. Slower compaction was observed in the C2C12 constructs, compared to the ovine constructs. Additionally, the constructs stayed intact for a longer time. Detachment of the pillars occured after 19 days of culture. Moreover, the constructs exercised spontaneous contraction from day 7 onwards. The contractions occured without any external stimulation and when removed from the incubator and kept at room temperature for over 15 minutes, frequent contractions were mintained. The contractions started small and locally, but developed into full construct contractions on day 19. Due to time constraints, it could not be investigated what was causing the contractions, however they are expected to result from myosin and actin interaction. After culturing the constructs for 23 days in total, of which 20 days in differentiation medium, the constructs were stained for myosin following the protocol described in section 3.8.4. Myosin was expected to be expressed throughout the whole construct, but no clear expression of the protein was observed by confocal microscopy. As it is unlikely that myosin is not expressed by the cells, it is expected that the antibodies for immunofluorescence were not fully permeated into the constructs. Unfortunately, optimisation of the staining protocol was not successful during the limited amount of time.

The spontaneous contraction of the C2C12 constructs motivated the investigation of the difference between the C2C12 constructs and ovine cell constructs. Fresh ovine constructs were made with the aim to closely monitor all constructs during the developmental process and to investigate if a part of the developmental process could be correlated with cell differentiation. For comparison, the goal was to assess the width of the constructs over time. Moreover, if the constructs would stay intact for at least 4 days the cells in the constructs would be analysed on myogenin and myosin expression. Unfortunately, all six constructs detached from the pillars on

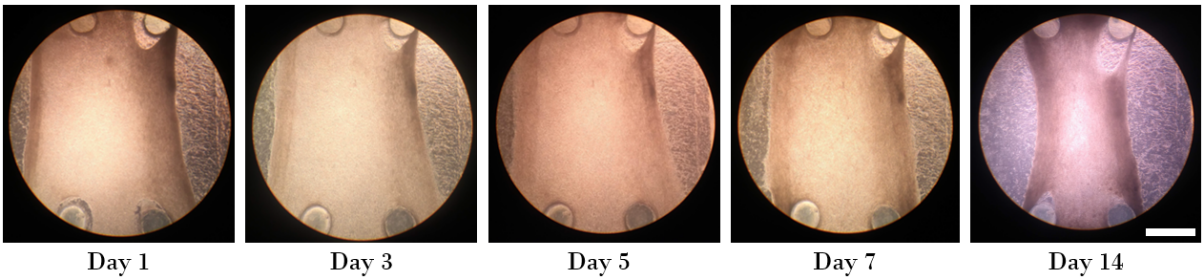


Figure 4.19.: 3D constructs made with C2C12 cells at passage 9. Cell seeding density: $32 * 10^6$ cells/ml. Scalebar: 1 mm.

day 3. Figure 4.20 presents an overview of three of the ovine constructs. It was observed that the ovine constructs compacted faster than the C2C12 constructs and that the width of the constructs was smaller. The ovine constructs display a construct width on day 1 that is only seen in the C2C12 constructs on day 14. This indicates that the ovine constructs experience a higher tension than the C2C12 constructs. A distinct difference between the two cell samples is that the C2C12 sample is a purified myoblast population, while the ovine cell sample is expected to be 89% myogenic cells and 11% fibroblasts. An interesting additional experiment would be to create 3D constructs of purified ovine SCs for comparison. Moreover, it would be interesting to investigate the effect of fibroblasts in the culture, by preparing constructs with different ratios of SCs and fibroblasts.

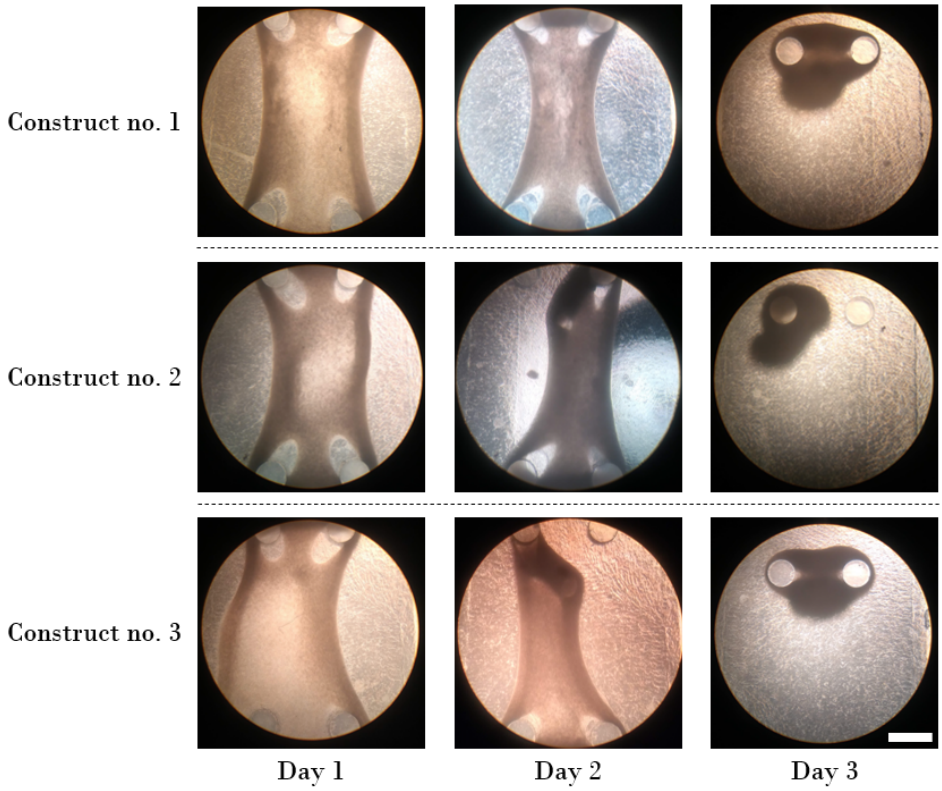


Figure 4.20.: 3D constructs made with enzymatic isolated ovine B1 ST cells at passage 5. Cell seeding density: $32 * 10^6$ cells/ml. Scalebar: 1 mm.

The system of figure 3.3a was initially used while optimising the cell seeding density. However, when the seeding density was increased it was concluded that a smaller distance between the pillars and a smaller diameter of the pillars was preferred to limit the required amount of

hydrogel and cells. The system depicted in figure 3.3b was therefore used for the experiments elaborated on above. Additonally, the systems depicted in figure 3.3c and 3.3d were tested. Due to time constraints they were not as intensively studied as the other systems, however, construct formation was observed in both systems when seeded with C2C12s or ovine cells. Figure 4.21 presents brightfield images of both systems. It was expectation that the cells would integrate in and around the pillars of the 16 pillar system, and that a homogenous compacted tissue would be formed. However, it was observed that the pillar array was treated as one large pillar and most of the cells compacted around the outer bounds of the pillar array. For both ovine cells and C2C12 cells it was observed that the pillars do not excert the expected tension on the tissue and that the tissue compacts in clusters randomly distributed along the outside of the pillar array, as demonstrated in figure 4.21a and 4.21b. The four pillar system with a smaller pillar distance, presented in figure 4.21c and 4.21d, was designed to avoid construct detachment off of the pillars. It was observed that the constructs stayed intact for longer and started detaching on day 6 when seeded with ovine cells. When seeded with C2C12s, detaching started on day 22. The 16 pillar system and both the four pillar systems presented in this section were seeded with the identical C2C12-laden hydrogel at the same moment. In all systems, spontaneous contraction was observed from culture day 4 onwards.

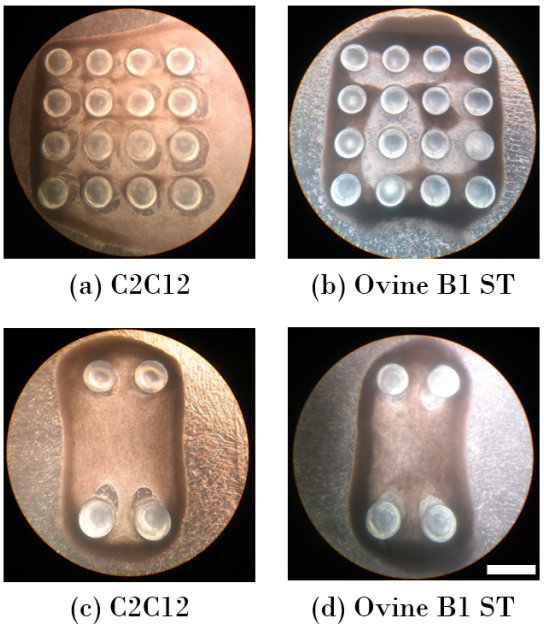

(a) C2C12 (b) Ovine B1 ST

(c) C2C12 (d) Ovine B1 ST

Figure 4.21.: 3D constructs made in the (a-b) 16 pillar array system and (c-d) four pillar system with decreased pillar distance. C2C12 cells at passage 9, enzymatic isolated ovine B1 ST cells at passage 5. Cell seeding density: $32 * 10^6$ cells/ml. Scalebar: 1 mm.

The arrangement of the pillars did not affect the initiation of spontaneous contraction. However, the four pillar system containing the smallest pillar distance, presented in figure 4.21c, resulted in the longest time period of an intact tissue construct. Therefore, future research is recommended to proceed with the smaller pillar system depicted in figure 3.3c.

## 4.7. A cost effective alternative for DMEM

Various energy drinks were selected as cost effective alternatives for DMEM. The osmolarity and pH of the drinks were measured and are presented in table 4.4. Three drinks were selected for the cell culture experiment and were adjusted to a similar osmolarity and pH of DMEM by addition of baking powder, NaOH, and MilliQ. As described in section 3.7, V-energy was

selected because it contains guarana extract, LIVE+ was selected because it contains ginseng extract, and Gatorade was selected because it approaches the osmolarity and pH of DMEM. The selected energy drinks and their final osmolarity and pH are presented in bolt in table 4.4.

Table 4.4.: Osmolarity and pH of selected energy drinks, including the adjusted values for the cell culture experiment.

| Energy drink | Osmolarity (mmol/kg) | pH | Final osmolarity (mmol/kg) | Final pH |
|---|---|---|---|---|
| **V-energy Original Guarana** | 521 | 3.33 | **324** | **7.45** |
| **Persist LIVE+** | 582 | 2.60 | **327** | **7.71** |
| Mountain Dew | 611 | 3.12 | | |
| **Gatorade Fierce Berry** | 288 | 6.18 | **319** | **7.57** |
| Powerade ION4 Berry Ice | 234 | 3.40 | | |
| Monster Energy Original | 611 | 3.57 | | |
| Other fluids | | | | |
| DMEM, 10569 | 333 | 7.67 | | |
| MilliQ | 0 | 6.93 | | |

Each energy drink was mixed with DMEM in gradually increasing amounts ranging from 10% to 90% with intervals of 10%. 0% energy drink was used as control. The culture medium was composed by supplementing these solutions with 10% FBS and 1% A-A. The experiment was performed once with three wells per condition. An MTT assay was performed on day 4 of culturing the cells in the medium, to measure the cell metabolism during proliferation. The experiment was performed with enzymatic isolated B1 ST cells and C2C12 cells as control. Of the three selected energy drinks, cells cultured in Gatorade performed best. Figure 4.22 presents the results of the MTT assay performed on the cells cultured in Gatorade. The absorbance is normalised to the control group of 0% Gatorade. The condition containing 10% of Gatorade shows a large decrease in cell metabolism, and a continuous decrease is seen in cell metabolism for the conditions containing 20% and 30% of Gatorade. Metabolism approaches zero when 50% or more of DMEM is replaced by Gatorade, which indicates low cell viability. C2C12 cells are slightly more persistant at 20% and 30% of DMEM replacement, however the conditions containing 50% and higher do not support cell metabolism.

An additional MTT assay was performed on day 10 of cell culturing, without medium refreshment meanwhile. Cell alignment and fusion was observed by brightfield microscopy. Similar to during proliferation, cells cultured in Gatorade performed best. Figure 4.23 presents brightfield images of the cells cultured in medium containing 0-50% of Gatorade. The cells reached a high confluency in the conditions containing 0-40% of Gatorade, indicating that the cells are viable in these medium compositions. Cell alignment and fusion is observed, which is expected to be caused by serum starvation or the high level of confluency. The cells are not assessed on protein expression and it is therefore not possible to conclude at which stage of maturation the cells currently are, and if they are capable of full differentiation into myotubes. Figure 4.24 presents the results of the MTT assay after 10 days of culture. It can be seen that the conditions containing up to 40% of Gatorade return a higher metabolism rate than after 4 days of culture. It is expected that this is due to a longer period of time for proliferation, resulting in a larger amount of cells and reaching the threshold of confluency, therefore yielding a higher metabolism rate of the MTT solvent. However, more experiments should be performed to support this theory.

Although more experiments should be performed to draw a conclusion, these results indicate that the cell performance is affected by replacing the DMEM with energy drinks. However, partial replacement by energy drink seems to suppress some cell functions rather than being

completely toxic. Therefore, potential in DMEM replacement is seen and further research is recommended to investigate if more cost effective alternatives can be produced.

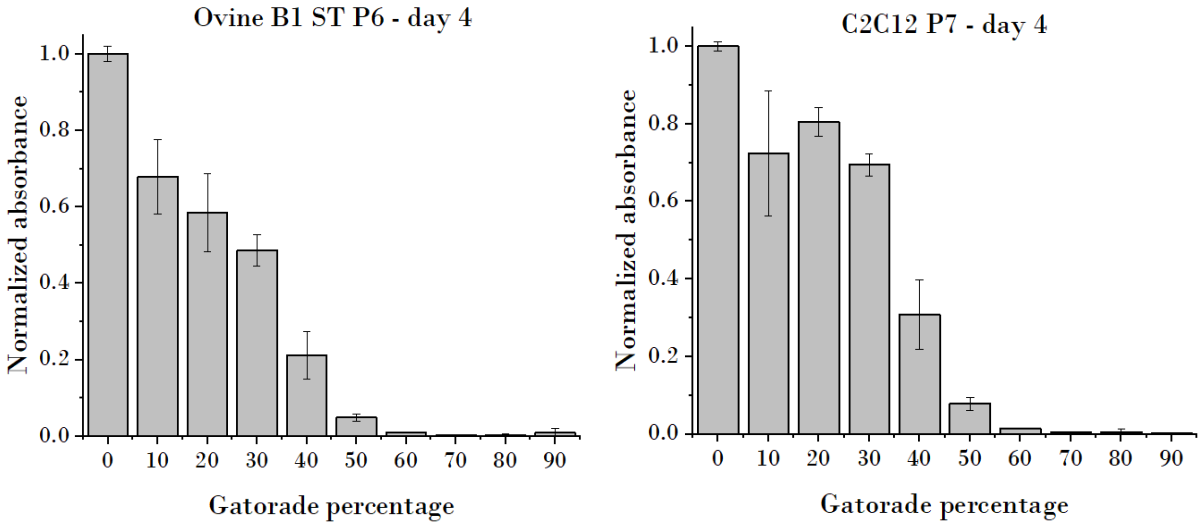


(a) Ovine cells

(b) C2C12 cells

Figure 4.22.: MTT assay results of cells cultured in various percentages of Gatorade for 4 days. The results are normalised to the control group of 0% Gatorade.

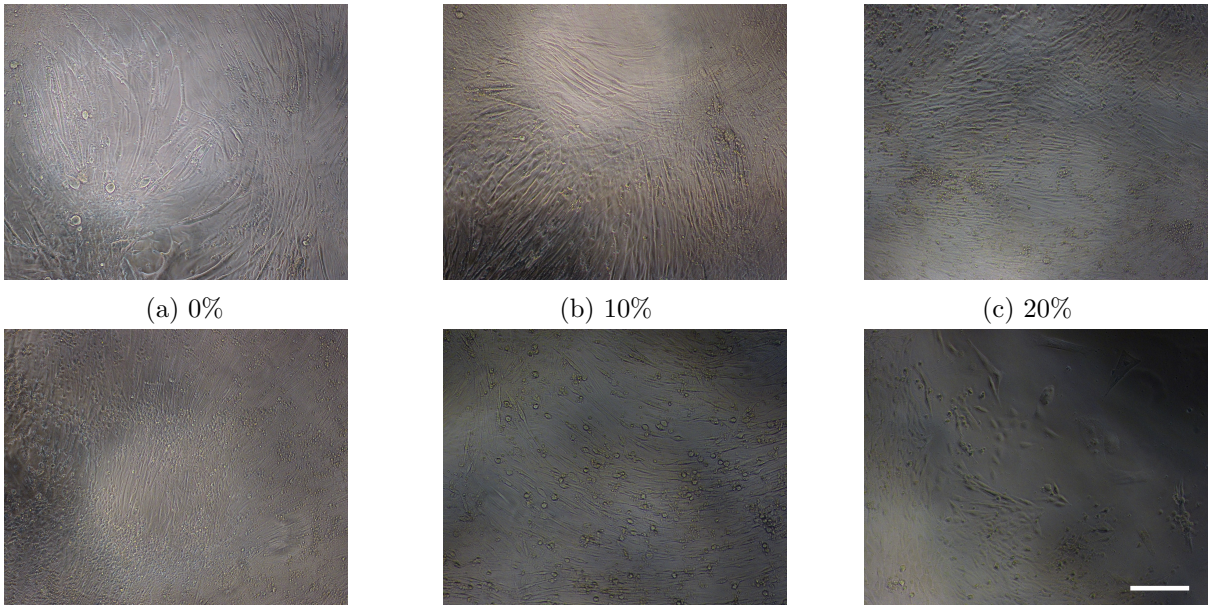

(a) 0%

(b) 10%

(c) 20%

(d) 30%

(e) 40%

(f) 50%

Figure 4.23.: Brightfield microscopy images of the cells cultured in growth medium where DMEM was partially replaced by Gatorade. The subcaptions present the percentage of Gatorade. Scalebar: 200 $\mu$m.

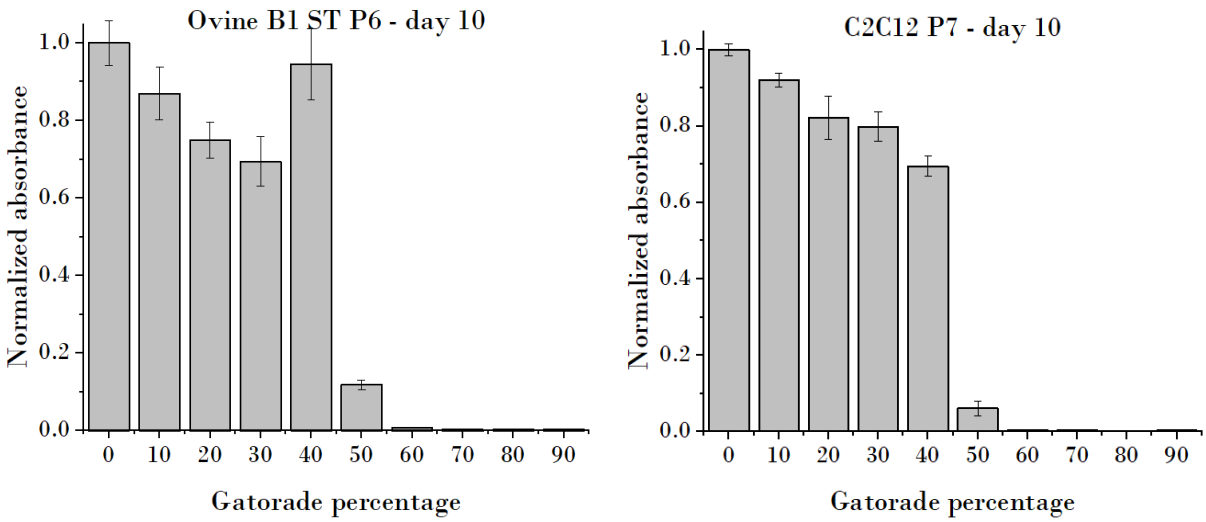


(a) Ovine cells

(b) C2C12 cells

Figure 4.24.: MTT assay results of cells cultured in various percentages of Gatorade for 10 days. The results are normalised to the control of 0% Gatorade.

# 5 Discussion

The aim of the research presented in this thesis is to lay the groundwork for research to cultured meat with an interest in ovine as a cell source. However, the research presented here is not limited to cultured meat and is also applicable to muscle tissue engineering for clinical applications. In this thesis, the whole process of isolation and characterisation of a cell sample is described, proceeding to investigate the proliferation and differentation properties and ultimately engineering 3D tissue constructs. This process can be applied to other mammalian cell sources, although optimisation is advised. The model used to create the tissue constructs was tested with the commonly used C2C12 myoblast cell line and construct formation was observed. The spontaneous contraction of the tissue constructs suggests that the cells in the constructs have differentiated and are expressing myosin. The expression of myosin has not been confirmed by immunofluorescence protein expression, so further research is advised to confirm this theory. Nevertheless, the spontaneous contraction indicates that the cells in the constructs are viable and communicating which is important for tissue formation. Therefore, the presented 3D system is interesting for muscle tissue engineering and could for example be explored for *in vitro* modelling of cardiac tissue or as a stepping stone for development of a skeletal muscle tissue regeneration system for muscular dystrophy research. The system provides a uniaxial tension on the constructs and supports cell alignment and fusion, which are important steps before reaching myofibre formation. The model allows for observation of compaction over time. Using four pillars instead of two can be argued to be an advantage, as more pillars maintain the tension on the construct. If the construct detaches from one pillar, the construct does not instantly transform into a tension-lacking cluster of cells. Ovine cells have shown potential regarding the formation of myofibres in this system. Optimisation is required, but the observations presented in this thesis indicate that this system could potentially result in successful myofibre formation with ovine cells. This is relevant for clinical purposes, as humans are more closely related to ovine than to mice.

## 5.1. Isolation

As the goal of cultured meat is to produce meat without the need of slaughtering animals, cells are ideally isolated from biopsies taken from living animals, instead of *post mortem* biopsies as described in this thesis. Due to regulations it was not possible to obtain a biopsy from a living ovine. However, the biopsies were taken from euthanised ovines after they were used for animal experiments and their bodies were categorised as waste. Therefore no animal was harmed for the cause of cell isolation during this research. As the animals were not alive at the time of biopsy retrieval, tissue samples could also have been retrieved more conveniently be making a large cut and cutting a large piece of tissue out. However, taking a biopsy is more accurately mimicking the approach of the cultured meat industry to create the least amount of harm [50, 61]. Approaches for cell isolation that inflict even less harm on the animals are to isolate cells from for example the umbilical cord [190, 191], hair follicles [192, 193], or urine [194, 195]. These samples have demonstrated to produce myogenic and adipogenic cells. An experiment was set up to isolate cells from an ovine umbilical cord and to induce myogenic differentiation, but unfortunately sudden COVID-19 restrictions disrupted this. It would be

interesting to explore the possibilities of isolating cells from other tissue samples than skeletal muscle and to compare the properties of the isolated cells.

In section 1.4 it was mentioned that around 10,000 cells can be isolated from a 0.5 gram biopsy, according to Post *et al.* [50]. The weight of the tissues obtained from the biopsies was logged during the second biopsy. The isolated cells were counted directly after isolation and the cell counts were $1.8*10^6$ and $4.0*10^6$ cells per 0.5 gram biopsy for the ST and SM, respectively. This is a relatively high cell count, when compared to the cell count of Post *et al.* However, when the cells were plated and cells attached, a lower amount of cells was observed than expected. As described in section 4.1, it was not possible to determine the amount of attaching cells before proliferation was initiated. Visual observations did not agree with the previously mentioned cell count and therefore the cell count is not treated as reliable. Isolating more cells from a tissue results in more proliferating cells, retaining the stemness of the cell sample for longer. Wu *et al.* reported that freshly isolated ovine satellite cells have difficulty attaching to the bottom of untreated culture plates [70]. Therefore, it could be beneficial to provide the plates with a coating before seeding the cells. Another strategy is to increase the enzyme concentration and investigate if this results in a higher cell yield, as various enzyme concentrations are reported in literature [66, 69, 196].

Moreover, a large difference in myogenic cell percentage was observed between biopsy 1 and 2. The difference in protocol was the use of collagenase type 1 during the first biopsy and collagenase type 2 during the second biopsy. Collagenase type 2 was used for the second isolation due to collagenase type 1 being out of stock. Furthermore, the tissues were obtained from different ovine, which means that physiological differences are probable. Therefore, it is not possible to conclude if the difference is caused by enzyme type or by the tissue isolated from. More data needs to be obtained, by isolating cells from the ST and SM from different ovines, following the identical protocol. The tissue biopsies should be retrieved from ovines in a similar age range. It has been found that the fibre type composition and gene expression of ovine muscles can differ significantly depending on the age of the animal [128]. For example, the fibre type composition of the SM switches to a fast phenotype over the course of the first six months in age. This could have an effect on the muscle texture of the ovine, resulting in cell population differences. Additionally, it suggests a reason for the difference in taste of meat from a young lamb and an older mutton. Future research is advised to determine the difference between cells isolated from different age ranges. This could be relevant as it can affect cell stemness and taste.

## 5.2. FACS

Cell identification was performed by FACS using the markers CD29, CD56, ITGA7, CD31, and CD45. All antibodies were titrated beforehand and the cells used for titration were the enzymatic isolated ovine B1 ST cells. During titration, no expression was observed for CD31 and CD45. It was therefore expected that all cell samples came out negative for these markers during FACS. CD31 targets endothelial cells and CD45 targets immune cells, and as these cells are not necessarily expected in the samples it was assumed that they were successfully removed during cell isolation. When combining the percentages of ITGA7+ and CD29+ cells, the total approaches 100% in all samples. It is therefore save to assume that endothelial cells and immune cells are not present in the sample. However, for future experiments with this FACS panel it would be advised to titrate CD31 and CD45 on a sample containing the targeted cell types. This was not possible during the research presented here, as ovine endothelial cells or immune cells were not available. Moreover, for future research it is advised to optimise the whole FACS panel, as the panel used in this research was a primary design. The presented FACS panel is recommended as a panel used for preliminary experiments and can be optimised to specific

species. Antibodies included in this panel are specifically tested against ovine and will therefore be most relevant for ovine derived cell samples. FACS panels for skeletal muscle samples of different species are advised to search for similar markers tested against the specific species.

CD56 and ITGA7 were both expected to target SCs. Uncertainty about the exact moment of expression during maturation of the cells was raised in literature, but the cells were expected to target approximately the same cell population. Instead, three different populations were observed in the FACS results: ITGA7-/CD56-/+, ITGA7+/CD56high, and ITGA7+/CD56-. As elaborately discussed in section 4.2.2, it is suggested that the ITGA7-/CD56-/+ population is fibroblasts, the ITGA7+/CD56high population is satellite cells, and the ITGA7+/CD56- population is myogenic cells in a later stage of maturation than satellite cells. If this observation is confirmed, it is relevant for skeletal muscle engineering of any species. For confirmation, Pax7 expression and a differentiation assay can determine if the cells are myogenic. To confirm the moment of expression during maturation, ITGA7 and CD56 could be analysed on co-expression with markers that are known to express at certain points of maturation. This could be applied to the biomarker profile markers. The unexpected difference in expression of ITGA7 and CD56 supports the observations of Castiglioni *et al.* and raises the question if ITGA7 and CD56 are reliable markers [155]. Validation of the markers for skeletal muscle FACS purposes is required, as the purity of cell populations can be severely affected by unreliable markers.

## 5.3. Tissue constructs

If time had allowed, the spontaneous contraction of the C2C12 constructs would have been investigated. The contraction is expected to be caused by calcium spikes [197, 198, 199]. An ad-hoc experiment to confirm if calcium plays a crucial role in the process could be to closely monitor a spontaneously contracting construct while mixing or partly replacing the culture medium with an EGTA solution at similar pH. EGTA chelates calcium ions and is therefore expected to instantly disrupt the process of spontaneous contraction if it relies on calcium. If this process is understood and appears to support myogenesis, it might be an option to artificially mimic the process when forming myofibres containing mammalian cells other than C2C12s.

An approach that could be investigated to keep the ovine constructs intact for longer, is including fibrinogen in the hydrogel. As mentioned in 2.5, Bian *et al.* showed with C2C12-laden hydrogels that detaching of the constructs occured 6 days later when fibrinogen was included.

It should be noted that collagen and Matrigel are both animal derived. The aim is to exclude animals from the meat production process, and therefore no animal derived products should be included in the hydrogel. Excluding animal products from a hydrogel for skeletal muscle tissue engineering purposes is an extensive research on its own and was therefore not included in the scope of this research. However, it is an important subject for future cultured meat research. Multiple plant-based hydrogels are being studied, such as cellulose, starch, or pectin based hydrogels [200]. A benefit of using plant-based hydrogels is that most plant-based content is already approved for consumption. The tissue construct system presented in this thesis is suitable for research and development of a cell-laden plant-based hydrogel.

The tissue construct system is applicable to muscle tissue engineering in general. The pillars provide anchor points to the cells, and by using PDMS as material the pillars are flexible and potential bending can be monitored, which can be useful for cardiac tissue engineering research [201]. However, the relatively high cell seeding density of $32 * 10^6$ cells/ml is not ideal. It is therefore advised to test the system with a lower seeding density or to alter the hydrogel composition.

## 5.4. A cost effective alternative for DMEM

The effect of partially replacing DMEM by cost effective alternatives was measured by MTT assays. It should be noted that the results of MTT assays must always be interpreted with caution. For example, in the case of assessing cytotoxicity, some drugs can directly affect the MTT measurements [184]. In this experiment, where DMEM was partly replaced by energy drinks, it is assumed that no component of the drinks directly interacts with the MTT. However, this has not been tested or confirmed. The osmolarity of the energy drinks was increased by addition of baking soda. Lab grade sodium bicarbonate was available, however baking soda is more cost effective. As the aim of the experiment was to explore cost effective alternatives for medium composition, it was decided to use baking soda. The experiment based on partially replacing DMEM with energy drinks was performed once and the data is therefore not conclusive. However, the results indicate that energy drinks affect cell performance, as replacing 10% of DMEM results in at least a 30% decrease of cell metabolism. It is not determined if the decrease is caused by lower proliferation rate, lower cell activity, or lower cell viability. Although a decrease in cell metabolism is not preferred, it is promising that energy drinks are not instantly toxic to the cells. Labs performing cell culture could greatly benefit from a cost effective alternative. It is not advised to replace DMEM by energy drink, however these results are relevant as they suggest that potentially a cost-effective alternative for DMEM could be developed to be suitable for primary cells. Moreover, a solution could be developed to be used for educational purposes not requiring long term culture.

## 5.5. Future outlook

An important goal of tissue engineering for cultured meat applications is to scale up the production process. The 3D system presented in this thesis is currently designed to grow a small individual myofibre around four pillars. Expansion of the design into a pillar array, maintaining the same pillar distances as in the current design, could potentially result in the formation of a sheet-like structure. It should be confirmed if the current pillar distances and an increased hydrogel volume allow the hydrogel to integrate into the array, instead of the disintegrating as observed in the 16 pillar system in figure 4.21a and 4.21b. If a sheet structure could be obtained, it would be interesting to combine this with the stacking method presented in the research of Furuhashi *et al.*, described in section 2.5. Experiments could be performed to determine the best composition of hydrogel in between the stacked sheets; non cell-laden, satellite cell-laden, or adipogenic cell-laden. Combining the sheet-structure with the stacking method of Furuhashi *et al.* could potentially be a step towards development of larger constructs of cultured meat.

The texture, appearance, and flavour of the 3D constructs were not assessed in this research, as the constructs did not reach that stage of development. When formation of a 3D construct expressing myosin is achieved, it is recommended to assess the texture of the construct by measuring the Young's modulus of the tissue. Subsequently, a more complete texture analysis can be performed by a method called texture profile analysis. Through a double compression cycle aspects as cohesiveness, adhesiveness, resiliency, fracturability, guminess, and chewiness can be assessed [202]. The appearance of cultured meat can be enhanced by growing the cells in the presence of myoglobin, which is reported to result in a colour similar to meat, while meanwhile increasing proliferation and metabolic activity of cells [203]. To identify food flavour components in cultured meat, the products can best be assessed by combination of olfactometry (measurements of smell based on sensory analysis by human participants) and gas chromatography. This combination is an appropriate approach, as odour-active components in complex mixtures can be assessed through specific correlation with the chromatographic peaks of interest [204].

# 6 Conclusion

The research presented in this thesis lays the groundwork for tissue engineering research with interest in ovine as a cell source. Cells were successfully isolated from *post mortem* biopsies of two ovines from the *m. semitendinosus* and *m. semimembranosus*. Explant isolation and enzymatic isolation performed with collagenase type 1 and collagenase type 2 resulted in six ovine cell samples. Cell identification was performed with the markers CD29, CD56, ITGA7, CD31, and CD45, and the cells in the samples were identified to be fibroblasts, satellite cells, and myogenic cells in an undefined stage of maturation. Myogenic properties of the cells were confirmed by starving the cells from serum and thereby initiating differentiation. The cells aligned, fused, and expressed the myogenic marker myosin. The sample used for all experiments was enzymatically isolated by collagenase type 1 from the *m. semitendinosus* (sample B1 ST enzymatic) and was mostly used at passage 4. This sample contained 24% fibroblasts and 76% of myogenic cells (8.4% satellite cells and 66% myogenic cells in an undefined stage of maturation). By tracking the population doublings of the cells, it was observed that the samples with a higher percentage of myogenic cells presented a higher population doubling rate. Moreover, all ovine samples were proliferated on non-coated, collagen coated, and Matrigel coated tissue culture plates. It was observed that all ovine samples achieved highest cell growth on collagen coated plates and lowest cell growth on Matrigel coated plates. It is noteworthy that this data is not conclusive and repeatability should be confirmed.

A four pillar system was designed for formation of a myofibre. A cell-laden hydrogel containing collagen and Matrigel was seeded in the system. Optimal compaction was observed at a cell seeding density of $32 * 10^6$ cells/ml. Ovine cells isolated by enzymatic digestion with collagenase type 1 from the *m. semitendinosus* were observed to form constructs around the pillars in one day of culture. A visual tension was seen in the construct, excerted by the cells itself, and the constructs detached after three days. C2C12 cells were likewise observed to form constructs in one day of culture, but less tension was observed in the constructs. Instead of detaching from the pillars, the constructs expressed spontaneous contraction from day 4 onwards.

According to the results presented in this thesis, ovine is an eligible cell source for cultured meat applications. The proliferation rate and differentiation capacity are comparable to purified bovine cells that are currently used for cultured meat development. Ovine isolated myogenic cells are therefore expected to meet the requirements of cultured meat research. Moreover, the cells were capable of forming a 3D tissue construct. However, optimisation of the 3D system should be performed to maintain the constructs for a longer time. The 3D construct system presented in this research is suitable for skeletal muscle research in general, and can therefore also be used for clinical applications.

# Titration

# A

The titration results of CD56, CD29, and ITGA7 are presented in this Appendix. Expression of CD31 and CD45 was not observed in the titration sample and therefore no results are presented. Titration of antibodies is an essential step to undertake when designing flow cytometry panels. It is required to validate the activity of the antibodies, and to optimize the antibody concentration [149]. Use of a suboptimal concentration enables excess antibody to bind at low afinity, resulting in an increased chance of non-specific background staining [148].

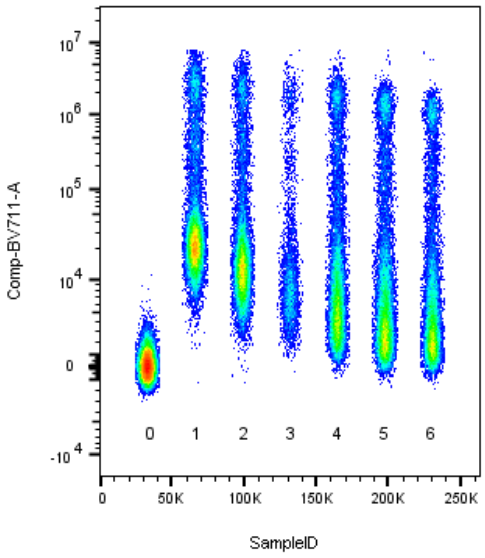


Figure A.1.: Titration of CD56.

Table A.1.: Concentrations with corresponding stain index. One test denotes a total volume of 100 $\mu$l staining $1 * 10^6$ cells.

| Tube no. | Concentration [$\mu$l/ test] | Stain index |
|---|---|---|
| 1 | 5 | 42.9 |
| 2 | 2.5 | 43.8 |
| 3 | 1.25 | 52.0 |
| 4 | 0.63 | 47.2 |
| 5 | 0.31 | 45.1 |
| 6 | 0.16 | 41.4 |

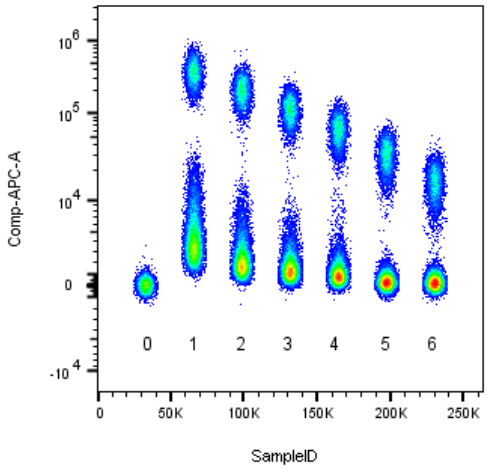


Figure A.2.: Titration of CD29.

Table A.2.: Concentrations with corresponding stain index. One test denotes a total volume of 100 $\mu$l staining $1 * 10^6$ cells.

| Tube no. | Concentration [$\mu$l/ test] | Stain index |
|---|---|---|
| 1 | 5 | 85.1 |
| 2 | 2.5 | 97.2 |
| 3 | 1.25 | 73.6 |
| 4 | 0.63 | 52.4 |
| 5 | 0.31 | 34.9 |
| 6 | 0.16 | 16.8 |

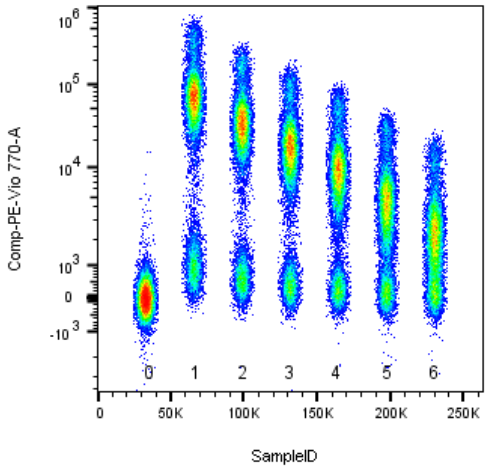


Figure A.3.: Titration of ITGA7.

Table A.3.: Concentrations with corresponding stain index. One test denotes a total volume of 100 $\mu$l staining $1 * 10^6$ cells.

| Tube no. | Concentration [$\mu$l/test] | Stain index |
|---|---|---|
| 1 | 5 | 59.7 |
| 2 | 2.5 | 37.3 |
| 3 | 1.25 | 21.9 |
| 4 | 0.63 | 13.1 |
| 5 | 0.31 | 5.77 |
| 6 | 0.16 | 3.4 |

# B

# FACS results

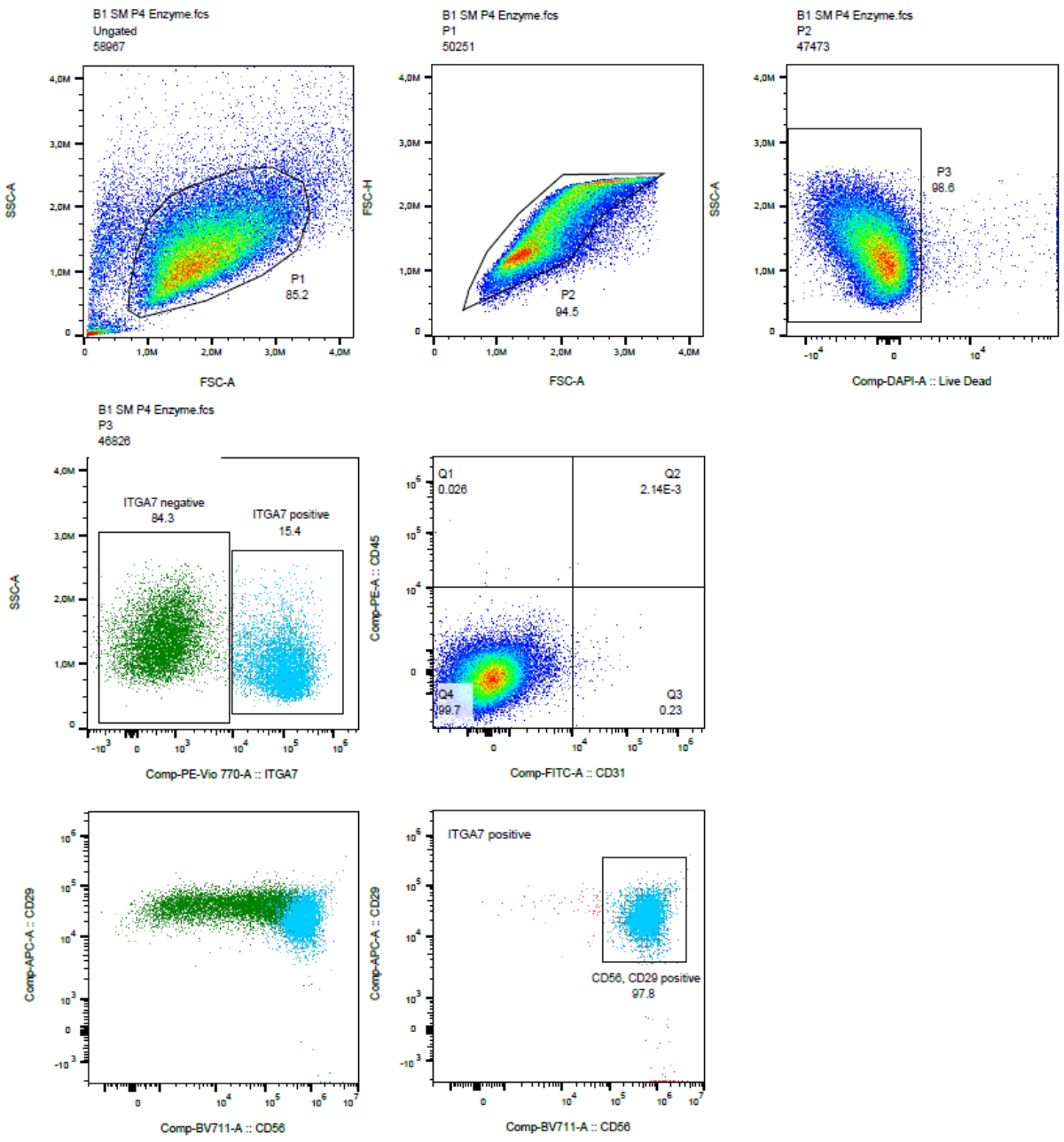


Figure B.1.: FACS plots of enzymatic isolated ovine B1 SM P4 cells.

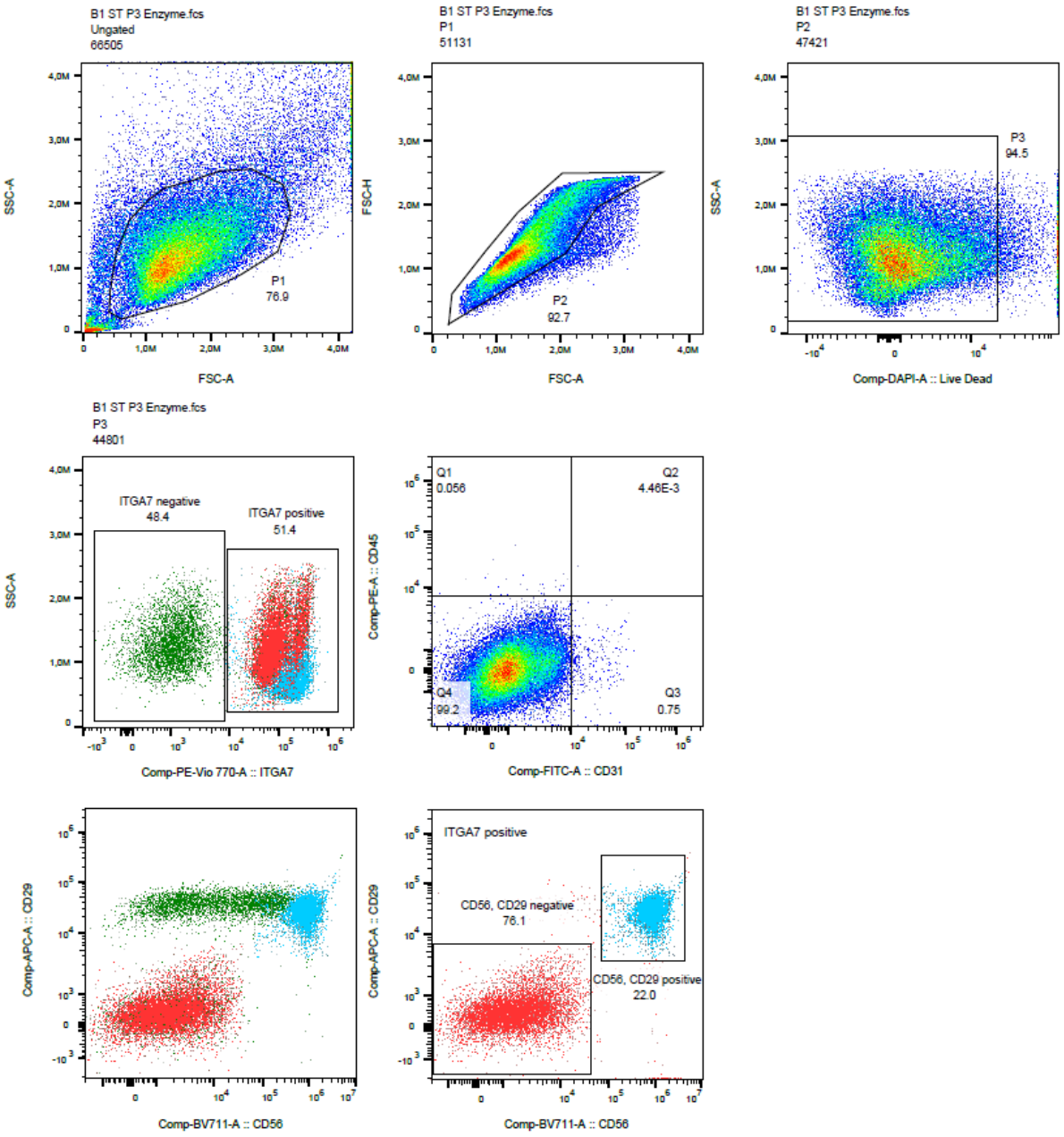


Figure B.2.: FACS plots of enzymatic isolated ovine B1 ST P3 cells.

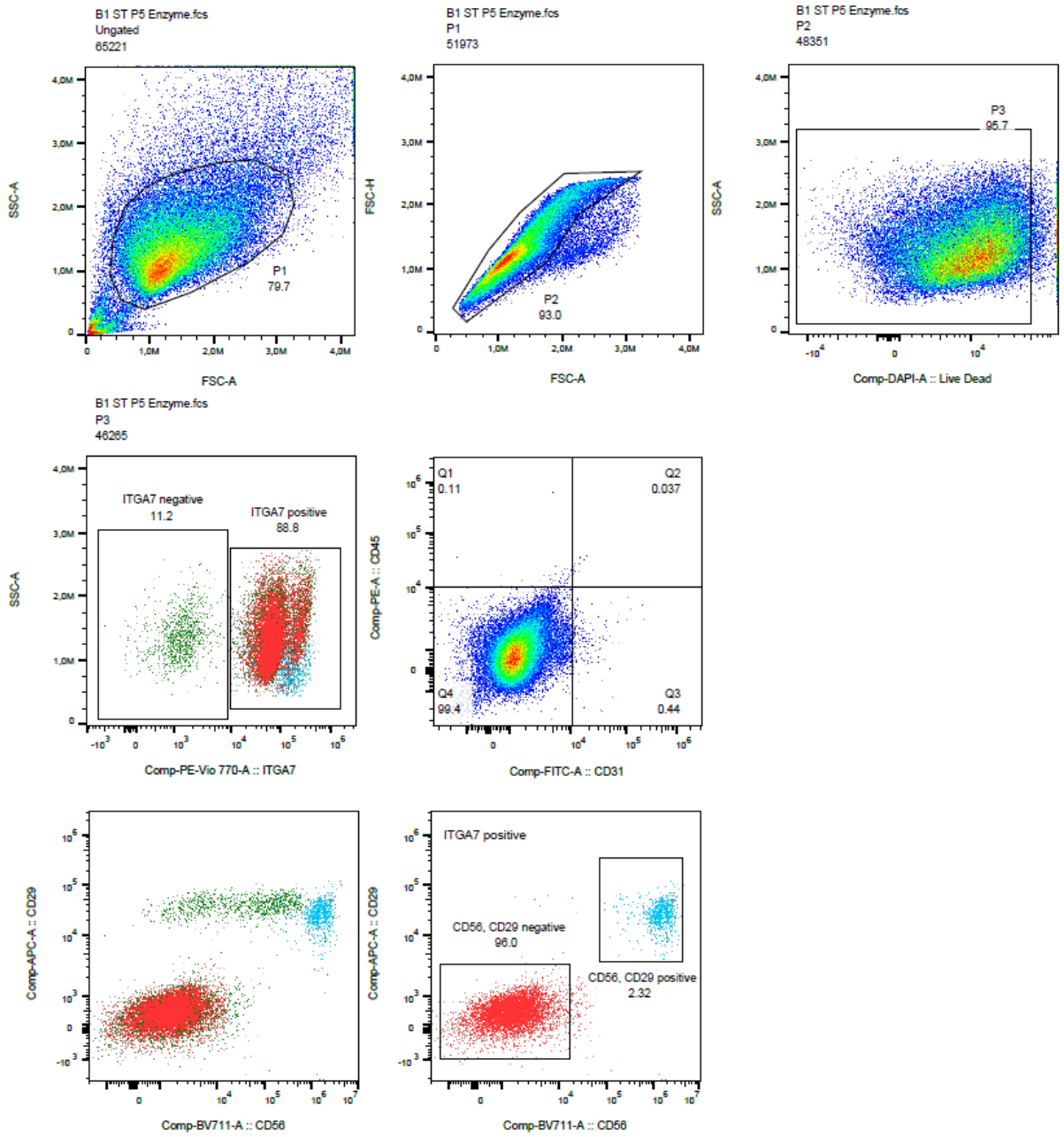


Figure B.3.: FACS plots of enzymatic isolated ovine B1 ST P5 cells.

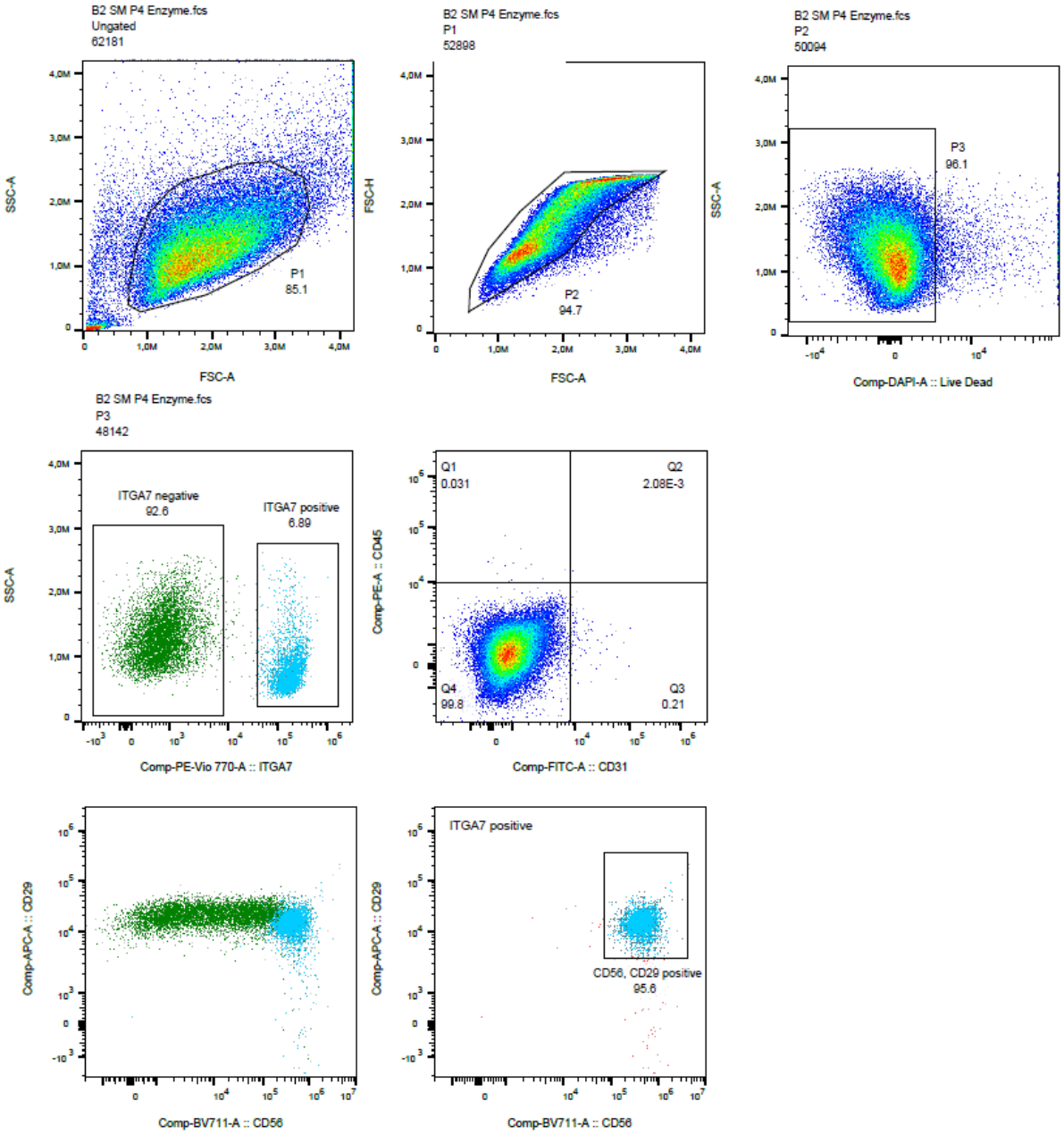


Figure B.4.: FACS plots of enzymatic isolated ovine B2 SM P4 cells.

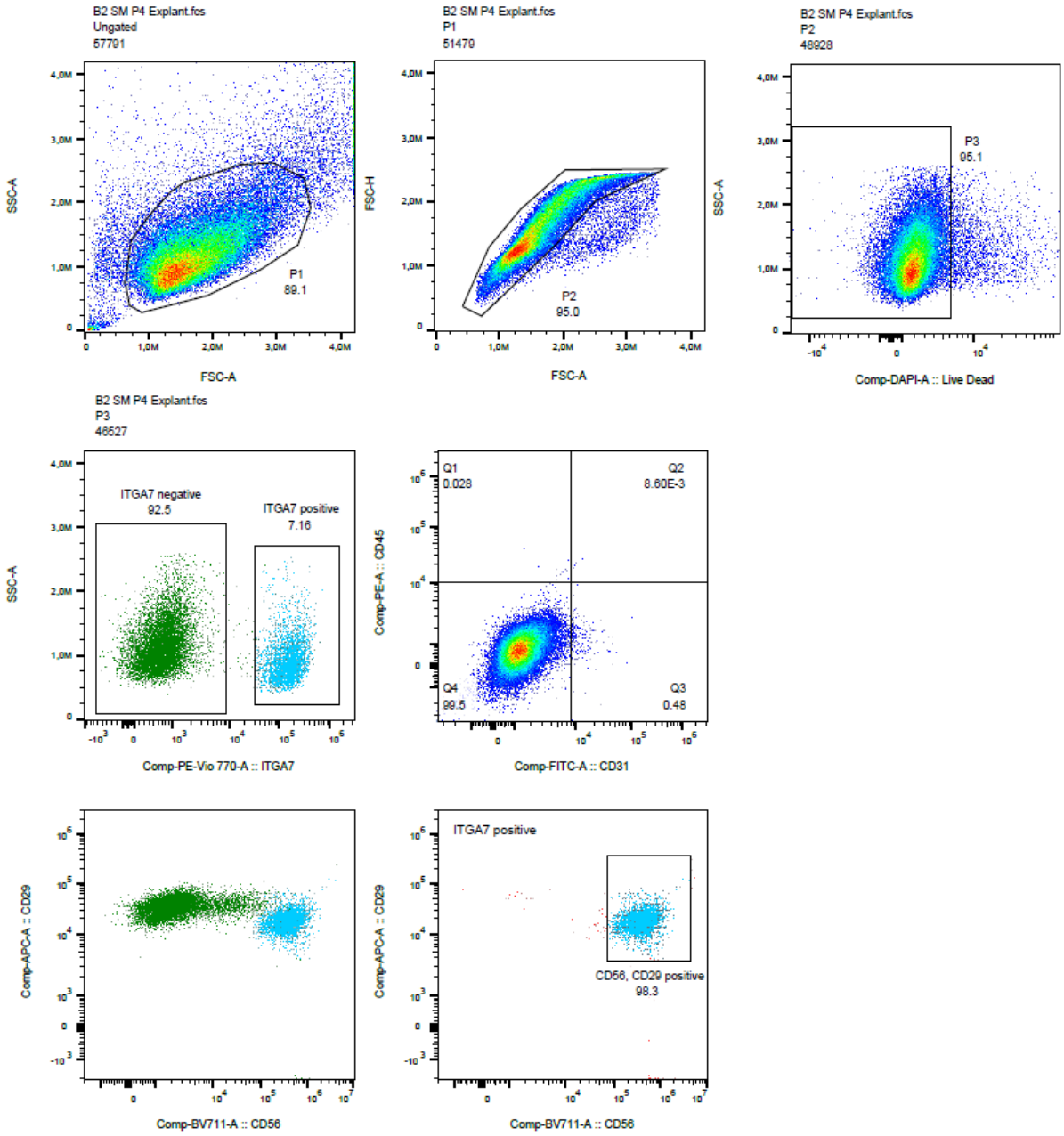


Figure B.5.: FACS plots of explant isolated ovine B2 SM P4 cells.

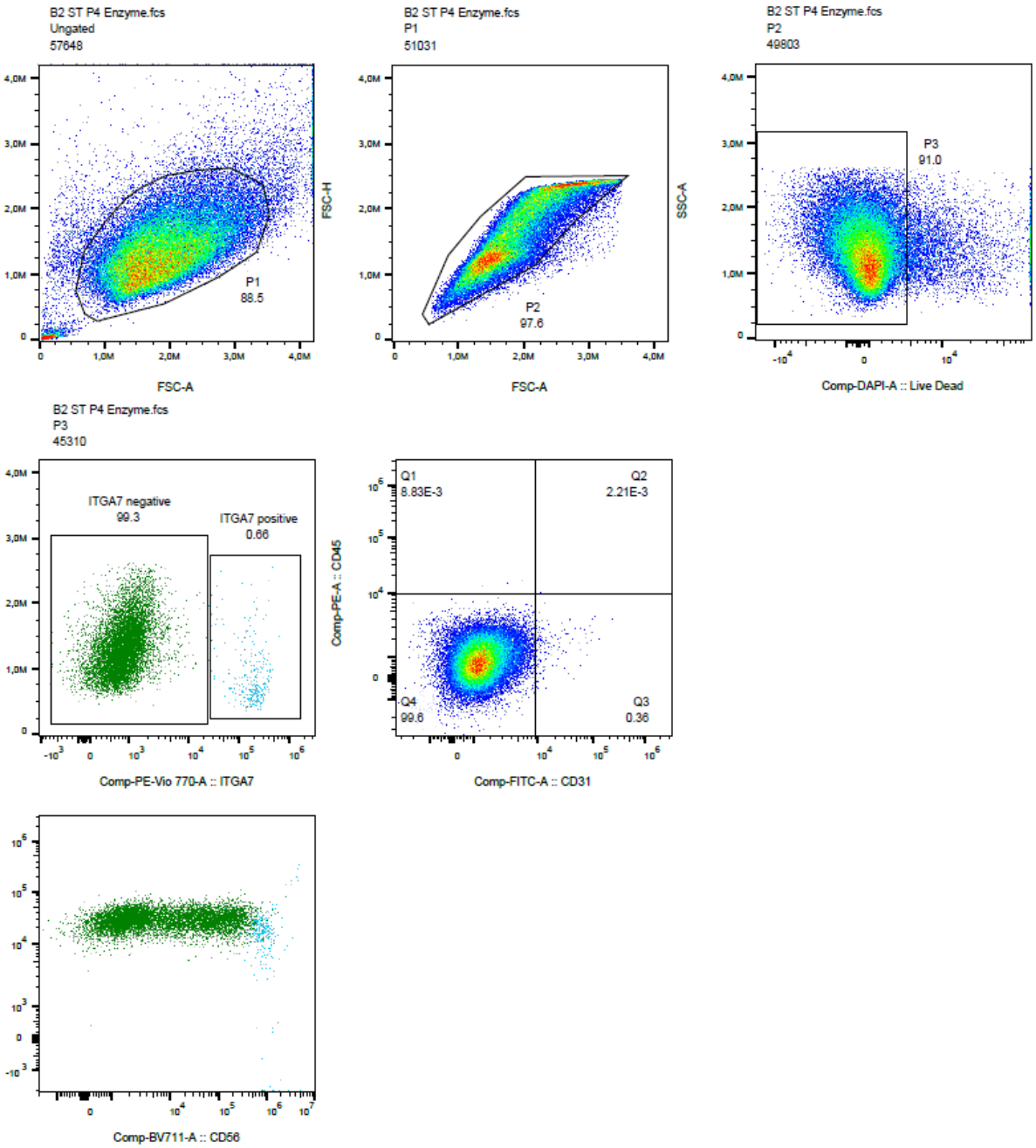


Figure B.6.: FACS plots of enzymatic isolated ovine B2 ST P4 cells.

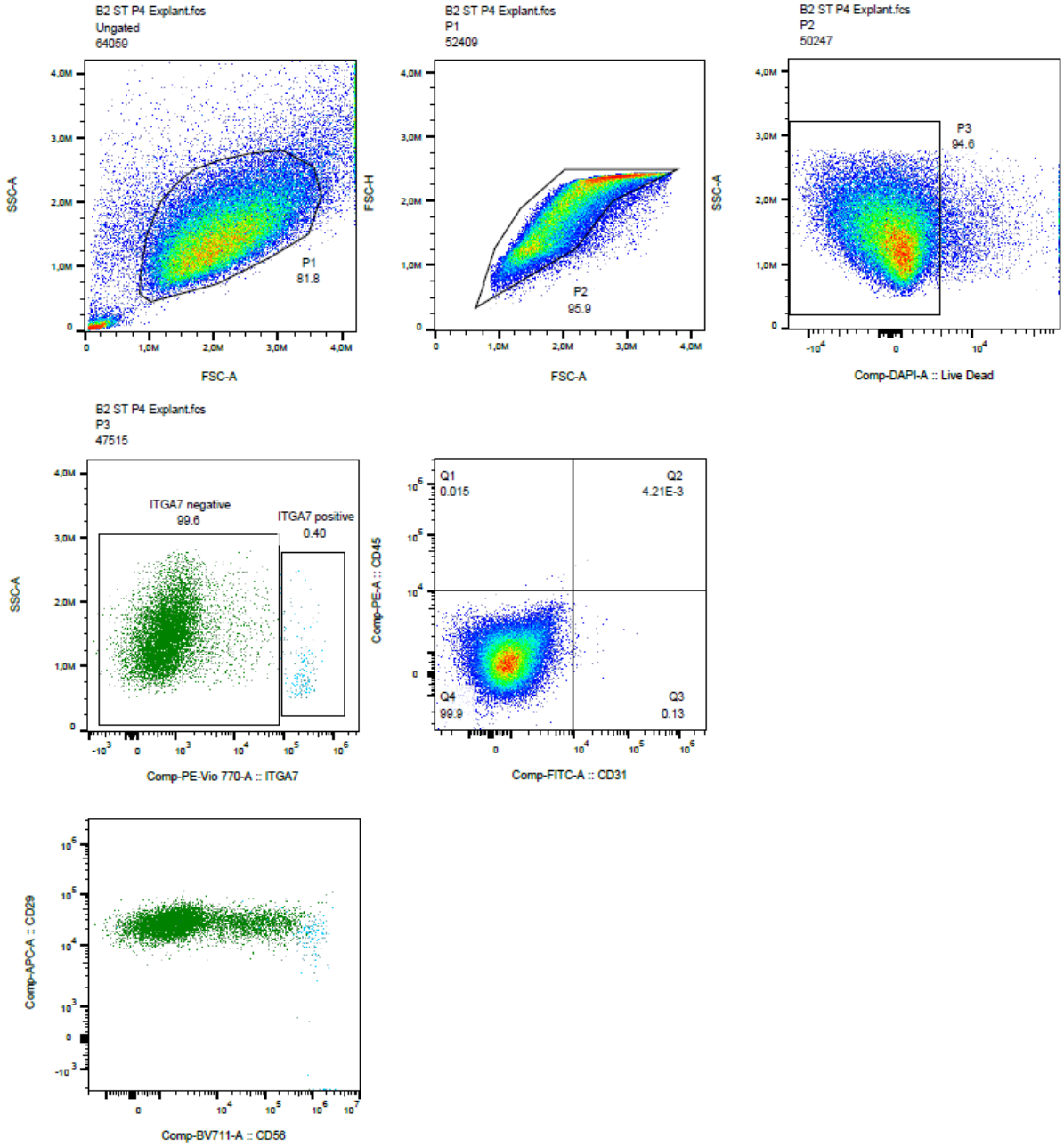


Figure B.7.: FACS plots of explant isolated ovine B2 ST P4 cells.

# C

# The influence of coating

The graphs of figure C.1 present the individual results of all ovine isolated samples. It is demonstrated that all ovine cell samples, regardless of the specific cell type ratio in the samples, favour the collagen coated surface over the other conditions, as the highest cell count and therefore proliferation rate is observed on the collagen coating. C2C12 cells likewise demonstrate this preference.

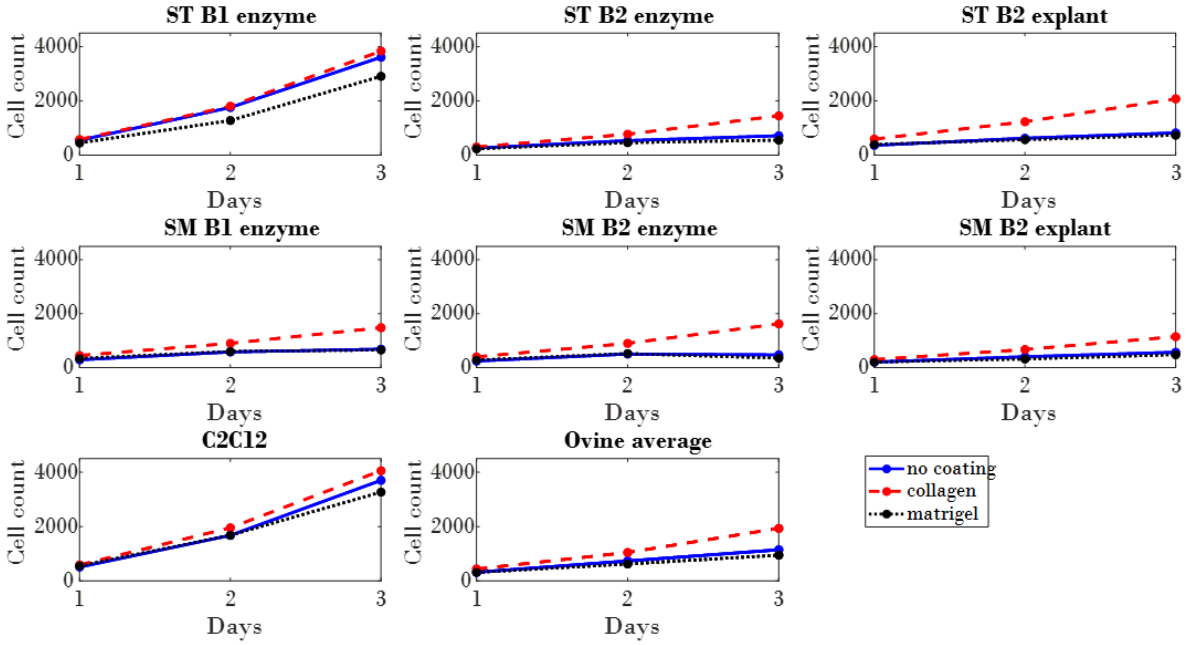


Figure C.1.: Cell count of all isolated samples and C2C12 cells on non-coated, collagen coated, and Matrigel coated tissue culture plates.

# A cost effective alternative for DMEM

# D

In this Appendix the MTT assay results of V-energy and LIVE+ are presented.

## D.1. Proliferation

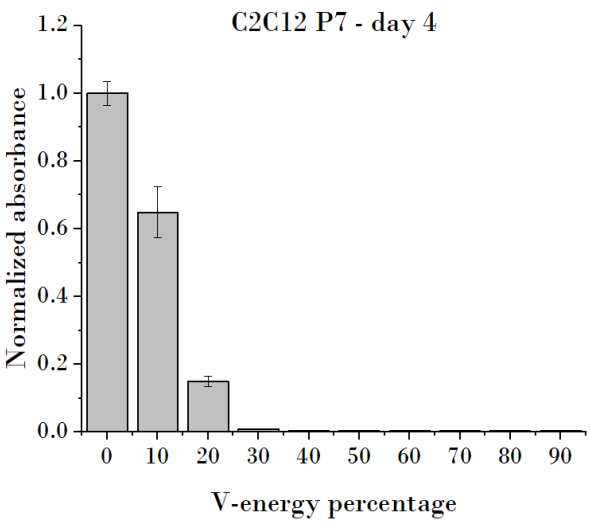


(a) C2C12 cells cultured in various percentages of V-energy.

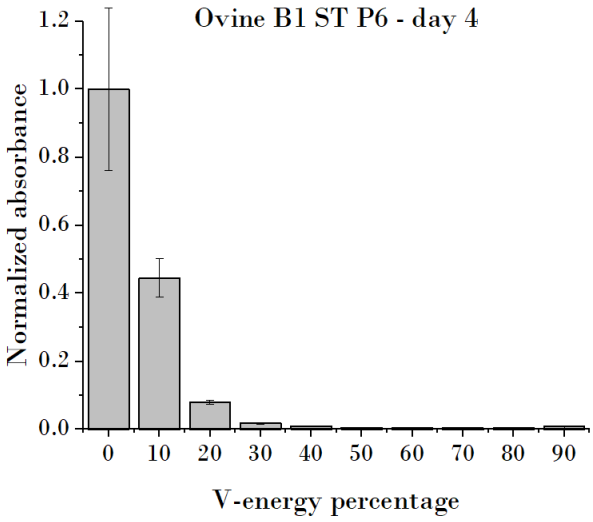


(b) Ovine cells cultured in various percentages of V-energy.

Figure D.1.: MTT assay results normalized to the control of 0% V-energy. Cells are cultured for 4 days.

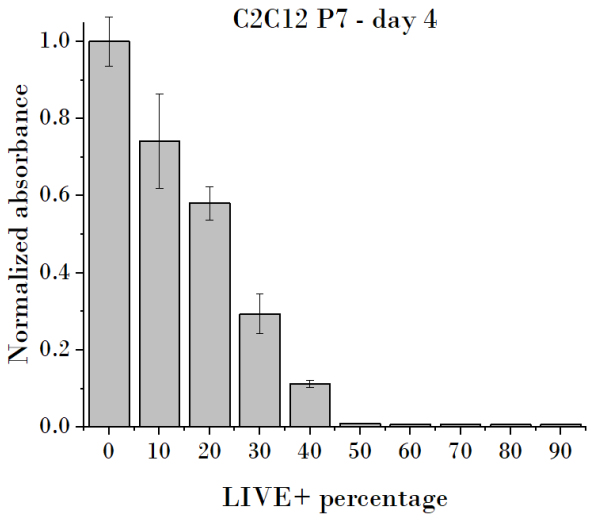


(a) C2C12 cells cultured in various percentages of LIVE+.

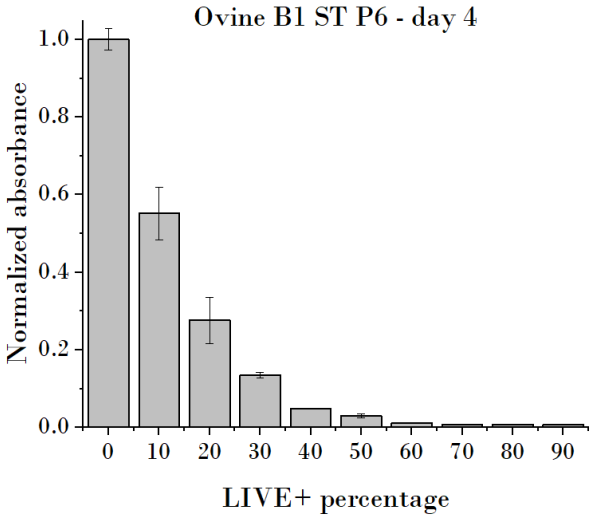


(b) Ovine cells cultured in various percentages of LIVE+.

Figure D.2.: MTT assay results normalized to the control of 0% LIVE+. Cells are cultured for 4 days.

## D.2. Differentiation

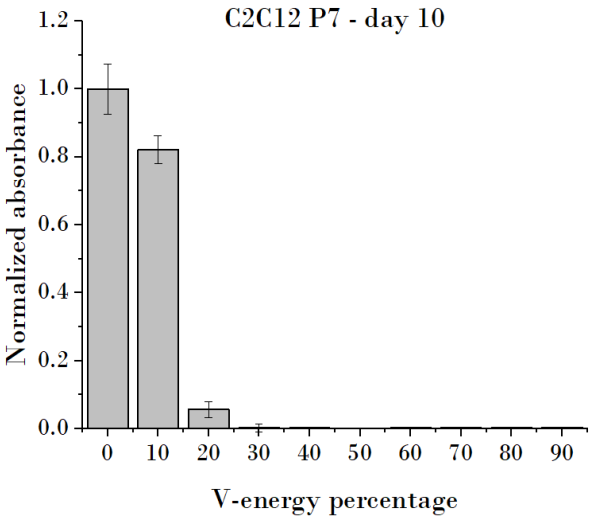


(a) C2C12 cells cultured in various percentages of V-energy.

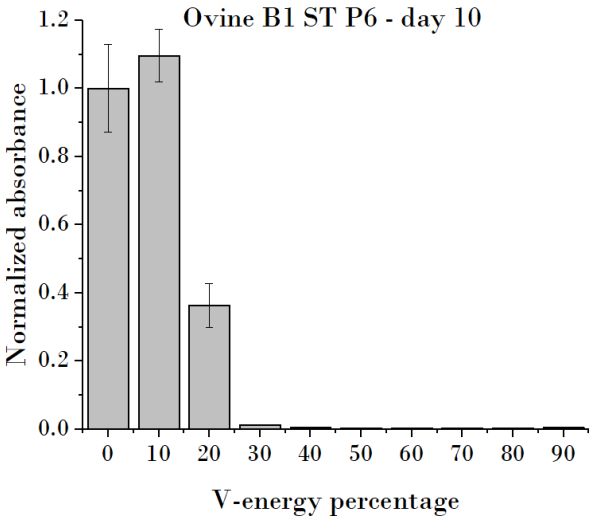


(b) Ovine cells cultured in various percentages of V-energy.

Figure D.3.: MTT assay results normalized to the control of 0% V-energy. Cells are cultured for 10 days.

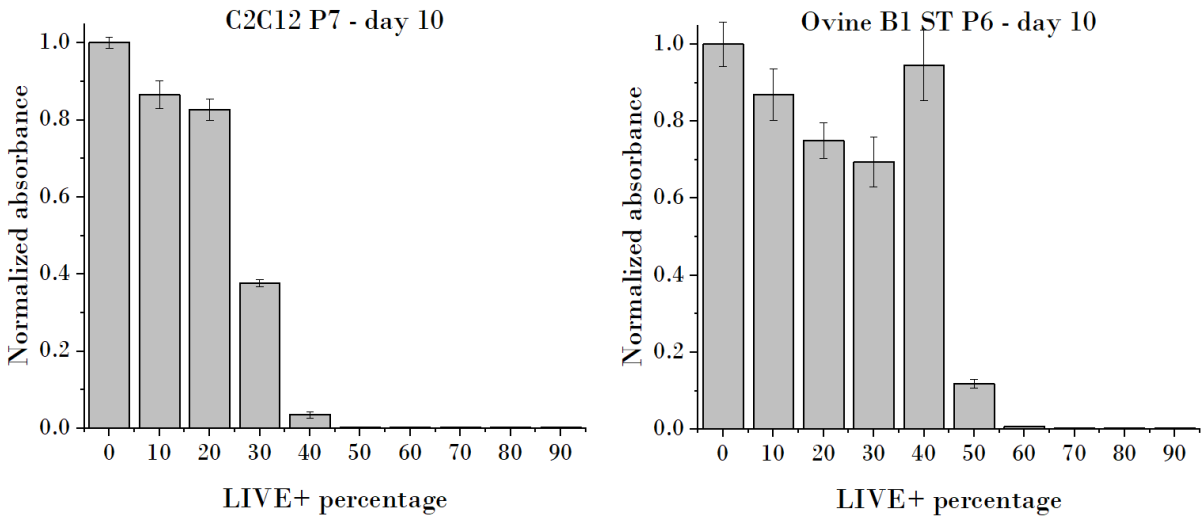


(a) C2C12 cells cultured in various percentages of LIVE+.

(b) Ovine cells cultured in various percentages of LIVE+.

Figure D.4.: MTT assay results normalized to the control of 0% LIVE+. Cells are cultured for 10 days.

# Bibliography


[1] Sandra Banholzer, James Kossin, and Simon Donner. The impact of climate change on natural disasters. In *Reducing disaster: Early warning systems for climate change*, pages 21–49. Springer, 2014.

[2] Thomas J Crowley. Causes of climate change over the past 1000 years. *Science*, 289(5477):270–277, 2000.

[3] Hannah Ritchie and Max Roser. Environmental impacts of food production. *Our World in Data*, 2020. https://ourworldindata.org/environmental-impacts-of-food.

[4] Joseph Poore and Thomas Nemecek. Reducing food's environmental impacts through producers and consumers. *Science*, 360(6392):987–992, 2018.

[5] Robert WR Parker, Julia L Blanchard, Caleb Gardner, Bridget S Green, Klaas Hartmann, Peter H Tyedmers, and Reg A Watson. Fuel use and greenhouse gas emissions of world fisheries. *Nature Climate Change*, 8(4):333–337, 2018.

[6] Dina Anwar and EL-CHAGHABY Ghadir. Nutritional quality, amino acid profiles, protein digestibility corrected amino acid scores and antioxidant properties of fried tofu and seitan. *Food and Environment Safety Journal*, 18(3), 2019.

[7] Shahin Homaeigohar and Mady Elbahri. Graphene membranes for water desalination. *NPG Asia Materials*, 9(8):e427–e427, 2017.

[8] Dan Yan, Mingtian Yao, Fulco Ludwig, Pavel Kabat, He Qing Huang, Ronald WA Hutjes, and Saskia E Werners. Exploring future water shortage for large river basins under different water allocation strategies. *Water Resources Management*, 32(9):3071–3086, 2018.

[9] P Winnie Gerbens-Leenes, Mesfin M Mekonnen, and Arjen Ysbert Hoekstra. The water footprint of poultry, pork and beef: A comparative study in different countries and production systems. *Water Resources and Industry*, 1:25–36, 2013.

[10] David Morales-Hidalgo, Sonja N Oswalt, and E Somanathan. Status and trends in global primary forest, protected areas, and areas designated for conservation of biodiversity from the global forest resources assessment 2015. *Forest Ecology and Management*, 352:68–77, 2015.

[11] Hannah Ritchie and Max Roser. Land use. *Our World in Data*, 2020. https://ourworldindata.org/land-use.

[12] Willandia A Chaves, Martha C Monroe, and Kathryn E Sieving. Wild meat trade and consumption in the central amazon, brazil. *Human Ecology*, 47(5):733–746, 2019.

[13] Hannah Ritchie and Max Roser. Meat and dairy production. *Our World in Data*, 2017. https://ourworldindata.org/meat-production.

[14] Vaclav Smil. Eating meat: evolution, patterns, and consequences. *Population and development review*, 28(4):599–639, 2002.

[15] FAO, IFAD, UNICEF, WFP and WHO. The state of food security and nutrition in the world 2018. building climate resilience for food security and nutrition. *FAO*, 2018.

[16] Shruti Sharma, Sukhcharanjit Singh Thind, and Amarjeet Kaur. In vitro meat production system: why and how? *Journal of food science and technology*, 52(12):7599–7607, 2015.

[17] Wettenbank. Regeling houders van dieren, geldend van 16-01-2020. *Article 6.5*, 2020.

[18] Jennifer Dillard. A slaughterhouse nightmare: Psychological harm suffered by slaughterhouse employees and the possibility of redress through legal reform. *Geo. J. on Poverty L. & Pol'y*, 15:391, 2008.

[19] Carola Schouten, Minister van Landbouw, Natuur en Voedselkwaliteit. Aanbieding rapport 2solve inzake onderzoek naar kleine- en middelgrote slachthuizen. *Overheidsidentificatienummer: 1858272854000, kenmerk: BPZ/19221338*, 2019.

[20] Centraal Bureau Statistiek. Biologische landbouw groeit, July 2018.

[21] Jace Reese Anthis. US factory farming estimates. Sentience Institute, April 2019.

[22] Kathleen N Morgan and Chris T Tromborg. Sources of stress in captivity. *Applied animal behaviour science*, 102(3-4):262–302, 2007.

[23] Stephen P Oliver, Shelton E Murinda, and Bhushan M Jayarao. Impact of antibiotic use in adult dairy cows on antimicrobial resistance of veterinary and human pathogens: a comprehensive review. *Foodborne pathogens and disease*, 8(3):337–355, 2011.

[24] Gaverick Matheny and Cheryl Leahy. Farm-animal welfare, legislation, and trade. *Law & Contemp. Probs.*, 70:325, 2007.

[25] Geert van der Peet, Ferry Leenstra, Izak Vermeij, Nico Bondt, Linda Puister, and Jaap van Os. Feiten en cijfers over de Nederlandse veehouderijsectoren 2018. Technical report, Wageningen Livestock Research, 2018.

[26] DM Broom. The effects of production efficiency on animal welfare. *European Association for Animal Production*, 67:201–201, 1992.

[27] NG Gregory. Animal welfare at markets and during transport and slaughter. *Meat science*, 80(1):2–11, 2008.

[28] Frédéric Leroy and Istvan Praet. Animal killing and postdomestic meat production. *Journal of Agricultural and Environmental Ethics*, 30(1):67–86, 2017.

[29] Jeff Welty. Humane slaughter laws. *Law and contemporary problems*, 70(1):175–206, 2007.

[30] Donna Mo. Unhappy cows and unfair competition: Using unfair competition laws to fight farm animal abuse. *UCLA L. Rev.*, 52:1313, 2004.

[31] Thomas P Van Boeckel, Charles Brower, Marius Gilbert, Bryan T Grenfell, Simon A Levin, Timothy P Robinson, Aude Teillant, and Ramanan Laxminarayan. Global trends in antimicrobial use in food animals. *Proceedings of the National Academy of Sciences*, 112(18):5649–5654, 2015.

[32] Alan G Mathew, Robin Cissell, and S Liamthong. Antibiotic resistance in bacteria associated with food animals: a united states perspective of livestock production. *Foodborne pathogens and disease*, 4(2):115–133, 2007.

[33] Wolfgang Witte. Selective pressure by antibiotic use in livestock. *International journal of antimicrobial agents*, 16:19–24, 2000.

[34] Vincent Perreten. Resistance in the food chain and in bacteria from animals: relevance to human infections. In *Frontiers in Antimicrobial Resistance*, pages 446–464. American Society of Microbiology, 2005.

[35] Bonnie M Marshall and Stuart B Levy. Food animals and antimicrobials: impacts on human health. *Clinical microbiology reviews*, 24(4):718–733, 2011.

[36] Karen Victor and Antoni Barnard. Slaughtering for a living: A hermeneutic phenomenological perspective on the well-being of slaughterhouse employees. *International journal of qualitative studies on health and well-being*, 11(1):30266, 2016.

[37] Jessica H Leibler, Patricia A Janulewicz, and Melissa J Perry. Prevalence of serious psychological distress among slaughterhouse workers at a united states beef packing plant. *Work*, 57(1):105–109, 2017.

[38] Hester J Lipscomb, John M Dement, Carol A Epling, Bradley N Gaynes, Mary Anne McDonald, and Ashley L Schoenfisch. Depressive symptoms among working women in rural North Carolina: A comparison of women in poultry processing and other low-wage jobs. *International journal of law and psychiatry*, 30(4-5):284–298, 2007.

[39] Amy J Fitzgerald, Linda Kalof, and Thomas Dietz. Slaughterhouses and increased crime rates: An empirical analysis of the spillover from "the jungle" into the surrounding community. *Organization & Environment*, 22(2):158–184, 2009.

[40] Peter Clarys, Tom Deliens, Inge Huybrechts, Peter Deriemaeker, Barbara Vanaelst, Willem De Keyzer, Marcel Hebbelinck, and Patrick Mullie. Comparison of nutritional quality of the vegan, vegetarian, semi-vegetarian, pesco-vegetarian and omnivorous diet. *Nutrients*, 6(3):1318–1332, 2014.

[41] David Pimentel and Marcia Pimentel. Sustainability of meat-based and plant-based diets and the environment. *The American journal of clinical nutrition*, 78(3):660S–663S, 2003.

[42] Phillip Tuso, Scott R Stoll, and William W Li. A plant-based diet, atherogenesis, and coronary artery disease prevention. *The Permanente Journal*, 19(1):62, 2015.

[43] Philip J Tuso, Mohamed H Ismail, Benjamin P Ha, and Carole Bartolotto. Nutritional update for physicians: plant-based diets. *The Permanente Journal*, 17(2):61, 2013.

[44] Julieanna Hever. Plant-based diets: A physician's guide. *The permanente journal*, 20(3), 2016.

[45] Pippa Bailey. An exploration into diets around the world. Technical Report Version 1, Ipsos, August 2018.

[46] Cynthia Rosenzweig Cheikh Mbow. *Special report on climate change and land*, volume Chapter 5 of *Food Security*. United Nations, 2019.

[47] Lyudmila Kopteva, Lyudmila Shabalina, and Elena Kashirina. Ecological aspects of the world food security. In *E3S Web of Conferences*, volume 91, page 06011. EDP Sciences, 2019.

[48] AM Kolkmann, MJ Post, MAM Rutjens, ALM Van Essen, and P Moutsatsou. Serum-free media for the growth of primary bovine myoblasts. *Cytotechnology*, 72(1):111–120, 2020.

[49] Muhammad Sajid Arshad, Miral Javed, Muhammad Sohaib, Farhan Saeed, Ali Imran, and Zaid Amjad. Tissue engineering approaches to develop cultured meat from cells: a mini review. *Cogent Food & Agriculture*, 3(1):1320814, 2017.

[50] Mark J Post, Shulamit Levenberg, David L Kaplan, Nicholas Genovese, Jianan Fu, Christopher J Bryant, Nicole Negowetti, Karin Verzijden, and Panagiota Moutsatsou. Scientific, sustainability and regulatory challenges of cultured meat. *Nature Food*, 1(7):403–415, 2020.

[51] Mark J Post. Cultured beef: medical technology to produce food. *Journal of the Science of Food and Agriculture*, 94(6):1039–1041, 2014.

[52] Hanna L Tuomisto and M Joost Teixeira de Mattos. Environmental impacts of cultured meat production. *Environmental science & technology*, 45(14):6117–6123, 2011.

[53] Carolyn S Mattick, Amy E Landis, Braden R Allenby, and Nicholas J Genovese. Anticipatory life cycle analysis of in vitro biomass cultivation for cultured meat production in the united states. *Environmental science & technology*, 49(19):11941–11949, 2015.

[54] John Lynch and Raymond Pierrehumbert. Climate impacts of cultured meat and beef cattle. *Frontiers in sustainable food systems*, 3:5, 2019.

[55] I. Odegard P. Sinke. LCA of cultivated meat. Future projections for different scenarios. Technical report, Committed to the Environment Delft, February 2021.

[56] Peter Alexander, Calum Brown, Almut Arneth, Clare Dias, John Finnigan, Dominic Moran, and Mark DA Rounsevell. Could consumption of insects, cultured meat or imitation meat reduce global agricultural land use? *Global Food Security*, 15:22–32, 2017.

[57] Patrick D Hopkins. Cultured meat in western media: the disproportionate coverage of vegetarian reactions, demographic realities, and implications for cultured meat marketing. *Journal of Integrative Agriculture*, 14(2):264–272, 2015.

[58] Zuhaib Fayaz Bhat, Sunil Kumar, and Hina Fayaz Bhat. In vitro meat: A future animal-free harvest. *Critical reviews in food science and nutrition*, 57(4):782–789, 2017.

[59] Nathalie CM Rolland, C Rob Markus, and Mark J Post. The effect of information content on acceptance of cultured meat in a tasting context. *PLoS One*, 15(4):e0231176, 2020.

[60] Christopher J Bryant and Julie C Barnett. What's in a name? Consumer perceptions of in vitro meat under different names. *Appetite*, 137:104–113, 2019.

[61] Mark J Post. An alternative animal protein source: cultured beef. *Annals of the New York Academy of Sciences*, 1328(1):29–33, 2014.

[62] Vincent Bodiou, Panagiota Moutsatsou, and Mark J Post. Microcarriers for upscaling cultured meat production. *Frontiers in nutrition*, 7:10, 2020.

[63] Ingrid Odegard Robert Vergeer, Pelle Sinke. TEA of cultivated meat. future projections of different scenarios. Technical report, Committed to the Environment Delft, February 2021.

[64] CHAFEA European Union. Multi call awarded grant proposals v4. Technical report, 2017.

[65] CHAFEA European Union. List of programmes selected for Union's financial contribution, page 1. Technical report, 2020.

[66] Tom Ben-Arye, Yulia Shandalov, Shahar Ben-Shaul, Shira Landau, Yedidya Zagury, Iris Ianovici, Neta Lavon, and Shulamit Levenberg. Textured soy protein scaffolds enable the generation of three-dimensional bovine skeletal muscle tissue for cell-based meat. *Nature Food*, 1(4):210–220, 2020.

[67] Shijie Ding, GN M Swennen, Tobias Messmer, Mick Gagliardi, Daniël GM Molin, Chunbao Li, Guanghong Zhou, and Mark J Post. Maintaining bovine satellite cells stemness through p38 pathway. *Scientific reports*, 8(1):1–12, 2018.

[68] Nicholas J Genovese, Timothy L Domeier, Bhanu Prakash VL Telugu, and R Michael Roberts. Enhanced development of skeletal myotubes from porcine induced pluripotent stem cells. *Scientific reports*, 7(1):1–11, 2017.

[69] Brittany L Rodriguez, Matthew H Nguyen, Rachel E Armstrong, Emmanuel E Vega-Soto, Phillip M Polkowski, and Lisa M Larkin. A comparison of ovine facial and limb muscle as a primary cell source for engineered skeletal muscle. *Tissue Engineering Part A*, 26(3-4):167–177, 2020.

[70] Haiqing Wu, Yu Ren, Shuo Li, Wei Wang, Jianlong Yuan, Xudong Guo, Dongjun Liu, and Ming Cang. In vitro culture and induced differentiation of sheep skeletal muscle satellite cells. *Cell biology international*, 36(6):579–587, 2012.

[71] S. Burgham. Overseas merchandise trade: February 2020, March 2020.

[72] Vaikundamoorthy Ramalingam, Zhen Song, and Inho Hwang. The potential role of secondary metabolites in modulating the flavor and taste of the meat. *Food research international*, 122:174–182, 2019.

[73] Charles Spence. Multisensory flavour perception. *Current Biology*, 23(9):R365–R369, 2013.

[74] Jason R Stokes, Michael W Boehm, and Stefan K Baier. Oral processing, texture and mouthfeel: From rheology to tribology and beyond. *Current Opinion in Colloid & Interface Science*, 18(4):349–359, 2013.

[75] Muhammad Issa Khan, Cheorun Jo, and Muhammad Rizwan Tariq. Meat flavor precursors and factors influencing flavor precursors—a systematic review. *Meat science*, 110:278–284, 2015.

[76] Donald S Mottram. Flavour formation in meat and meat products: a review. *Food chemistry*, 62(4):415–424, 1998.

[77] Marianne N Lund and Colin A Ray. Control of maillard reactions in foods: Strategies and chemical mechanisms. *Journal of Agricultural and Food Chemistry*, 65(23):4537–4552, 2017.

[78] Surendranath P Suman and Poulson Joseph. Myoglobin chemistry and meat color. *Annual review of food science and technology*, 4:79–99, 2013.

[79] Shane B Kanatous and Pradeep PA Mammen. Regulation of myoglobin expression. *Journal of Experimental Biology*, 213(16):2741–2747, 2010.

[80] Guoqiang Zhang, Xinrui Zhao, Xueliang Li, Guocheng Du, Jingwen Zhou, and Jian Chen. Challenges and possibilities for bio-manufacturing cultured meat. *Trends in Food Science & Technology*, 97:443–450, 2020.

[81] Florence Croisier and Christine Jérôme. Chitosan-based biomaterials for tissue engineering. *European polymer journal*, 49(4):780–792, 2013.

[82] In-Yong Kim, Seog-Jin Seo, Hyun-Seuk Moon, Mi-Kyong Yoo, In-Young Park, Bom-Chol Kim, and Chong-Su Cho. Chitosan and its derivatives for tissue engineering applications. *Biotechnology advances*, 26(1):1–21, 2008.

[83] I Yuvarani, S Senthilkumar, Jayachandran Venkatesan, Se-Kwon Kim, Abdul Aziz Al-Kheraif, Sukumaran Anil, and PN Sudha. Chitosan modified alginate-polyurethane scaffold for skeletal muscle tissue engineering. *Journal of Biomaterials and Tissue Engineering*, 5(8):665–672, 2015.

[84] Kyle D Fish, Natalie R Rubio, Andrew J Stout, John SK Yuen, and David L Kaplan. Prospects and challenges for cell-cultured fat as a novel food ingredient. *Trends in food science & technology*, 98:53–67, 2020.

[85] B Guo and BP Dalrymple. Transcriptomics of meat quality. In *New Aspects of Meat Quality*, pages 259–320. Elsevier, 2017.

[86] Han Zhu, Marion O'Farrell, Eddy Walther Hansen, Petter Vejle Andersen, Per Berg, and Bjørg Egelandsdal. The potential for predicting purge in packaged meat using low field NMR. *Journal of Food Engineering*, 206:98–105, 2017.

[87] Yiu H Hui. *Handbook of meat and meat processing*. CRC press, 2012.

[88] Tom Ben-Arye and Shulamit Levenberg. Tissue engineering for clean meat production. *Frontiers in Sustainable Food Systems*, 3:46, 2019.

[89] James A Olzmann and Pedro Carvalho. Dynamics and functions of lipid droplets. *Nature reviews Molecular cell biology*, 20(3):137–155, 2019.

[90] Fiona Louis, Pauline Pannetier, Zied Souguir, Didier Le Cerf, Philippe Valet, Jean-Pierre Vannier, Guillaume Vidal, and Elise Demange. A biomimetic hydrogel functionalized with adipose ECM components as a microenvironment for the 3D culture of human and murine adipocytes. *Biotechnology and bioengineering*, 114(8):1813–1824, 2017.

[91] Yimin Qin, Jinju Jiang, Lili Zhao, Jian Zhang, and Fahe Wang. Applications of alginate as a functional food ingredient. In *Biopolymers for food design*, pages 409–429. Elsevier, 2018.

[92] Dong-Hee Yong, Min-Kyung Song, and Hye-Hyun Yoon. Effects of sodium alginate concentration on physical and sensory characteristics of persimmon calcium alginate beads. *Korean journal of food and cookery science*, 27(5):497–505, 2011.

[93] Rob Vreeker, Liangbin Li, Yapeng Fang, Ingrid Appelqvist, and Eduardo Mendes. Drying and rehydration of calcium alginate gels. *Food Biophysics*, 3(4):361–369, 2008.

[94] Jon A Rowley, Gerard Madlambayan, and David J Mooney. Alginate hydrogels as synthetic extracellular matrix materials. *Biomaterials*, 20(1):45–53, 1999.

[95] Michal Shachar, Orna Tsur-Gang, Tal Dvir, Jonathan Leor, and Smadar Cohen. The effect of immobilized RGD peptide in alginate scaffolds on cardiac tissue engineering. *Acta biomaterialia*, 7(1):152–162, 2011.

[96] Brian R MacIntosh, Phillip F Gardiner, and Alan J McComas. *Skeletal muscle: form and function*. Human Kinetics, 2006.

[97] H. Schmalbruch. *Skeletal Muscle*. Handbuch der mikroskopischen Anatomie des Menschen Handbook of Mikroscopic Anatomy. Springer Berlin Heidelberg, 2012.

[98] R. Korthuis. *Skeletal Muscle Circulation*. Colloquium Series on Integrated Systems Physiology: From Molecule to Function to Disease. Biota Publishing, 2011.

[99] E.N. Marieb and K. Hoehn. *Human Anatomy & Physiology*. Pearson Benjamin Cummings, 2007.

[100] Peter S Zammit, Terence A Partridge, and Zipora Yablonka-Reuveni. The skeletal muscle satellite cell: the stem cell that came in from the cold. *Journal of Histochemistry & Cytochemistry*, 54(11):1177–1191, 2006.

[101] Laura E Sidney, Matthew J Branch, Siobhán E Dunphy, Harminder S Dua, and Andrew Hopkinson. Concise review: evidence for CD34 as a common marker for diverse progenitors. *Stem cells*, 32(6):1380–1389, 2014.

[102] Julia von Maltzahn, Andrew E Jones, Robin J Parks, and Michael A Rudnicki. Pax7 is critical for the normal function of satellite cells in adult skeletal muscle. *Proceedings of the National Academy of Sciences*, 110(41):16474–16479, 2013.

[103] Aleksandra Klimczak, Urszula Kozlowska, and Maciej Kurpisz. Muscle stem/progenitor cells and mesenchymal stem cells of bone marrow origin for skeletal muscle regeneration in muscular dystrophies. *Archivum immunologiae et therapiae experimentalis*, 66(5):341–354, 2018.

[104] Susan M Abmayr and Grace K Pavlath. Myoblast fusion: lessons from flies and mice. *Development*, 139(4):641–656, 2012.

[105] Joseph W Sanger, Songman Kang, Cornelia C Siebrands, Nancy Freeman, Aiping Du, Jushuo Wang, Andrea L Stout, and Jean M Sanger. How to build a myofibril. *Journal of Muscle Research & Cell Motility*, 26(6-8):343, 2005.

[106] J.M. Lackie. *The Dictionary of Cell & Molecular Biology*. Elsevier Science, 2007.

[107] Peter S Zammit, Frederic Relaix, Yosuke Nagata, Ana Pérez Ruiz, Charlotte A Collins, Terence A Partridge, and Jonathan R Beauchamp. Pax7 and myogenic progression in skeletal muscle satellite cells. *Journal of cell science*, 119(9):1824–1832, 2006.

[108] Masakazu Yamamoto, Nicholas P Legendre, Arpita A Biswas, Alexander Lawton, Shoko Yamamoto, Shahragim Tajbakhsh, Gabrielle Kardon, and David J Goldhamer. Loss of MyoD and Myf5 in skeletal muscle stem cells results in altered myogenic programming and failed regeneration. *Stem cell reports*, 10(3):956–969, 2018.

[109] Fiona C Wardle. Master control: transcriptional regulation of mammalian MyoD. *Journal of muscle research and cell motility*, 40(2):211–226, 2019.

[110] Stephen J Tapscott. The circuitry of a master switch: MyoD and the regulation of skeletal muscle gene transcription. *Development*, 132(12):2685–2695, 2005.

[111] Michael A Rudnicki, Patrick NJ Schnegelsberg, Ronald H Stead, Thomas Braun, Hans-Henning Arnold, and Rudolf Jaenisch. MyoD or Myf-5 is required for the formation of skeletal muscle. *Cell*, 75(7):1351–1359, 1993.

[112] Thomas Braun, Eva Bober, Michael A Rudnicki, Rudolf Jaenisch, and Hans-Henning Arnold. MyoD expression marks the onset of skeletal myogenesis in Myf-5 mutant mice. *Development*, 120(11):3083–3092, 1994.

[113] Boris Kablar, Kirsten Krastel, Chuyan Ying, Atsushi Asakura, Stephen J Tapscott, and Michael A Rudnicki. MyoD and Myf-5 differentially regulate the development of limb versus trunk skeletal muscle. *Development*, 124(23):4729–4738, 1997.

[114] Luc A Sabourin, Adele Girgis-Gabardo, Patrick Seale, Atsushi Asakura, and Michael A Rudnicki. Reduced differentiation potential of primary MyoD-/- myogenic cells derived from adult skeletal muscle. *The Journal of cell biology*, 144(4):631–643, 1999.

[115] Zipora Yablonka-Reuveni, Michael A Rudnicki, Anthony J Rivera, Michael Primig, Judy E Anderson, and Priscilla Natanson. The transition from proliferation to differentiation is delayed in satellite cells from mice lacking MyoD. *Developmental biology*, 210(2):440–455, 1999.

[116] Melissa L Conerly, Zizhen Yao, Jun Wen Zhong, Mark Groudine, and Stephen J Tapscott. Distinct activities of Myf5 and MyoD indicate separate roles in skeletal muscle lineage specification and differentiation. *Developmental cell*, 36(4):375–385, 2016.

[117] RN Cooper, S Tajbakhsh, V Mouly, G Cossu, M Buckingham, and GS Butler-Browne. In vivo satellite cell activation via Myf5 and MyoD in regenerating mouse skeletal muscle. *J Cell Sci*, 112(17):2895–2901, 1999.

[118] Jeff Ishibashi, Robert L Perry, Atsushi Asakura, and Michael A Rudnicki. MyoD induces myogenic differentiation through cooperation of its NH2- and COOH-terminal regions. *The Journal of cell biology*, 171(3):471–482, 2005.

[119] Aref Shahini, Kalyan Vydiam, Debanik Choudhury, Nika Rajabian, Thy Nguyen, Pedro Lei, and Stelios T Andreadis. Efficient and high yield isolation of myoblasts from skeletal muscle. *Stem cell research*, 30:122–129, 2018.

[120] Christel Becker, Bruno Della Gaspera, Michèle Guyot, Evelyne Donsez, Anne-Sophie Armand, Frédéric Charbonnier, Thierry Launay, and Christophe Chanoine. Expression of MRF4 protein in adult and in regenerating muscles in xenopus. *Developmental dynamics: an official publication of the American Association of Anatomists*, 227(3):445–449, 2003.

[121] Irene Moretti, Stefano Ciciliot, Kenneth A Dyar, Reimar Abraham, Marta Murgia, Lisa Agatea, Takayuki Akimoto, Silvio Bicciato, Mattia Forcato, Philippe Pierre, et al. MRF4 negatively regulates adult skeletal muscle growth by repressing MEF2 activity. *Nature communications*, 7(1):1–12, 2016.

[122] Massimo Ganassi, Sara Badodi, Huascar Pedro Ortuste Quiroga, Peter S Zammit, Yaniv Hinits, and Simon M Hughes. Myogenin promotes myocyte fusion to balance fibre number and size. *Nature communications*, 9(1):1–17, 2018.

[123] Yusaku Kodaka, Gemachu Rabu, and Atsushi Asakura. Skeletal muscle cell induction from pluripotent stem cells. *Stem cells international*, 2017, 2017.

[124] William F Harrington and Michael E Rodgers. Myosin. *Annual review of biochemistry*, 53(1):35–73, 1984.

[125] Jonathan S Berg, Bradford C Powell, and Richard E Cheney. A millennial myosin census. *Molecular biology of the cell*, 12(4):780–794, 2001.

[126] David M Brown, Tim Parr, and John M Brameld. Myosin heavy chain mrna isoforms are expressed in two distinct cohorts during C2C12 myogenesis. *Journal of muscle research and cell motility*, 32(6):383–390, 2012.

[127] Ana Soriano-Arroquia, Peter D Clegg, Andrew P Molloy, and Katarzyna Goljanek-Whysall. Preparation and culture of myogenic precursor cells/primary myoblasts from skeletal muscle of adult and aged humans. *Journal of visualized experiments: JoVE*, (120), 2017.

[128] Lina Cancellara, Silvia Quartesan, Luana Toniolo, Carlo Reggiani, Francesco Mascarello, Luca Melotti, Maura Francolini, Lisa Maccatrozzo, and Marco Patruno. Age-dependent variations in the expression of myosin isoforms and myogenic factors during the involution of the proximal sesamoidean ligament of sheep. *Research in veterinary science*, 124:270–279, 2019.

[129] Jordan D Jones, Alex S Rebello, and Glenn R Gaudette. Decellularized spinach: An edible scaffold for laboratory-grown meat growing meat on spinach. *Food Bioscience*, page 100986, 2021.

[130] W-H Zimmermann, K Schneiderbanger, P Schubert, M Didie, F Munzel, JF Heubach, S Kostin, WL Neuhuber, and Thomas Eschenhagen. Tissue engineering of a differentiated cardiac muscle construct. *Circulation research*, 90(2):223–230, 2002.

[131] Zhengwei Li, Yongbeom Seo, Onur Aydin, Mohamed Elhebeary, Roger D Kamm, Hyunjoon Kong, and M Taher A Saif. Biohybrid valveless pump-bot powered by engineered skeletal muscle. *Proceedings of the National Academy of Sciences*, 116(5):1543–1548, 2019.

[132] M. Post J. Breemhaar. Apparatus and process for production of tissue from cells, 2019.

[133] Andrew J Capel, Rowan P Rimington, Jacob W Fleming, Darren J Player, Luke A Baker, Mark C Turner, Julia M Jones, Neil RW Martin, Richard A Ferguson, Vivek C Mudera, et al. Scalable 3D printed molds for human tissue engineered skeletal muscle. *Frontiers in bioengineering and biotechnology*, 7:20, 2019.

[134] Gaurav Agrawal, Aereas Aung, and Shyni Varghese. Skeletal muscle-on-a-chip: an in vitro model to evaluate tissue formation and injury. *Lab on a Chip*, 17(20):3447–3461, 2017.

[135] Weining Bian and Nenad Bursac. Engineered skeletal muscle tissue networks with controllable architecture. *Biomaterials*, 30(7):1401–1412, 2009.

[136] Herman Vandenburgh, Janet Shansky, Frank Benesch-Lee, Victoria Barbata, Jonathan Reid, Lieven Thorrez, Robert Valentini, and Gregory Crawford. Drug-screening platform based on the contractility of tissue-engineered muscle. *Muscle & nerve*, 37(4):438–447, 2008.

[137] B Kalman, C Monge, A Bigot, V Mouly, C Picart, and T Boudou. Engineering human 3D micromuscles with co-culture of fibroblasts and myoblasts. *Computer methods in biomechanics and biomedical engineering*, 18(sup1):1960–1961, 2015.

[138] Mohammad E Afshar, Haben Y Abraha, Mohsen A Bakooshli, Sadegh Davoudi, Nimalan Thavandiran, Kayee Tung, Henry Ahn, Howard J Ginsberg, Peter W Zandstra, and Penney M Gilbert. A 96-well culture platform enables longitudinal analyses of engineered human skeletal muscle microtissue strength. *Scientific reports*, 10(1):1–16, 2020.

[139] Celia Snyman, Kyle Peter Goetsch, Kathryn Helen Myburgh, and Carola Ulrike Niesler. Simple silicone chamber system for 3D skeletal muscle tissue formation. *Frontiers in physiology*, 4:349, 2013.

[140] Joshua R Gershlak, Sarah Hernandez, Gianluca Fontana, Luke R Perreault, Katrina J Hansen, Sara A Larson, Bernard YK Binder, David M Dolivo, Tianhong Yang, Tanja Dominko, et al. Crossing kingdoms: using decellularized plants as perfusable tissue engineering scaffolds. *Biomaterials*, 125:13–22, 2017.

[141] Gianluca Fontana, Joshua Gershlak, Michal Adamski, Jae-Sung Lee, Shion Matsumoto, Hau D Le, Bernard Binder, John Wirth, Glenn Gaudette, and William L Murphy. Biofunctionalized plants as diverse biomaterials for human cell culture. *Advanced healthcare materials*, 6(8):1601225, 2017.

[142] Katja Jansen, Marianna Evangelopoulou, Carla Pou Casellas, Sarina Abrishamcar, Jitske Jansen, Tina Vermonden, and Rosalinde Masereeuw. Spinach and chive for kidney tubule engineering: the limitations of decellularized plant scaffolds and vasculature. *The AAPS Journal*, 23(1):1–7, 2021.

[143] Serkan Dikici, Frederik Claeyssens, and Sheila MacNeil. Decellularised baby spinach leaves and their potential use in tissue engineering applications: studying and promoting neovascularisation. *Journal of biomaterials applications*, 34(4):546–559, 2019.

[144] Mai Furuhashi, Yuya Morimoto, Ai Shima, Futoshi Nakamura, Hiroshi Ishikawa, and Shoji Takeuchi. Formation of contractile 3D bovine muscle tissue for construction of millimetre-thick cultured steak. *npj Science of Food*, 5(1):1–8, 2021.

[145] JS Raja, ML Hoffman, KE Govoni, SA Zinn, and SA Reed. Restricted maternal nutrition alters myogenic regulatory factor expression in satellite cells of ovine offspring. *Animal*, 10(7):1200–1203, 2016.

[146] MR Hathaway, Mary S Pampusch, JR Hembree, and William R Dayton. Transforming growth factor beta-1 facilitates establishing clonal populations of ovine muscle satellite cells. *Journal of animal science*, 72(8):2001–2007, 1994.

[147] Wu Rihan, Yun Yueying, Feng Qinghui, Qin Xia, He Xige, Chen Lu, Sha Lina, Nishiumi Tadayuki, and Borjigin Gerelt. Expression of myogenic regulatory factor genes in skeletal muscle satellite cells from Wuzhumuqin sheep in vitro. *Small Ruminant Research*, 193:106251, 2020.

[148] Sreemanti Basu, Hope M Campbell, Bonnie N Dittel, and Avijit Ray. Purification of specific cell population by fluorescence activated cell sorting (FACS). *Journal of visualized experiments: JoVE*, (41), 2010.

[149] Enrico Lugli, Veronica Zanon, Domenico Mavilio, and Alessandra Roberto. FACS analysis of memory T lymphocytes. In *T-Cell Differentiation*, pages 31–47. Springer, 2017.

[150] Ana Costa, Yann Kieffer, Alix Scholer-Dahirel, Floriane Pelon, Brigitte Bourachot, Melissa Cardon, Philemon Sirven, Ilaria Magagna, Laetitia Fuhrmann, Charles Bernard, et al. Fibroblast heterogeneity and immunosuppressive environment in human breast cancer. *Cancer cell*, 33(3):463–479, 2018.

[151] Camila F Almeida, Stephanie A Fernandes, Antonio F Ribeiro Junior, Oswaldo Keith Okamoto, and Mariz Vainzof. Muscle satellite cells: exploring the basic biology to rule them. *Stem cells international*, 2016, 2016.

[152] Akshay Bareja, Jason A Holt, Guizhen Luo, Calvin Chang, Junyu Lin, Aaron C Hinken, Johannes M Freudenberg, William E Kraus, William J Evans, and Andrew N Billin. Human and mouse skeletal muscle stem cells: convergent and divergent mechanisms of myogenesis. *PloS one*, 9(2):e90398, 2014.

[153] N Arrighi, C Moratal, N Clement, S Giorgetti-Peraldi, P Peraldi, A Loubat, JY Kurzenne, C Dani, ANGELE Chopard, and CA Dechesne. Characterization of adipocytes derived from fibro/adipogenic progenitors resident in human skeletal muscle. *Cell death & disease*, 6(4):e1733–e1733, 2015.

[154] Bruno Péault, Michael Rudnicki, Yvan Torrente, Giulio Cossu, Jacques P Tremblay, Terry Partridge, Emanuela Gussoni, Louis M Kunkel, and Johnny Huard. Stem and progenitor cells in skeletal muscle development, maintenance, and therapy. *Molecular therapy*, 15(5):867–877, 2007.

[155] Alessandra Castiglioni, Simone Hettmer, Matthew D Lynes, Tata Nageswara Rao, Daria Tchessalova, Indranil Sinha, Bernard T Lee, Yu-Hua Tseng, and Amy J Wagers. Isolation of progenitors that exhibit myogenic/osteogenic bipotency in vitro by fluorescence-activated cell sorting from human fetal muscle. *Stem cell reports*, 2(1):92–106, 2014.

[156] Nicolas A Dumont, Yu Xin Wang, Julia Von Maltzahn, Alessandra Pasut, C Florian Bentzinger, Caroline E Brun, and Michael A Rudnicki. Dystrophin expression in muscle stem cells regulates their polarity and asymmetric division. *Nature medicine*, 21(12):1455–1463, 2015.

[157] Ryan R Driskell, Beate M Lichtenberger, Esther Hoste, Kai Kretzschmar, Ben D Simons, Marika Charalambous, Sacri R Ferron, Yann Herault, Guillaume Pavlovic, Anne C Ferguson-Smith, et al. Distinct fibroblast lineages determine dermal architecture in skin development and repair. *Nature*, 504(7479):277–281, 2013.

[158] Elizabeth E Crouch and Fiona Doetsch. FACS isolation of endothelial cells and pericytes from mouse brain microregions. *Nature protocols*, 13(4):738–751, 2018.

[159] Kaveh Baghaei, Seyed Mohmoud Hashemi, Samaneh Tokhanbigli, Ali Asadi Rad, Hamid Assadzadeh-Aghdaei, Abdolhamid Sharifian, and Mohammad Reza Zali. Isolation, differentiation, and characterization of mesenchymal stem cells from human bone marrow. *Gastroenterology and hepatology from bed to bench*, 10(3):208, 2017.

[160] Daniel Eberli, Shay Soker, Anthony Atala, and James J Yoo. Optimization of human skeletal muscle precursor cell culture and myofiber formation in vitro. *Methods*, 47(2):98–103, 2009.

[161] L. Galluzzi and N.P. Rudqvist. *Tumor Immunology and Immunotherapy - Cellular Methods Part B*. Elsevier Science, 2020.

[162] S Grefte, S Vullinghs, AM Kuijpers-Jagtman, R Torensma, and JW Von den Hoff. Matrigel, but not collagen I, maintains the differentiation capacity of muscle derived cells in vitro. *Biomedical materials*, 7(5):055004, 2012.

[163] Janine Treter, Fernando Bonatto, Cristiano Krug, Gabriel Vieira Soares, Israel Jacob Rabin Baumvol, and Alexandre Jose Macedo. Washing-resistant surfactant coated surface is able to inhibit pathogenic bacteria adhesion. *Applied surface science*, 303:147–154, 2014.

[164] J Van der Valk, D Brunner, K De Smet, Å Fex Svenningsen, P Honegger, Lisbeth E Knudsen, T Lindl, J Noraberg, A Price, ML Scarino, et al. Optimization of chemically defined cell culture media–replacing fetal bovine serum in mammalian in vitro methods. *Toxicology in vitro*, 24(4):1053–1063, 2010.

[165] Gerhard Gstraunthaler, Toni Lindl, and Jan van der Valk. A plea to reduce or replace fetal bovine serum in cell culture media. *Cytotechnology*, 65(5):791–793, 2013.

[166] Carlo EA Jochems, Jan BF Van Der Valk, Frans R Stafleu, and Vera Baumans. The use of fetal bovine serum: ethical or scientific problem? *Alternatives to Laboratory Animals*, 30(2):219–227, 2002.

[167] Gerhard Gstraunthaler. Alternatives to the use of fetal bovine serum: serum-free cell culture. *ALTEX-Alternatives to animal experimentation*, 20(4):275–281, 2003.

[168] Ann H Ryu, Walter L Eckalbar, Anat Kreimer, Nir Yosef, and Nadav Ahituv. Use antibiotics in cell culture with caution: genome-wide identification of antibiotic-induced changes in gene expression and regulation. *Scientific reports*, 7(1):1–9, 2017.

[169] Aleksandra Skubis, Joanna Gola, Bartosz Sikora, Jolanta Hybiak, Monika Paul-Samojedny, Urszula Mazurek, and Marek J Łos. Impact of antibiotics on the proliferation and differentiation of human adipose-derived mesenchymal stem cells. *International journal of molecular sciences*, 18(12):2522, 2017.

[170] H Babich, EJ Liebling, RF Burger, HL Zuckerbraun, and AG Schuck. Choice of DMEM, formulated with or without pyruvate, plays an important role in assessing the in vitro cytotoxicity of oxidants and prooxidant nutraceuticals. *In Vitro Cellular & Developmental Biology-Animal*, 45(5-6):226–233, 2009.

[171] Thermo Fisher Scientific. Media formulation technical resources - 10569 - DMEM, high glucose, Glutamax$^{TM}$, pyruvate. Accessed on 24-02-2021.

[172] Thermo Fisher Scientific. DMEM, high glucose, Glutamax$^{TM}$ supplement, pyruvate, March 2021. Accessed on 01-03-2021.

[173] Thermo Fisher Scientific. DMEM, high glucose, March 2021. Accessed on 01-03-2021.

[174] Shojinmeat Project. Open source cell-ag, 2021. Accessed on 24-02-2021.

[175] MA Heckman, Kendle Sherry, and E Gonzalez De Mejia. Energy drinks: an assessment of their market size, consumer demographics, ingredient profile, functionality, and regulations in the United States. *Comprehensive Reviews in food science and food safety*, 9(3):303–317, 2010.

[176] Kaia Kordosky-Herrera and Wade A Grow. Caffeine and nicotine decrease acetylcholine receptor clustering in C2C12 myotube culture. *Cell and tissue research*, 335(2):341–348, 2009.

[177] David S Enyart, Chelsea L Crocker, Jennifer R Stansell, Madeleine Cutrone, Meghann M Dintino, Stephen T Kinsey, Stephan L Brown, and Bradley L Baumgarner. Low-dose caffeine administration increases fatty acid utilization and mitochondrial turnover in C2C12 skeletal myotubes. *Physiological reports*, 8(1):e14340, 2020.

[178] Fengyu Li, Xiaoxue Li, Xuewei Peng, Lili Sun, Shengnan Jia, Ping Wang, Shuang Ma, Hongyan Zhao, Qingmiao Yu, and Hongliang Huo. Ginsenoside Rg1 prevents starvation-induced muscle protein degradation via regulation of AKT/mTOR/FoxO signaling in C2C12 myotubes. *Experimental and therapeutic medicine*, 14(2):1241–1247, 2017.

[179] Szu-Hsien Yu, Chih-Yang Huang, Shin-Da Lee, Ming-Fen Hsu, Ray-Yau Wang, Chung-Lan Kao, and Chia-Hua Kuo. Decreased eccentric exercise-induced macrophage infiltration in skeletal muscle after supplementation with a class of ginseng-derived steroids. *PloS one*, 9(12):e114649, 2014.

[180] Samuel Mettler, Carmen Rusch, and Paolo C Colombani. Osmolality and ph of sport and other drinks available in switzerland. *Schweizerische Zeitschrift fur Sportmedizin und Sporttraumatologie*, 54(3):92, 2006.

[181] The Serum Specialist Biowest. Technical data sheet DMEM high glucose. *Catalogue number L0104*, 2013.

[182] HiMedia Cell Culture. Dulbeccoś Modified Eagle Medium Product Information. *Product code AT186*, 2012.

[183] Thermo Fisher Scientific. DMEM, high glucose, NEAA, no glutamine, March 2021. Accessed on 21-03-2021.

[184] Juan C Stockert, Alfonso Blázquez-Castro, Magdalena Cañete, Richard W Horobin, and Ángeles Villanueva. MTT assay for cell viability: Intracellular localization of the formazan product is in lipid droplets. *Acta histochemica*, 114(8):785–796, 2012.

[185] Priti Kumar, Arvindhan Nagarajan, and Pradeep D Uchil. Analysis of cell viability by the MTT assay. *Cold Spring Harbor Protocols*, 2018(6):pdb–prot095505, 2018.

[186] M Gaster, H Beck-Nielsen, and HD Schrøder. Proliferation conditions for human satellite cells the fractional content of satellite cells. *Apmis*, 109(11):726–734, 2001.

[187] Brian C Syverud, Jonah D Lee, Keith W VanDusen, and Lisa M Larkin. Isolation and purification of satellite cells for skeletal muscle tissue engineering. *Journal of regenerative medicine*, 3(2), 2014.

[188] Colin Venter and Carola Niesler. A triple co-culture method to investigate the effect of macrophages and fibroblasts on myoblast proliferation and migration. *BioTechniques*, 64(2):52–58, 2018.

[189] ST Cooper, AL Maxwell, E Kizana, M Ghoddusi, EC Hardeman, IE Alexander, DG Allen, and KN North. C2C12 co-culture on a fibroblast substratum enables sustained survival of contractile, highly differentiated myotubes with peripheral nuclei and adult fast myosin expression. *Cell motility and the cytoskeleton*, 58(3):200–211, 2004.

[190] Lu-Lu Lu, Yong-Jun Liu, Shao-Guang Yang, Qin-Jun Zhao, Xin Wang, Wei Gong, Zhi-Bo Han, Zhen-Shu Xu, Yong-Xin Lu, Delong Liu, et al. Isolation and characterization of human umbilical cord mesenchymal stem cells with hematopoiesis-supportive function and other potentials. *haematologica*, 91(8):1017–1026, 2006.

[191] Eun Ji Gang, Ju Ah Jeong, Seung Hyun Hong, Soo Han Hwang, Seong Whan Kim, Il Ho Yang, Chiyoung Ahn, Hoon Han, and Hoeon Kim. Skeletal myogenic differentiation of mesenchymal stem cells isolated from human umbilical cord blood. *Stem cells*, 22(4):617–624, 2004.

[192] NW Rufaut, NT Goldthorpe, JE Wildermoth, and OAM Wallace. Myogenic differentiation of dermal papilla cells from bovine skin. *Journal of cellular physiology*, 209(3):959–966, 2006.

[193] Colin AB Jahoda, Claire J Whitehouse, Amanda J Reynolds, and Nicholas Hole. Hair follicle dermal cells differentiate into adipogenic and osteogenic lineages. *Experimental dermatology*, 12(6):849–859, 2003.

[194] Wei Chen, Minkai Xie, Bin Yang, Shantaram Bharadwaj, Lujie Song, Guihua Liu, Shanhong Yi, Gang Ye, Anthony Atala, and Yuanyuan Zhang. Skeletal myogenic differentiation of human urine-derived cells as a potential source for skeletal muscle regeneration. *Journal of Tissue Engineering and Regenerative Medicine*, 11(2):334–341, 2017.

[195] Shantaram Bharadwaj, Guihua Liu, Yingai Shi, Rongpei Wu, Bin Yang, Tongchuan He, Yuxin Fan, Xinyan Lu, Xiaobo Zhou, Hong Liu, et al. Multipotential differentiation of human urine-derived stem cells: Potential for therapeutic applications in urology. *Stem cells*, 31(9):1840–1856, 2013.

[196] Ling Liu, Tom H Cheung, Gregory W Charville, and Thomas A Rando. Isolation of skeletal muscle stem cells by fluorescence-activated cell sorting. *Nature protocols*, 10(10):1612–1624, 2015.

[197] Heping Cheng, W Jonathan Lederer, and Mark B Cannell. Calcium sparks: elementary events underlying excitation-contraction coupling in heart muscle. *Science*, 262(5134):740–744, 1993.

[198] Paola Lorenzon, Aldo Giovannelli, Davide Ragozzino, Fabrizio Eusebi, and Fabio Ruzzier. Spontaneous and repetitive calcium transients in C2C12 mouse myotubes during in vitro myogenesis. *European Journal of Neuroscience*, 9(4):800–808, 1997.

[199] Michael J Berridge and Antony Galione. Cytosolic calcium oscillators. *The FASEB Journal*, 2(15):3074–3082, 1988.

[200] Reza Mohammadinejad, Hajar Maleki, Eneko Larrañeta, André R Fajardo, Amirala Bakhshian Nik, Amin Shavandi, Amir Sheikhi, Mansour Ghorbanpour, Mehdi Farokhi, Praveen Govindh, et al. Status and future scope of plant-based green hydrogels in biomedical engineering. *Applied Materials Today*, 16:213–246, 2019.

[201] Nomin-Erdene Oyunbaatar, Deok-Hyu Lee, Swati J Patil, Eung-Sam Kim, and Dong-Weon Lee. Biomechanical characterization of cardiomyocyte using pdms pillar with microgrooves. *Sensors*, 16(8):1258, 2016.

[202] F Ruiz De Huidobro, E Miguel, B Blázquez, and E Onega. A comparison between two methods (warner–bratzler and texture profile analysis) for testing either raw meat or cooked meat. *Meat science*, 69(3):527–536, 2005.

[203] Robin Simsa, John Yuen, Andrew Stout, Natalie Rubio, Per Fogelstrand, and David L Kaplan. Extracellular heme proteins influence bovine myosatellite cell proliferation and the color of cell-based meat. *Foods*, 8(10):521, 2019.

[204] Barbara d'Acampora Zellner, Paola Dugo, Giovanni Dugo, and Luigi Mondello. Gas chromatography–olfactometry in food flavour analysis. *Journal of Chromatography a*, 1186(1-2):123–143, 2008.